A THESIS
FOR THE DEGREE OF DOCTOR OF PHILOSOPHY

Development of Organic and Inorganic Nanostructured Thin Films through Electrohydrodynamic Atomization towards Multifunctional Applications

Navaneethan Duraisamy

Department of Mechatronics Engineering
GRADUATE SCHOOL
JEJU NATIONAL UNIVERSITY

August, 2013

Development of Organic and Inorganic Nanostructured Thin Films through Electrohydrodynamic Atomization towards Multifunctional Applications

Navaneethan Duraisamy

(Supervised by Professor Kyung Hyun Choi)

A thesis submitted in partial fulfillment of the requirement for the degree of Doctor of Philosophy

2013. 08

The thesis has been examined and approved.

Chul Ung Kang

Thesis director, Chul Ung Kang, Professor, Department of Mechatronics Engineering

Ki Rin Kwon

Ki Rin Kwon, Professor, Department of Mechanical Engineering

Jinho Bae

Jin Ho Bae, Professor, Department of Ocean System Engineering

Jeongdai Jo

Jeongdai Jo, Director, Korea Institute of Machinery & Materials

Kyung Hyun Choi

Kyung Hyun Choi, Professor, Department of Mechatronics Engineering

Date

Department of Mechatronics Engineering
GRADUATE SCHOOL
JEJU NATIONAL UNIVERSITY
REPUBLIC OF KOREA

Dedicated

To

My Parents

Acknowledgments

I would like to express my sincere gratitude to the individuals who contributed to in success of my work. First of all, I would like to thank my research advisor, Prof. KyungHyun Choi. Through his positive and open-minded attitude, and his enthusiasm and optimism toward research on printed electronics, he created the legacy of the free, vivid, intelligent, friendly and communicative research atmosphere in the lab. I feel really lucky to work in such environment. His experience, knowledge, and guidance have been an invaluable throughout my graduate career.

I extend my sincere thanks to my thesis advisors Prof. Jeongdai Jo, Prof. Jin Ho Bae, Prof. ChulUng Kang and Prof. Ki Rin Kwon. Their help and support in my thesis completion is highly gratified. I would like to thank Prof. K. Natarajan for his constant support and encouragement.

It is my great pleasure to thank my friend Mr. K. Bala krishnan and senior Mr. S. Sridharan, who introduced me in to this lab. I wish to express my deep gratitude to Dr. Nauman for his valuable suggestions and timely help. I owe my heartfelt thanks to the support rendered by my seniors Dr. Khalid, Mr. Naeem and friends Mr. Kamran, Mr. Zubair, Mr. Adnan, Ms. Maria, Mr. Hyun-Woo, Mr. Hyung Chan and Mr. Jeong-beom, Mr. Murtuza, Mr. Junaid and Mr. Shaid. I also thank to my friend Mr. K. Anand, who inspired me to do PhD in abroad. I would be thankful to Mr. Kyung-Hyun Lee, Ms. Jae-he Park and Ms. Ji-yeon for their helping presence around me always.

I must thank my better half Ms. K. Kavitha for bringing me in high spirit at all the times. Then, I would say my heartiest thanks to my lovable brothers Dr. Karthikeyan and Dr. Ganesh Thangaraj for their fruitful discussions and strong personnel support throught my research period whenever I disappoint. I also thank to my brother Dr. M. S. Gandhi for his healthy discussions and joyful fight with me. Next, I should place my overwhelming thanks to Dr. P. Prabu, R. Parthiban, M. Prabu, R. Suriyaprabha, Dr. Gunasekaran, Dr. M. Rajkumar and Dr. P. Manivasakan for their kind words and strong support. I also thank Mr. B. Saravanakumar, Mr. R. Ananthakumar, Mr. V. Ganesh Kumar, Mr. Umasuthan Navaneethaiyer, Mr. S. Radha Krishnan, Mr. A. Sebastian Ananth, Mr. K. Thiyagarajan, Dr. Anil, Dr. Dharanitharan, Dr. Purushothaman and Mrs. Saranya Purushothaman, Mr. Farrukh,Mr. Safdar, for providing good environment in Jeju.

I am also grateful for the Regional Instrument Center (RIC) at Jeju National University for providing me opportunities to handle many instrument facilities during my study and I thank Mr. Ko at RIC for their cheerful assistance in the work. Many thanks to Graduate school of Jeju University for their generous support in waiving the tuition fee for my doctoral studies.

My thanks from the bottom of the heart are to my sister's and grandfather's family who had taken over my responsibilities in my home and supported me to achieve my goal.

I would like to thank all those whom I have not mentioned above but helped me in numerous ways to my success.

Contents

List of Figures

List of Tables

Abstract

Electrohydrodynamic atomization (EHDA) is a new and emerging technology in the field of functional thin films. This process is capable of producing organic, inorganic and composite thin films on various substrates using solution based materials. The process parameters for achievinguniform and void free surface nature of thin films via Taylor cone formation are discussed in detail. Achieving the Taylor cone mainly depends upon the two main parameters such as process parameters (flow rate, applied potential, stand-off distance and nozzle diameter, etc.) and physico-chemical properties of precursor solution or inks. The deposition of thin films is achieved at room atmospheric conditions with less time period. In this dissertation, a detailed deposition and spectroscopic analysis of semiconducting polymeric materials, transition metal oxides and one dimensional silver embedded polymer matrix thin film on flexible and non-flexible substrates via EHDA.

In the first phase, development of poly(3,4ethylenedioxythiophene):poly(styrenesulfonate) (PEDOT:PSS) and multi-layered poly(3-hexylthiophene): poly(6,6-Phenyl C_{61}-butyric acid methyl ester) (P3HT:PCBM)/ PEDOT:PSS thin films on flexible polyethylene terephthalate (PET) substrate. The properties and process parameters of inks for achieving stable cone-jet are clearly explained through operating envelope.Crystallinity, surface morphology, film purity of deposited thin films is investigated to determine the film homogeneity and chemical compositions. Further, the optical and electrical properties of thin films are examined in terms of film transmittance, absorbance, sheet resistivity and diode behavior.

The nanostructured metal oxides thin films such as titanium (IV) oxide (TiO_2), zinc oxide (ZnO) and nickel oxide (NiO) are deposited on non-flexible substrate. The precursor solution of the respective metal oxides inks are prepared via wet chemical process using starting precursors with suitable surfactant to achieve a stable precursor solution or inks. Operating envelope of atomization process is varied with respective precursor solution. The film crystallinity, surface morphology, chemical composition and optical properties confirm the nature of thin films. Optoelectronic properties of ZnO are investigated by measuring the current density under the UV light illumination. In addition, electrochemical behavior of NiO thin film is analyzed by measuring the current values under redox reaction via cyclic voltammetry.

Utilizing EHDA process, the development of one dimensional nanostructured metal intercalated with polymer matrix is achieved for transparent conductive electrode applications. Here, we demonstratethe fabricationof silver nanowires embedded PEDOT:PSS matrix on flexible substrate. The optimization of flow rate and applied potential for achieving uniform thin film via Taylor cone formation are discussed in detail. The crystallinity, surface morphology and nature of chemical bonding of the as-deposited thin films are investigated. The optical and electrical studies reveal high transparency in the visible region and lower sheet resistance of the AgNWs/PEDOT:PSS thin films. These results indicate that the AgNWs embedded PEDOT:PSS is a key factor to enhance the film conductivity without any loss of optical properties which may create new horizon in their potential applications in optoelectronics. The unique advantage of EHDA technique play a significant role in the manufacture of functional thin films based printing devices at room atmospheric conditions and hence, it will create a new horizon in coating industry.

1.Introduction

1.1Thin film

The unique and intriguing properties of functional thin films are one of the highly exploiting researchfields in science and technology. Functional thin film technology could be referred to as old wine in the new bottle. Thin films are derived from the layer of different materials whose thickness ranges from few nanometers to several micrometers. Thin films are directly deposited on the substrates to achieve a better physico-chemical property than that of bulk materials. The deposited functional thin films are of significant interest in optical coatingand electronic industries.The surface engineering of functional thin films has a great impact on the physico-chemical properties of nanostructured thin films such as crystallinity, film thickness, surface morphology,optical properties, chemical compositions, surface purity and electronic transportations. The presence of two interfaces namely, air−thin films interface and film−substrate interface can induce the preferential orientation in deposited thin films. The interfacial energy between thin film and substrate has been altered by substrate treatments for achieving uniform orientations of nanostructured materials. Thin films are commonly used in several applications such as solar cells, light emitting diodes, anti-reflective coating, memory storage, supercapacitors, thin film transistors, wireless sensors, anti-corrections and paint industries(Jorgensen et al. 2011, Paul et al. 2010 and Nagashima et al. 2009). On the other hand, multilayer or composite based nanostructured thin films have tunable physico-chemical properties, which are significantly used for multifunctional applications such as light emitting transistors, light emitting memristors, radio frequency identification based sensors, and

electronic tattoos based bio-integrated devices (Yao et al. 2012, Hyeong et al. 2011, Hyeong et al. 2012 and Mannoor et al. 2012) .

Inorganic based nanostructured thin films playpivotal role in conferring exceptional chemical, electrical, optical properties and its potential applicationin diverse field.Pure and doped metal oxides such as nickel oxide (NiO), zinc oxide (ZnO), zirconium oxide (ZrO_2), iron oxide (Fe_2O_3), magnesium oxide (MnO_2), molybdenium oxide (MoO_3/Mo_2O_5), aluminum or nitrogen doped zinc oxide (AlZnO/NZnO) and silver doped titanium oxide ($AgTiO_2$) etc, can be employed fordifferent applications (photovoltaic, conductive electrode, resistive switching, bio/chemical sensors, self-cleaning, antibacterial activity and photo-catalysis) with respect to their physico-chemical and structural properties of thin films (Fortunato et al. 2012, Kim et al. 2012 and Cheng et al. 2005). On the other hand, one dimensional and two dimensional nanostructured thin films such as silver, copper nanowires, carbon nanotube graphene/graphene oxide and MoS_2 nanosheets are also having fabulous role in the current potential applications(Madaria et al. 2011, Radisavljevic et al. 2011 and Kaempgen et al. 2009).

The organic or polymer based thin films are also widely used these days. The organic polymers have tunable band gap, electron delocalization along with their polymer backbone andso enabling low-cost manufacture of large scalethin films. Additionally, polymer based materials havegood compatibility with flexible substrates(Wang et al. 2011 and Christos et al. 2002).In organic polymer, the charge transfer mechanism can occur via π- bond especially by hopping, tunneling and related mechanism. Molecular semiconductors such as conjugated polymers, small molecules and organic dyes are of very much interestfor thin film based electronic and biological applications. Usually, organic materials have lower conductivity as compared with inorganic metals due to weak electron mobility. This can be overcome by

introducing several doping materials such as fullerene derivatives or one dimensional nanostructured materials of silverand copper etc.These materials can easily intercalate with polymer matrix to enhance their electronic and optical properties of organic thin films(Yu et al. 2011, Boucle et al. 2007 and Kim et al. 2012). However, in order to achieve a flawless orientation of single or multilayered thin films for device fabrications, suitable thin film process is needed to deposit the nanostructured thin films on different substrates (silicone, glass, flexible and stretchable substrates).

1.2 Conventional deposition technique

The process engineering of functional thin filmdeposition is significantly varied with respect to physico-chemical properties of materials and device fabrications. Thin film deposition is classified into two ways

- Physical process
- Chemical process

Physical process of thin film fabrications are mainly depends on the evaporation or ejection of different materials from the respective sources. This process mainly consists of evaporation, sputtering techniques e.g. physical vapour depositions, vacuum evaporation, and electron beam evaporation etc. On the other hand, deposition of thin films through chemical methods mainly depends upon the definite chemical reactions and physical properties of materials. Typical chemical process are electroplating, chemical reduction plating, vapour phase depositions and precursors ingredients e.g. thermal growth, chemical vapour depositions and plasma enhanced vapour depositions etc,(Gupta et al. 2004, Penga et al. 2003, Teixeira et al. 2009 and Choi et al. 2005).

1.2.1Physical vapour deposition (PVD)

PVD process comprises the standard technologies for deposition of nanostructured materials. This process consists of the following sequence of steps:

- The deposition of solid material is physically converted into vapour phase
- The vapour phase material is transported across a region of reduced pressure from the source to substrate target
- The condensation of vapour on the substrate to achieve a uniform thin film

The initial phase conversion from solid to vapour is done by adding of heat in the evaporation deposition. This process is used to utilize any type of inorganic and some organic materials for achieving uniform surface coatings. The main drawback of PVD technologyis typically operate at very high temperature, vacuum, required cooling water system to dissipate large heat loads and need attention to operate the system due to process complexity.

1.2.2 Sputtering

Sputtering is a process in which the material is ejected from the source at low temperature as compared with evaporation process. The desired material is bombarded with energetic particles; it is possible to cause ejection of the surface atom. The ejected atoms undergo condensation on to a substrate to form thin film. The basic principle of sputtering is the same for all type of sputtering technologies such as ion-beam sputtering, reactive sputtering and gas flow sputtering etc (He et al. 1998 and Kelly et al. 1996).This method has better advantages over normal evaporation techniques in which no more impurities will occur. This technique is used to deposit the metals, alloys, superconducting and magnetic materials. This process has comparatively

slower reaction rate than that of thermal evaporation technique. Sputtering targets are often expensive. Most of the energy incident on the target becomes heat, which must be removed.

1.2.3 Chemical vapour deposition

Chemical vapour deposition (CVD) is a chemical reaction takes place in the vapour phase. The reaction undergoes condensation to form a solid thin film on surface of substrate. The chemical reaction of precursor materials is an important characteristic of this method. Therefore, the reaction rate and starting precursors or reactants must be well understood to attain homogeneous thin film on desired substrate. There are different types of CVD process exists such as low plasma enhanced CVD (PECVD), low pressure CVD (LPCVD) and oxidative CVD etc. The CVD process produces thin film with good uniformity and desired film thickness. In CVD process, different materials can be used for thin film deposition such as silicone, CNTs, graphene, high dielectric based materials (Al_2O_3, HfO_2, ZrO_2), metal carbides and nitrides. The main drawback associated with CVD process is that it requires high temperature with controlled environment and expensive equipment.

1.2.4 Atomic layer deposition

Atomic layer deposition (ALD) is a method to deposit thin film on several substrates with atomic scale precision. The chemistry of ALD process is almost similar as that of CVD process but the rate of reaction in ALD process is two steps, in which it breaks the CVD process into two half by keeping the starting precursors separatelythroughout the process. ALD film growth is self-limited by exposing the precursors to the growth surface repeatedly, which make uniform thin films. There are four main types of ALD reactors exist such as closed system chamber, open system chamber, semi-closed system chamber and semi-open system chamber. The atomic layer thickness in ALD process has uniformly controlled by adjusting the flow rate of precursors, rate

of chemical reaction on desired substrate and the number of deposition cycles. ALD process is widely used to deposit high –k dielectric materials, semiconductor memory, barrier layer (TiN, TaN) and deposition in porous structures. The main drawback of ALD process is that the reaction rate of ALD is slower than CVD process, requires very high vacuum system and also limited thin film growth by activation energy.

The above mention techniques are widely used for obtaining uniform deposition of thin film with desired film thickness. Hence, choice and selection of deposition process play energetic role in the formation of excellent quality of nanostructured functional thin films for large scale production with all desired physico-chemical properties. The selection of particular technique should be satisfied the following aspects

- Controlled Microstructure of thin films and deposition rate
- Deposition takes place at low temperature
- Easy to control the film thickness with desired materials properties
- Environmental friendly technique
- Cost effectiveness
- Large scale production
- Applicable to different substrates

With this motivation, we employed the new technique of electrohydrodynamic atomization (EHDA) in the present investigation.

1.3Electrohydrodynamic atomization technique

Electrohydrodynamic atomization (EHDA) technique holds more promises toward the deposition of functional thin films on different substrates (flexible, non-flexible and stretchable) and also

possesses several advantages such high speed, solution process, controlled film thickness and large scale production(Hayati et al. 1986 and Choi et al. 2013).In EHDA, when precursor solution or ink is supplied to the nozzle without applying electric field, a hemispherical meniscus is appeared at the nozzle tip (figure.1-1a). When the electric filed is applied over the liquid droplets, which lead to induce the surface charges in a liquid meniscus. At strong electric potential, the liquid droplets tend to overcome the liquid surface tension and deform into a conical shape, which is called as Taylor cone or stable cone-jet (figure.1-1b). Taylor is the first derived the stable-cone-jetusing analytical background in the atomization process. The shape of the Taylor cone is a result from the force balance of surface tension, gravity, applied electric potential in the liquid surface. The observed Taylor cone or stable cone-jet is essential for the production of atomized fine droplets in the rage of nanometer to micron-scale size, which is directly deposited on the desired substrate accompanied by the evaporation of solvents. Assuming a positively charged metal capillary tends to attract the negatively charged ions in the solution and the presence of positively charged ions leads to surface instabilities due to excess of positive ions to form fine droplets. The charged droplets transport onto the ground electrode, where the positive ions are reduced. This phenomenon is clearly explained in the figure.1-2. In EHDA, there are different mode is observed during atomization process of precursor solution or ink such as dripping, micro-dripping, unstable cone-jet, stable cone-jet and multi-jet. Usually, each mode is observed and sustained within a certain range of applied potential with respect to flow rate, stand-off distance between the spray nozzle tip and substrate, nozzle used and physico-chemical properties of the respective inks.

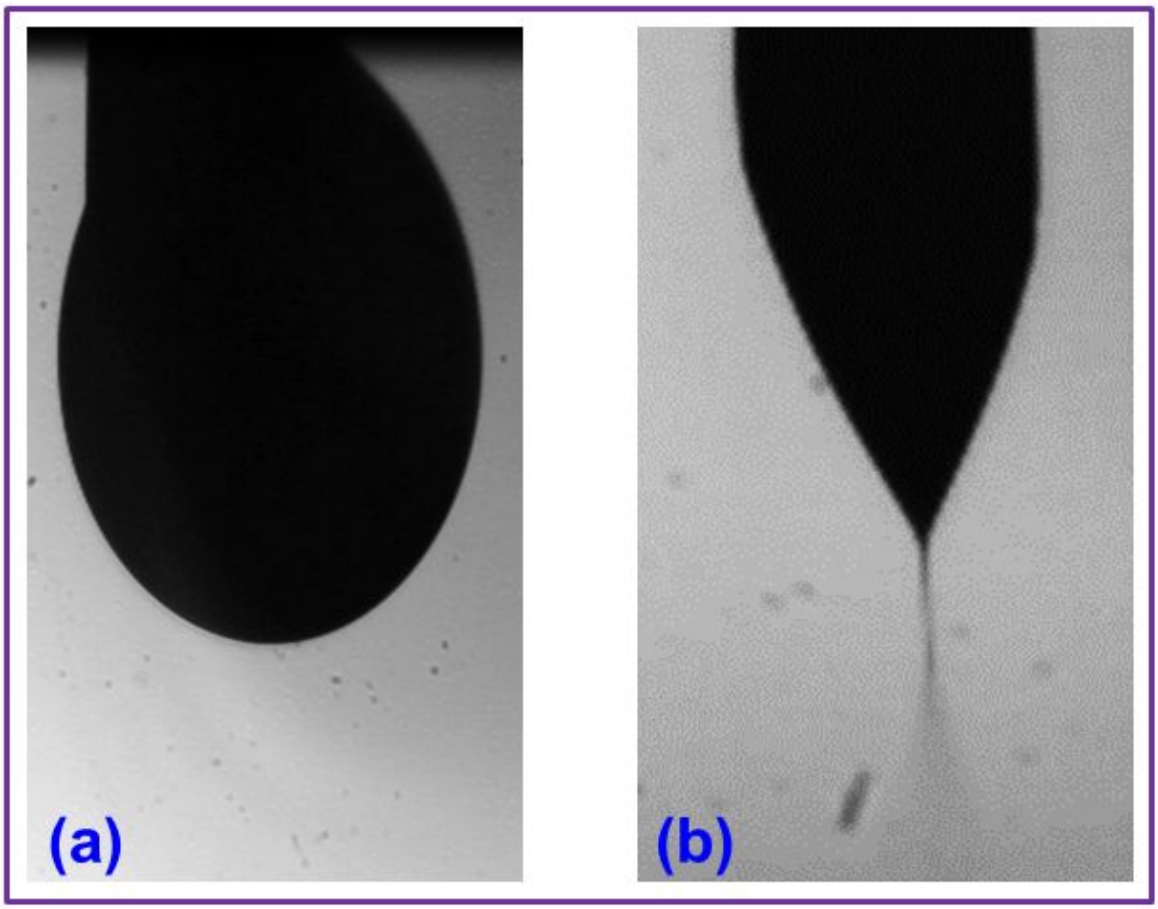

Figure 1-1 Atomization mode: (a) dripping, (b) Taylor cone

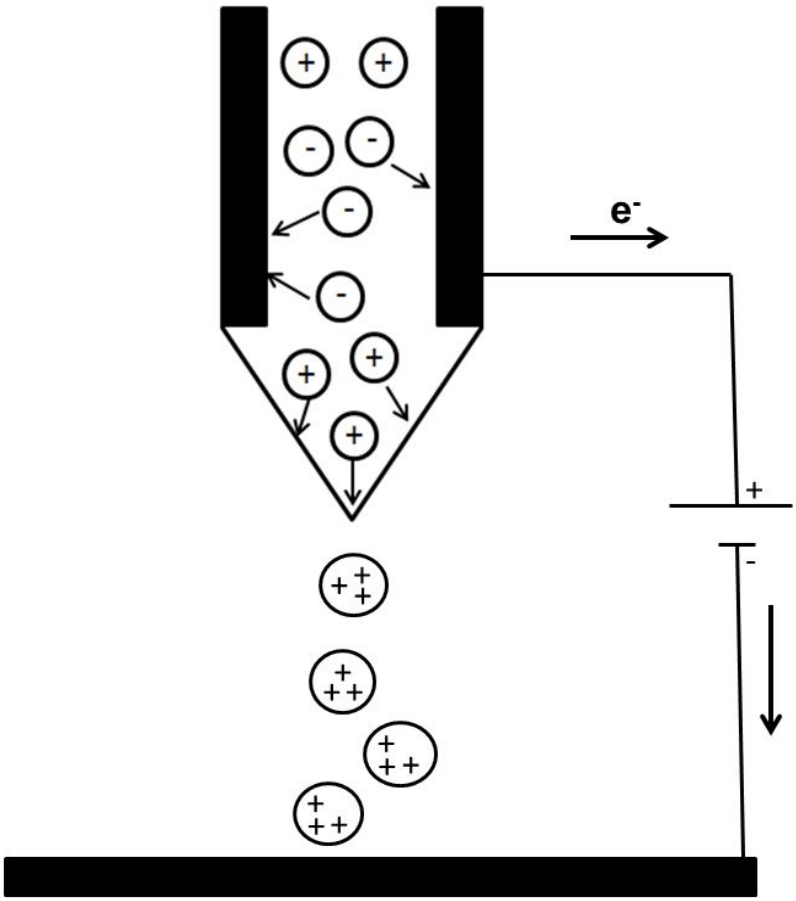

Figure 1-2 Block diagram of atomization process phenomenon

1.3.1 Atomization mode

(i) Dripping mode

The first step appearing in the EHDA is a dripping mode. The dripping mode is observed only by given flow rate without electric potential onto the liquid. The size of the droplets is almost same or larger than that of the nozzle tip. The drops are observed as regular sphere detaching from the nozzle capillary as the weight of the drop overcome the capillary forces.

(ii) Micro-dripping

In micro-dripping, the liquid flow tends to form a stable meniscus at the end of nozzle tip with respect to applied potential. The droplet size is much smaller than nozzle diameter. Herein, dripping mode is changed into micro-dripping mode in the presence of applied potential. A clear difference between the dripping and micro-dripping mode is the formation of Taylor cone. In the dripping mode, observed droplet is falling down without forming Taylor cone due to lack of applied potential but in case of micro-dripping mode, it undergoes further elementary process with the influence of applied potential.

Spindle mode is observed from the liquid meniscus under the influence of electric potential. Herein, the liquid meniscus elongate in the direction of applied potential and detaches as a massive spindle like fragment of liquid. This type of mode is called as spindle mode. In spindle mode, ejection of liquid droplets is in different sizes, hence, resulting in poly-dispersity of liquid droplets. This mode is completely differs from the dripping mode,where ejection of irregular droplets size from the meniscus is occurred. This mode is significantly controlled to avoid the jet irregularity during the atomization process.

(iii) Unstable cone-jet

Unstable cone-jet mode is exhibit when the applied potential is not enough to permanently overcome the liquid surface tension but these potential is enough to overcome the surface tension temporarily. The instability of cone-jet is also ejecting the number of droplets but the droplets are not in mono-dispersed nature due to the insufficient applied potential.

(iv) Stablecone-jet or Taylor cone

This is the most important atomization mode in EHDA process. Stable cone-jet is the results of precursor solution or ink forms a regular, axisymmetric cone with a uniform thin jet at nozzle tip.

The ejection of cone assumed that the three different forms (liner sides, convex or concave) according to Cloupeau and Prunet-Foch 1994.The cone-jet mode produces the charged droplets due to the influence of electric force. However, the ejection of charged droplets from the cone-jet is mainly depends upon the flow rate and applied potential. When the flow rate or applied potential has been increasedbeyondcertain limit, then the cone-jet did not break up due to axisymmetric or varicose instabilities. In this case, jet breaks only due to lateral or kink instabilities. Herein, the ejection of cone-jet and charged droplets (main and secondary droplets) does not follow the capillary axis or straight line in the atomization process. But in case of varicose instabilities, the cone-jet and ejection of monodispersed charge droplets do not leave from the capillary axis during the atomization process. Therefore the ejection of stable cone-jet followed either varicose instabilities or kink instabilities are mainly depends upon the liquid flow rate and applied potential.

(v) Multi-jet

Multi-jet is the spraying mode for ejection of charged droplets at higher production rate. By increasing the applied potential, the cone-jet mode is deformed into multi-jet. It is theoretically possible to produce a monodispersed charged droplets but in practical, the mondispersity of droplets are very difficult to control than that of cone-jet mode due to ejection of more number of spraying points instead of one under the influence of applied potential and nozzle diameter.

In EHDA, the above mentioned modes of atomization exist. However, the stable-cone jet or Taylor cone is the most important atomization mode for achieving homogeneous functional thin films due to ejection of monodispersed charged droplets under the influence of applied potential

and flow rate in a controlled manner. Samarasinghe et al. 2008 and Jaworek. 1999havediscussed the detailed deposition of functional thin films under the influence of stable-cone jet mode.

1.3.2 Parameters influencing the cone-jet

In EHDA, the cone-jet mode is significantly influenced by operating parameters and physico-chemical properties of precursor solution or ink

(i) Operating parameters

a) Flow rate

Flow rate has significant effects on cone-jet and size/width of the charged droplets with constant physico-chemical properties of ink. When the flow rate increases, the applied potential on the liquid cone increases, which is due to acceleration of liquid in the cone-jet at high flow rate. At high flow rate, the ejection of charged droplets with larger diameter is occurred due to formation of larger diameter of cone-jet with high applied potential. With an increasing flow rate, the jet diameter and kinetic energy of cone-jet increase and the jet break up due to kink instabilities. At minimum flow rate, the formation of cone-jet with smaller diameters and the jet break up into smaller charged droplets due to axisymmetric instabilities.The resulting smaller diameter of droplets with respect to just above the minimum flow rate and applied potential is of very much interest in the fabrication of nanoscale functional thin films through EHDA process.

b) Applied potential

The applied potential (electric field) is essential parameters in the atomization process. The above mentioned modes of atomization are occurred by the influence of applied potential at constant flow rate and ink properties. However, the applied potential has less effect on the jet diameter as compared with flow rate. The applied potential is varied with respect to flow rate for

achieving stable cone-jet. In case of low flow rate at high applied potential, the jet disintegrates into mist of smaller droplets for deposition of nano/micro sized functional thin films, which is also known as electrospray atomization process (figure.1-3).

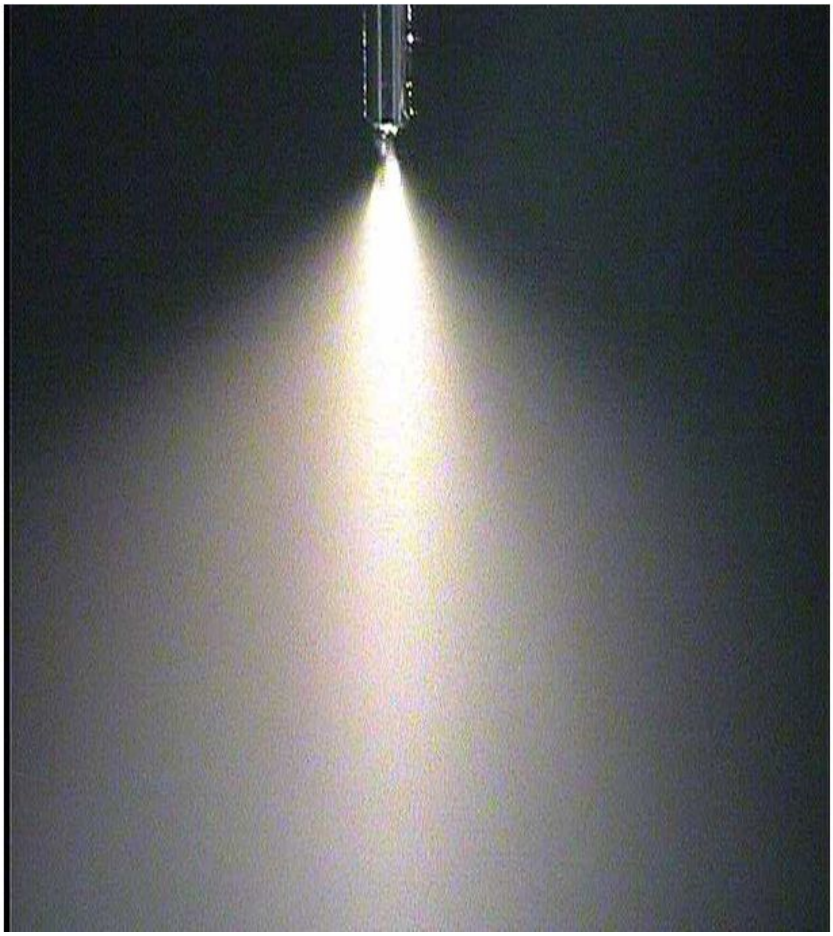

Figure 1-3 Electrospray atomization process

c) Stand-off distance

The distance between the nozzle tip and the substrate is called as stand-off distance. The flying time of monodispersed droplet and the rate of solvent evaporation are periodically controlled by stand-off distance. The rate of solvent evaporations havevery important role for achieving porous free thin films. In case of methanol, ethanol and isopropanol have a low boiling point (<80 ^{o}C),

which is very easy to evaporate at minimum stand-off distance but in case high boiling point solvents such as dichlorobenzene, dimethyl sulfoxide and N-methyl-2-pyrrolidone are not so easy to evaporate at minimum stand-off distance due to high boiling point. In order to evaporate these solvents, the stand-off distance should be higher.

d) Nozzle diameter

Nozzle diameter has a role of determining the shape and diameter of stable-cone with flow rate and applied potential. Smaller diameter of nozzle leads to eject the smaller droplets during atomization process and also limit flow rate. Achievinga stable cone at smaller diameter of nozzle is very easy when compared with larger diameter at minimum applied potential. The diameter of nozzle has been changed according to the spray area or patterns for different thin films and device applications.

(ii) Properties of ink

The above mentioned process parameters are significantly varied with respect to the properties of ink such as electrical conductivity, surface tension and viscosity.

a) Electrical conductivity

The electrical conductivity is an important parameter during the atomization process. Increase with precursor solution or ink conductivity, the current increases. The results of high surface charge density with good kinetic energy of cone-jet. The liquid which have good electrical conductivity can easily achieve a Taylor cone to overcome the surface tension of respective ink at lower electric field. On the other hand, the low conductivity inks need high electric field to

achieve a stable cone-jet due to weak polarization of ink. Non-polar based precursor solution or inks are not suitable for EHDA process due to lack of polarization.

b) Surface tension

The surface tension of solution is one of the parameters which influence the atomization process. In EHDA, the applied potential increases with respect to surface tension of respective inks to attain a conical shape of jet. The inks possessing low surface tension are very easy to spray at low applied potential but in case of water based inks such as PEDOT:PSS ink, it is very difficult to spray due to high surface tension, affects cone-stability. In order to achieve a stable cone-jet, the water based inks are modified by adding suitable co-solvents to reduce the surface tension of respective inks (Hartman. 1998).

c) Viscosity

Viscosity of precursor solution or inks has a little influence on the atomization process. The jet length increases with the increase of viscosity. However, the jet break up also becomes slower with respect to ink viscosity. The high viscosity based cone-jet is more suitable for patternsdue to longer cone−jet (Shigeta et al. 2012) but in case of spray process, low viscosity of inks are more suitable for thin film deposition due to jet breakup at smaller time period.

The above mentioned properties of precursor solution or ink are periodically influenced by chemical structure of desired materials and solvents. The chemical structures such as molecular geometry, electronic structure, crystal structure of molecules and solvents natures (polar, semi polar and non-polar) are directly influence theink properties.

1.3.3 Experimental setup of EHDA

The basic schematic and experimental setup of EHDA are shown in figure.1-4 and 1-5. The precursor solution or ink was filled in the syringe (Hamilton, model 1001 GASTIGHT syringe), which was driven by a syringe pump (Harvard Apparatus, PHD 2000 Infusion). The syringe was connected to the capillary nozzle holder via a Teflon tube. A stainless steel nozzle (NanoNC) was fixed at the bottom of a nozzle holder. A high potential was applied between the nozzle and the copper plate (ground) using a high-voltage DC power source (NanoNC, 30 kV) and the substrate (glass) was mounted on the copper plate. The movement of the substrate and nozzle holder could be controlled via the *x*-, *z*-axis stage and the *y*-axis stage, respectively. The whole experimental process was monitored by using a CCD camera (MotionPro X) which was interfaced with a high-performance PC.

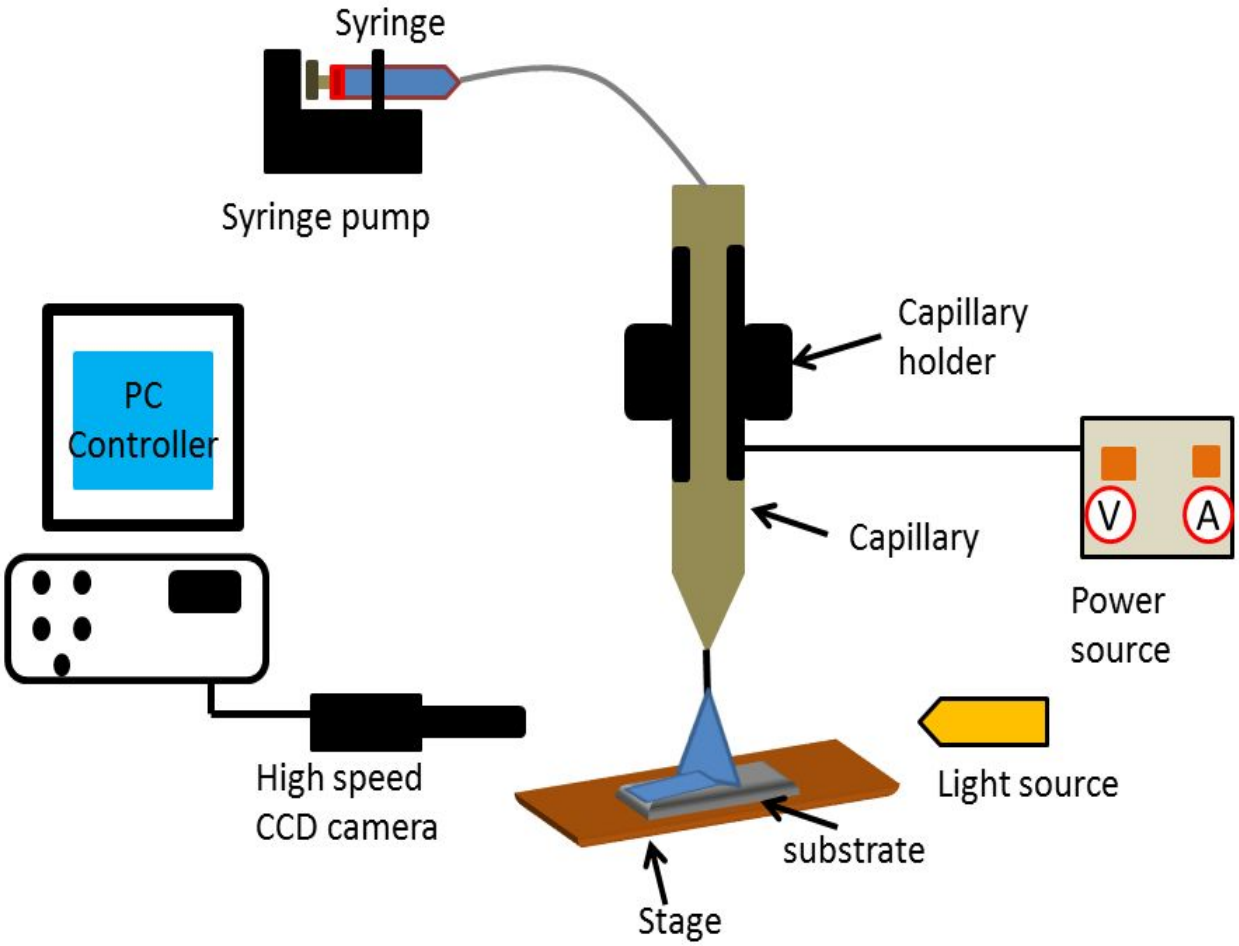

Figure 1-4 Schematic picture of EHDA

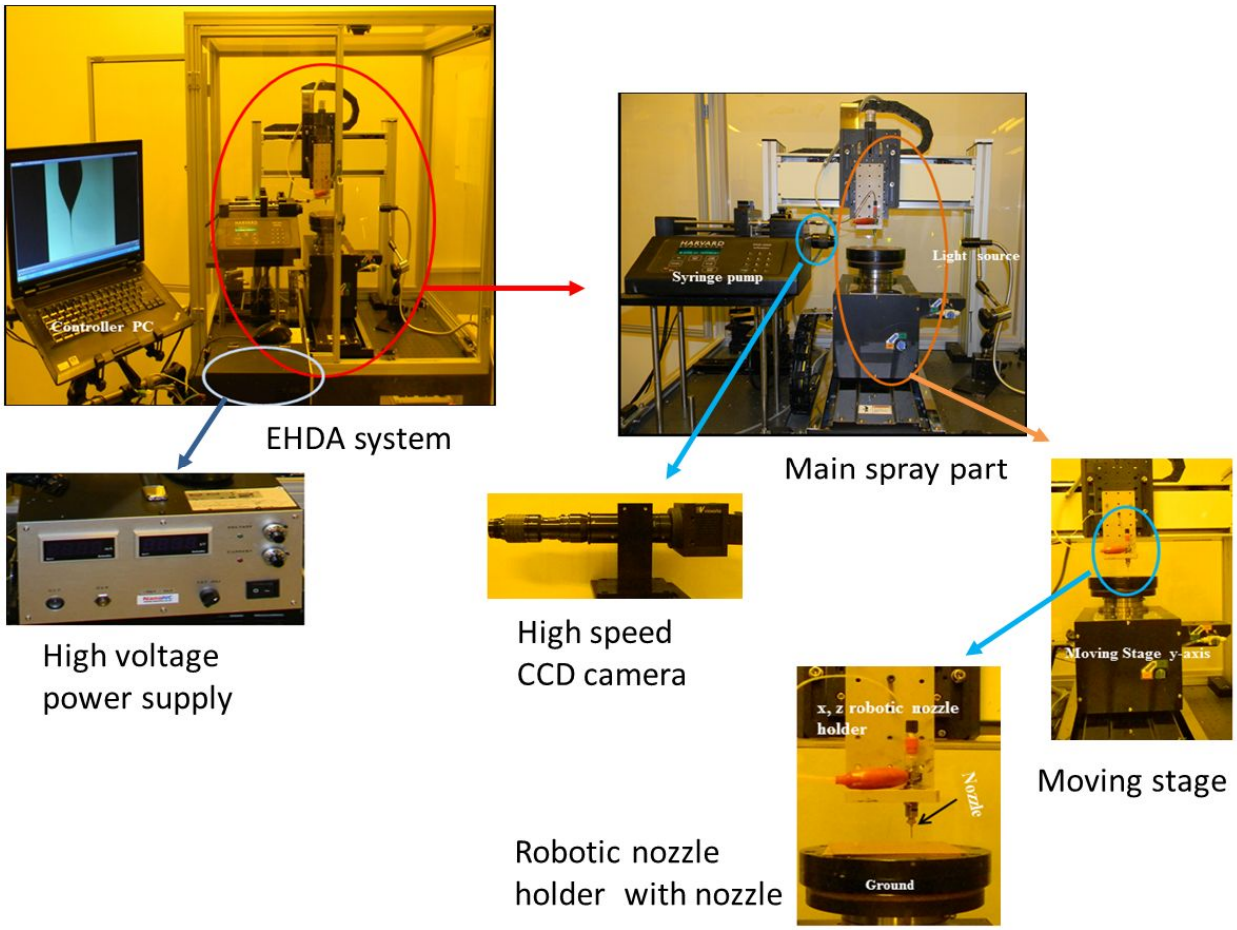

Figure 1-5 Experimental setup of EHDA

1.4 Focus of current research

Current research is mainly focused on the investigation of the properties of nanostructured functional thin films deposited via EHDA techniques towards multifunctional applications. Scheme 1 represents the focus of the current research work done in brief.

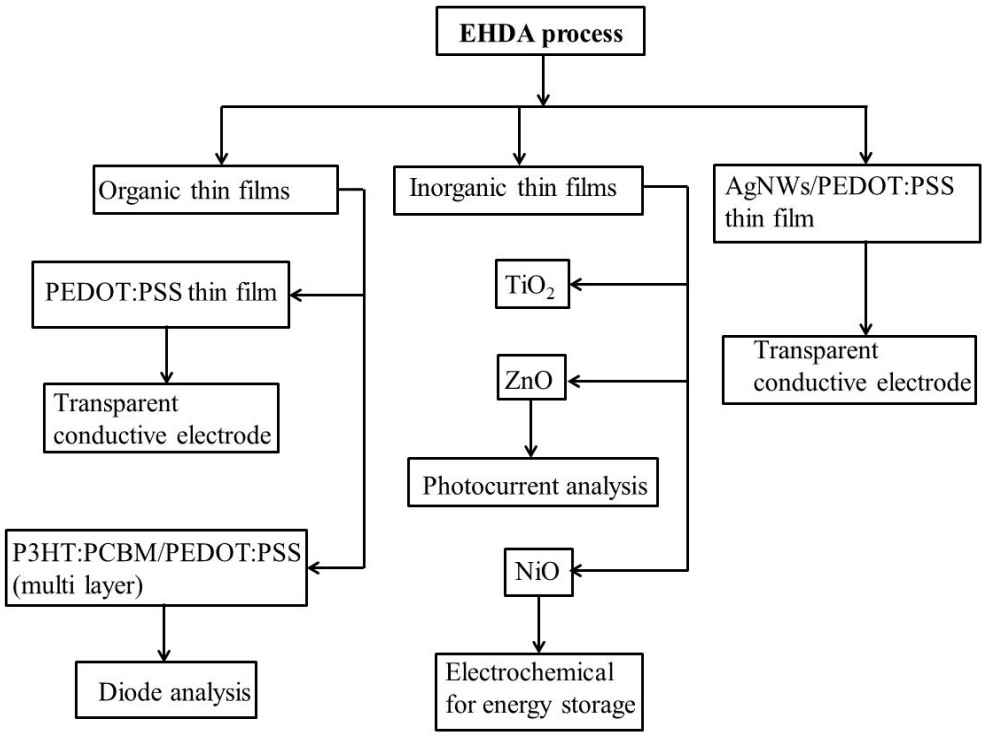

Scheme 1. Focus of current research work

Briefly, nanostructured functional thin films are fabricated through EHDA technique on different substrates. The organic polymer of poly(3,4-ethylenedioxythiophene) poly(styrenesulfonate) (PEDOT:PSS) has deposited on flexible PET substrate using modified PEDOT:PSS ink. Achieving Taylor cone at constant flow rate and applied potentialare discussed in detail. The chemical structure, optical and electrical properties of deposited PEDOT:PSS thin film are

investigated via FE-SEM, Raman analysis, UV-vis analysis and current−voltage (*I−V*) analysis. The deposited PEDOT:PSS thin film is applicable inoptoelectronics.

The multi-layer thin films such as P3HT:PCBM and PEDOT:PSS deposited on indium tin oxide (ITO) coated PET substrate. The selection of suitable co-solvents for preparation of composite ink (P3HT:PCBM) and fabrication of multi-layers (P3HT:PCBM/PEDOT:PSS) through EHDA process are clearly investigated. The X-ray diffraction, FE-SEM, FT-IR and optical analysis have been employed to understand the chemical and structural investigation of P3HT:PCBM. Further, the electrical study revealed that the diode analysis and capacitance properties of multi-layer.

We then focus on the energy related application using inorganic nanostructured thin films deposited via EHDA technique on glass and conductive substrates. Titanium oxide (TiO_2), zinc oxide (ZnO) and nickel oxide (NiO) are deposited on glass substrate using precursor solution. The optimum physical properties of precursor solution has been investigated and used for thin film fabrications. The crystallinity and surface morphology is investigated through XRD and FE-SEM analysis. The X-ray photoelectron spectra and FT-IR analysis revealed the chemical composition and purity of nanostructured functional thin films. The optical transmittance and energy band gap of deposited metal oxide thin film are clearly examined through UV-vis analysis. Further, the *I−V* analysis of revealed the sheet resistivity of TiO_2 thin film, which is well known material for electronic industries. Further, the photocurrent behavior of ZnO thin film is measured by the UV-assisted current−voltage analysis, suggesting ZnO has a potential application in optoelectronics. The unique electronic properties of inorganic materials show promising application in the energy storage devices. We evaluated the electrochemical properties of nanostructured NiO thin film for their application in energy storage devices.

Utilizing nanostructured composite thin film on the road to the development of large scale deposition of transparent conductive electrode via EHDA process are rapidly increasing in the field of printed electronic industries. In this regards, we demonstrated the fabrication of silver nanowires (AgNWs) embedded PEDOT:PSS thin film on flexible substrate by EHDA process using AgNWs/PEDOT:PSS ink. The fabricated AgNWs/PEDOT:PSS film shows good NWs intercalated polymer matrix with high quality of thin films. We also studied the optical and electrical properties of thin film for transparent conductive electrode application.

Overall the research work aims at understanding the basic phenomenon of functional thin film deposition via EHDA technique and focused on the multifunctional application in electronic industries such as transparent conductive electrode, optoelectronics, and energy storage devices.

2. Organic thin films

This chapter provides the detailed deposition of organic polymeric thin films on flexible PET substrate through EHDA process. The detailed structural, optical and electrical properties of deposited single or multilayered polymeric thin films are investigated in detail.

2.1 Deposition of PEDOT:PSS thin film

A π- conjugated conducting polymer of PEDOT (poly(3,4-ethylenedioxythiophene)) carries very much interest in organic optoelectronics because of its good optical transparency, high electrical conductivity and excellent stability (Burroughes et al. 1990). PEDOT has many applications in solar cells, light emitting diodes, sensors and thin film transistors (Yong et al. 2011, Stephan et al. 2005 and Marcus et al. 2002, Burroughes et al. 1990). Usually the pure form of PEDOT is insoluble in most of the solvents. This problem is overcome by introducing water soluble polymeric material of poly(styrenesulfonate) (PSS). The PSS polymer has the ability to attain equilibrium with cationic charge of PEDOT under polymerization process to generate PEDOT:PSS complex with homogeneous dispersion of PEDOT in water (Nardes et al. 2008).

Conventionally, the fabrication of thin film are achieved through dip and spin coating, chemical vapor deposition, physical vapor deposition and atomic layer deposition etc. (Youn et al. 2011 and Marin et al. 2009). These techniques produce good quality film but are expensive and have certain intricacies involved with them (Ganan-Calvo et al. 1997 and Jaworek et al. 1999). Therefore the development of new techniques such as electrohydrodynamic atomization (EHDA) becomes more relevant for thin film deposition (Hartman et al. 2000) as it offers simple process,

low cost and enables large area printing under ambient conditions. In addition to that, the working mechanism of EHDA is discussed in detail by Hayati et al in (Hayati et al. 1986).

In this investigation, commercially available PEDOT:PSS is modified by adding isopropanol to make it suitable for electrospray deposition on polyethylene terephthalate (PET) as a substrate. A field emission scanning electron microscopy is used to determine the surface morphology and thickness of the fabricated thin film. Transparency and electrical properties of deposited film have been characterized through UV-vis spectrum and current-voltage (*I–V*) measurements.

2.1.1 Materials and methods

2.1.1.1 Materials used

PEDOT:PSS (Orgacon) was purchased from Agfa Materials Japan Ltd, Japan. Isopropanol ($(CH_3)_2CHOH$) was obtained from Sigma-Aldrich, South Korea. Silver nanoparticle ink was received from NPK Ink Ltd, South Korea.

2.1.1.2 PEDOT:PSS ink preparation

In EHDA technique, the stable cone-jet is achieved when the electric stress overcomes the surface tension of the liquid meniscus at the end of the capillary (Choi et al. 2012). Liquids with high surface tension (e.g. H_2O) are very difficult to electrospray (Ijsebaert et al. 2002). Hence, water based inks are usually modified by adding suitable alcoholic co-solvents to reduce the surface tension of the inks (Erika et al. 2006). Based upon this phenomena PEDOT:PSS was modified by using isopropanol as a co-solvent to achieve low surface tension (figure 2-1a).

PEDOT:PSS ink was prepared by diluting (2.3 wt.%) PEDOT:PSS with 5 ml of isopropanol (2:1w/w) and stirring for 20 min at 1500 rpm. Then 2 ml of deionized-water was added drop by drop and stirring was continued for 2 h under ambient conditions. The obtained solution was

filtered through the polymeric filter (PTFE – 0.45 µm) to achieve homogeneous dispersion of modified PEDOT:PSS ink as shown in figure 2-1b. The physical properties of modified PEDOT:PSS ink are given in Table 2-1.

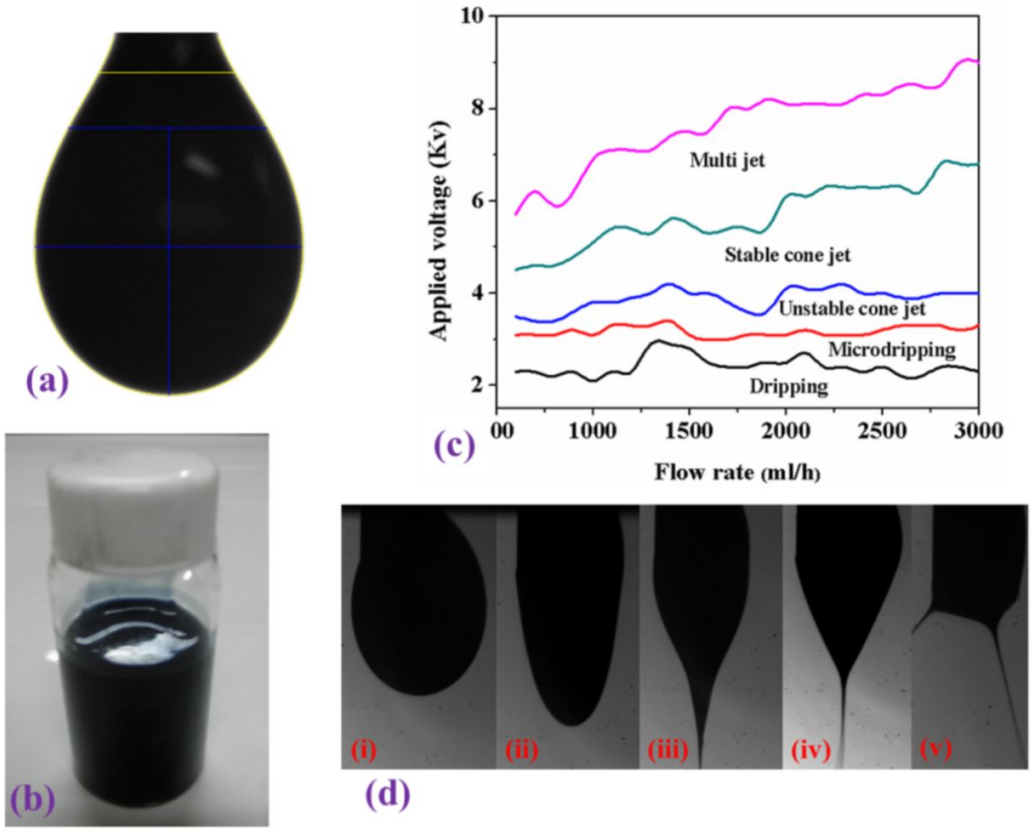

Figure 2-1 (a) Surface tension analysis of PEDOT:PSS ink, (b) photographic image of modified PEDOT:PSS ink, (c) operating envelop of PEDOT:PSS ink by using EHDA, (d) modes of atomization: (i) dripping, (ii) micro dripping, (iii) unstable cone jet, (iv) stable cone, (V) multi-jet

Physical properties	Values
Viscosity	114 mPa S
Electrical conductivity	7.2 μS cm^{-1}
Surface tension	14mN m^{-1}

Table 2-1 Properties of modified PEDOT:PSS ink for EHDA technique

2.1.1.3 Fabrication of PEDOT:PSS thin film

Before to the deposition of PEDOT:PSS, the substrates were treated with plasma in order to confirm the possibility of improving the adherence of PEDOT:PSS with the substrate. The modified PEDOT:PSS solution made a large contact angle of 72^{o} (figure 2-2a) on untreated polyethylene terephthalate (PET) substrate. The large contact angle caused reduced adherence between ink and substrate due to lowered wetting. The same substrate when treated with oxygen (O_2) plasma showed contact angle of 47^{o}(figure 2-2b) with the above solution. The reduced contact angle leads to improved wetting, which in turn improved the adherence of the thin film on substrate. Therefore it can be said that contact angle also plays a role in thin film deposition. Later on, thin film deposition of PEDOT:PSS was carried out on plasma treated PET substrates through EHDA technique at ambient conditions. During EHDA process, the stand -off distance between metallic nozzle and the substrate (PET) was maintained at 15 mm with the substrate

velocity of 8 mm/sec to achieve uniform deposition and the film were sintered at 110 ^{o}C for 10 minutes after deposition.

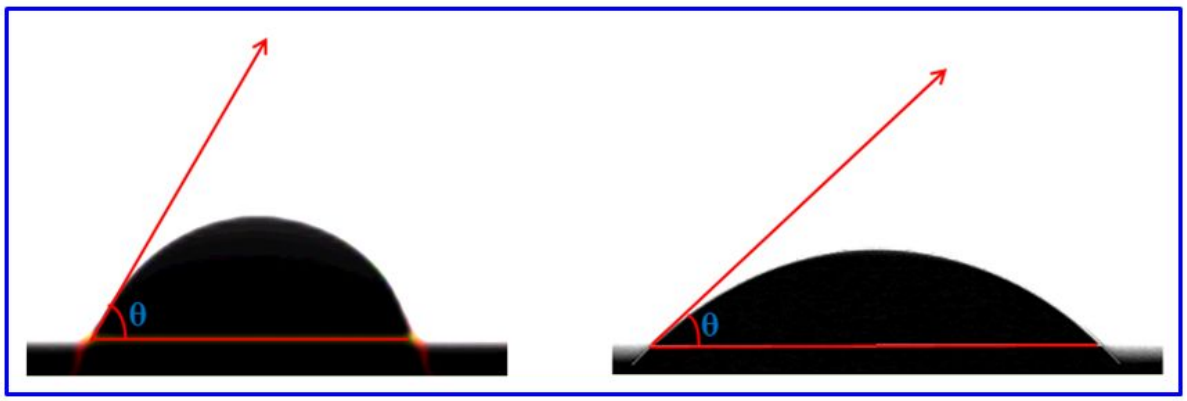

Figure 2-2 Contact angle of PEDOT:PSS solution (a) untreated PET substrate, (b) oxygen plasma treated PET substrate

2.1.1.4 Instrumentation

The electrical conductivity of the PEDOT:PSS ink was measured by a conductivity meter (EUTECH Instruments, ECOSCAN CON 6). The surface tension of the ink was measured by a surface tension meter (SEO-Phoenix). The viscosity of the ink was measured through a viscometer (ARES, TA Instruments, USA). The transparency of the film was recorded by a UV-vis spectrometer (Shimadzu UV-3150) with a range of 200–800 nm. The surface morphology and cross-section of the deposited thin film were analyzed by field emission scanning electron microscope (FESEM JEOL. Ltd., JEM 1200EX II). The Raman spectra were recorded with anIFS 66/S, FRA 106/S Raman system with laser frequency of 1064 nm as an excitation source. The *I–V* characteristics of the thin film were measured by a semiconductor device (B1500A, Agilent, USA) parameter analyzer.

2.1.2Results and discussion

2.1.2.1 Taylor cone and spray formation

Before the actual deposition process, working operating envelope (Choi et al. 2012)was identified as shown in figure 2-1c. At different flow rate and applied voltages, different spray modes such as dripping, micro-dripping, unstable cone jet, stable cone jet and multi jet were obtained. Figure 2-1d illustrates the different atomization modes which exist at constant flow rate of 1200 µl/h at varying voltages. Until 3.3 kV, only natural dripping appeared. Above 3.3 kV micro-dripping occurred until 3.9 kV. Further increase in voltage resulted in the ejection of unstable cone when the stable cone jet appeared at 5.4 kV which was maintained until 7.1 kV. Increasing the voltage beyond 7.1 kV resulted in multi jet mode. The thickness of the as−deposited thin films can be controlled by different parameters such as concentration of ink, flow rate, stand-off distance, substrate velocity and spray time (Muhammad et al. 2011).

2.1.2.2 UV-visible analysis

The fabricated PEDOT:PSS thin film showed the average transmittance of nearly 75-82 % in the visible region as illustrated in figure 2-3a. The absorption peak appeared below the 298 nm in the UV range. This results indicate that the deposited PEDOT:PSS thin film is more suitable for optoelectronic applications.

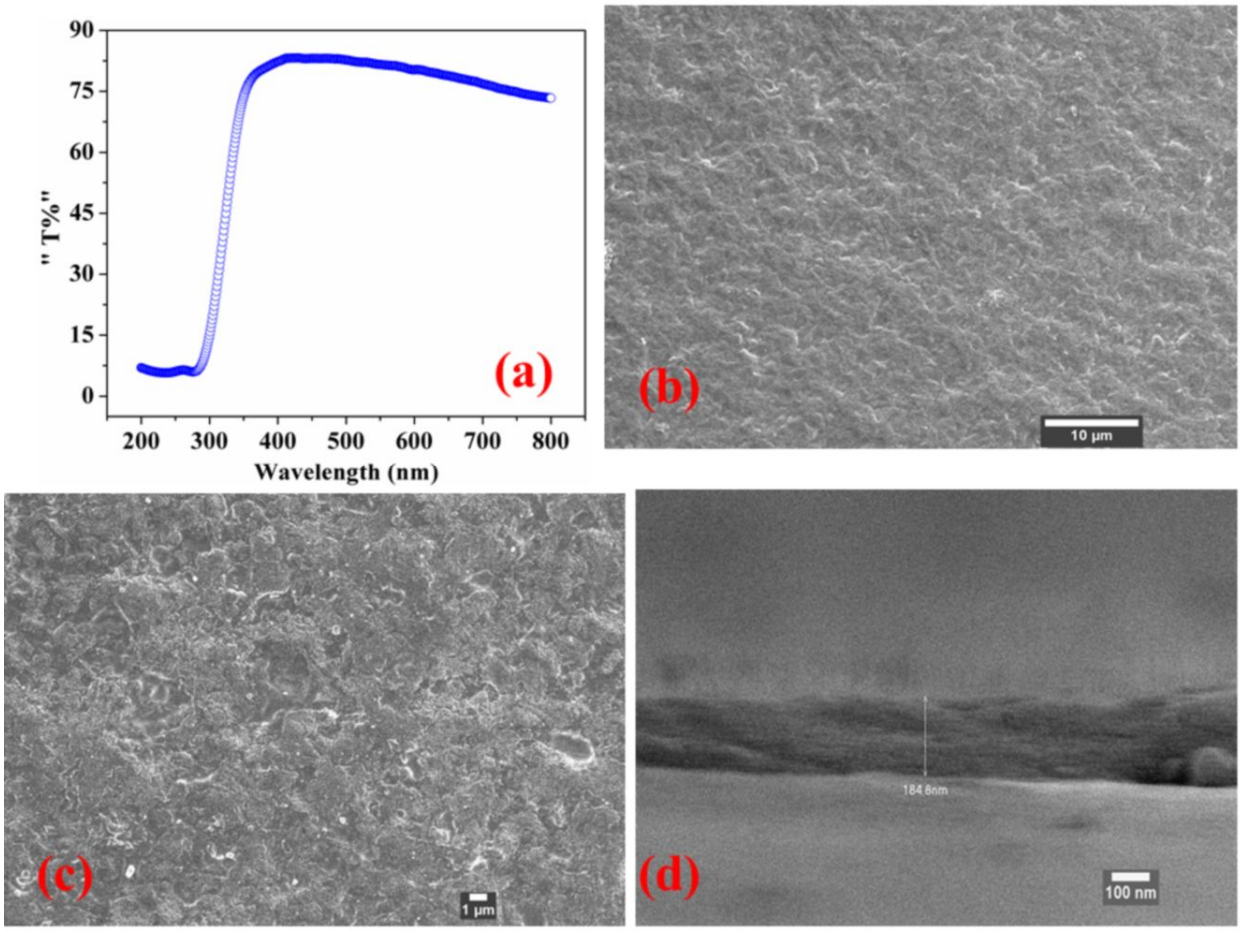

Figure 2-3 (a) Transmittance spectra of PEDOT:PSS thin film, surface morphology PEDOT:PSS thin film (b) low magnification FE-SEM image (c) high magnification FE-SEM image, (d) film cross-section

2.1.2.3 Surface morphology

The surface morphology of the as-deposited PEDOT:PSS thin film was analyzed using filed emission scanning electron microscope as shown in figure 2-3(b−d). The low magnification image (figure 2-3b) confirmed that the polymeric film showed surface uniformity with homogeneous deposition. Under high magnification, the FE-SEM image (figure 2-3c) revealed a small range of agglomeration occurred in the film with little voids. The cross sectional image as shown in figure 2-3d revealed the thickness of the film about 180 nm and it also shows good

adhesion between the PEDOT:PSS and PET substrate due to influence of jet based coating of EHDA (Jaworek et al. 2007).

2.1.2.4 Purity of thin film

The Raman spectra of deposited PEDOT:PSS film is illustrated in figure 2-4. In the spectrum of the thin film, a band with a strong intensity at 1426 cm^{-1}, which corresponds to the symmetrical stretching of C=C bond in the aromatic ring. The other three important bands found at 1530, 1365 and 1261 cm^{-1} are related to the anti-symmetric C_α–C_α stretching, C_β–C_β stretching deformations and C_α–C_α inter-ring stretching vibrations, respectively (Lapkowski and Pron. 2000 and Garreau et al. 2002). Although PSS does not give strong Raman peaks because of its non-conjugated backbone (Kim et al. 2002). The resulted spectrum did not show any significant change in the deposited PEDOT:PSS thin film, suggesting that the structure of the PEDOT:PSS film is more stable during atomization process in EHDA process.

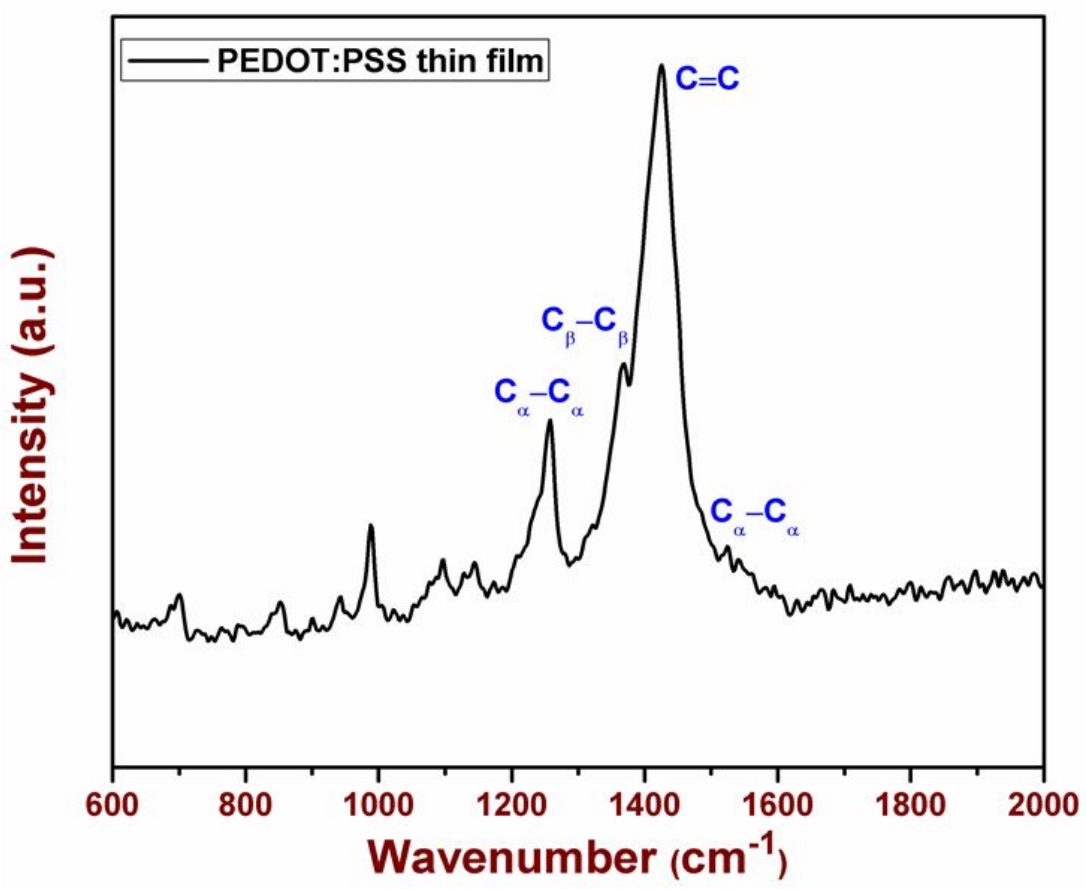

Figure 2-4 Raman analysis of PEDOT:PSS

2.1.2.5 Electrical study

Electrical characterization of PEDOT:PSS thin film was done through current-voltage (*I–V*) measurements. For contact purposes, silver patterns are printed on top of the film through EHDA technique (Arshad et al. 2011) as shown in the inset in figure 2-5 as a microscopic image (left) and a block diagram (right). Figure 2-5 explains the *I–V* curve of the film, which revealed a good ohmic contact between PEDOT:PSS thin film and metal electrode. The resistivity was calculated from the linear *I–V* curve by using sheet resistivity formula (Kyung et al. 2012).

$$\rho = \frac{\pi t}{ln2}\left(\frac{V}{I}\right) \quad \text{..... [1]}$$

Where, t is the film thickness and V and I are voltage and current from the I–V plot. The electrical resistivity was found out to be 49.6 mΩ cm respectively. The thin film showed the low resistivity due to excellent deposition through EHDA and the I–V analysis accords with the FE-SEM results as explained in previous discussion.

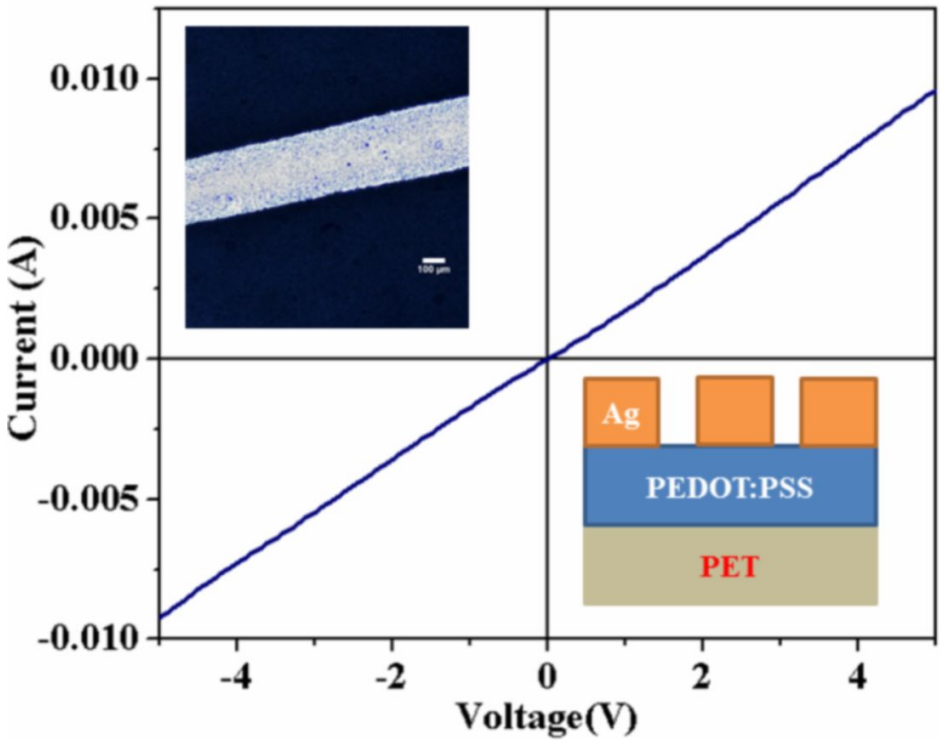

Figure 2-5*I*–*V* analysis of PEDOT:PSS thin film. In the inset, block diagram of Ag/PEDOT:PSS/PET configuration (right) and microscopic image of patterned silver on PEDOT:PSS thin film (left)

2.2 Multi-layer fabrication of P3HT:PCBM/ PEDOT:PSS thin film

In recent years, the π conjugated organic polymers have a promising role in electronic applications such as solar cells, organic light emitting diode, thin film transistors, and etc., (Currie et al. 2008 and Sekitani et al. 2009). The poly(3-hexylthiophene) (P3HT) is one of the most prospective conducting polymers, which is acts as a p-type semiconductor. Usually organic materials have lower charge mobility which can be improved by introducing several doping materials such as fullerene derivative, due to their influence of π electron carbon cluster (Forrest et al. 2004 and Haddon et al. 1992). The fullerene doped P3HT has good optical and electrical properties (Shah et al. 1999). The blended polymers would provide future scope in flexible electronics industry. There is always a demand for developing a unique method for the nanostructured thin film deposition with low cost that is environmentally benign and should be suitable for large-scale production.

As compared with the conventional thin film fabrication techniques such as spin-coating, PVD and CVD which have limitations for large scale production, EHDA holds more promises toward the deposition of nanostructured thin film and also possesses several advantages such as cost effectiveness, high speed and large scale production etc., (Choi et al. 2012 and Muhammad et al. 2012). This is due to the principle employed in this technique which is described as follows: EHDA employs a generation of stable cone jet from the precursor solution with diameter range from sub-micron to nanoscale with an applied potential. The stable cone jet further breaks up into mono-dispersed droplets with lesser diameter due to the influence of electrical stress, finally reaches the substrate, and results in the formation of nanostructured thin films (Duraisamy et al. 2012). Hence, a study in the processing, characterization and performance of organic

semiconductor thin films such as P3HT:PCBM using EHDA technique is an area of potential interest needs to be investigated.

In this work, we reported the deposition of P3HT:PCBM thin films on the poly(3,4-ethylenedioxythiophene):poly(styrenesulfonate) / Indium-tin oxide (PEDOT:PSS / ITO) coated polyethylene terephthalate (PET) substrates using EHDA technique. The physico-chemical characterizations of the as deposited films were investigated in detail using X-ray diffraction (XRD), UV−visible spectra, Fourier transform infra-red spectra (FT-IR) and field emission−scanning electron microscope (FE-SEM). The electrical study of the film was characterized through current−voltage measurement (*I*−*V*) and capacitance−voltage (*C*−*V*) analysis.

2.2.1 Materials and methods

2.2.1.1 Materials used

PEDOT:PSS (Orgacon) was purchased from Agfa Materials Japan Ltd, Japan. Poly (3-hexylthiophene) (P3HT), Poly (6,6-Phenyl C_{61}-butyric acid methyl ester) (PCBM), acetone, isopropanol and ITO coated PET substrate were received from Sigma-Aldrich, South Korea.

2.2.1.2 Preparation of ink and its physical properties

The P3HT:PCBM ink was prepared with dissolving P3HT and PCBM in a molar ratio of 1:0.8 using dichlorobenzene as a solvent. The entire solution is allowed to stirring for 24 h at 60°C in order to achieve a homogenous ink.

In EHDA techniques, the physical properties of the ink have a predetermining factor for the atomization process to achieve uniform thin films. The important physical properties such as

surface tensionand electrical conductivity and viscosity of the prepared P3HT:PCBM ink has been measured and given in the Table.2-2.

Physical Properties	**Values**
Viscosity	3 mPa S
Surface tension	17mN m^{-1}
Electrical conductivity	2.2 μS cm^{-1}

Table 2-2 Physical properties of P3HT:PCBM ink

The blended polymeric ink of P3HT:PCBM has been prepared by using dichlorobenzene (DCB) as a solvent. The DCB has good solubility effect of P3HT and PCBM to achieve a homogeneous solution. The prepared homogeneous mixture of blended polymeric P3HT:PCBM has lower surface tension (figure 2-6b) with viscosity of 3 m Pa s, which is more suitable parameters for electrospray process. However the polymeric ink has low electrical conductivity due to the influence of DCB, which leads to achieve cone-jet with higher applied potential. In addition, suitable co-solvent (acetone) is added to increase of the solution conductivity without affecting other properties and also to obtain a good homogeneity are shown in figure 2-6a. It gave a stable-cone jet with lower applied potential as compared with pure DCB due to the conductivity of ink.The prepared ink has good surface adherence on PEDOT:PSS coated ITO/PET with contact angle of 17 ^{o} (figure 2-6c).

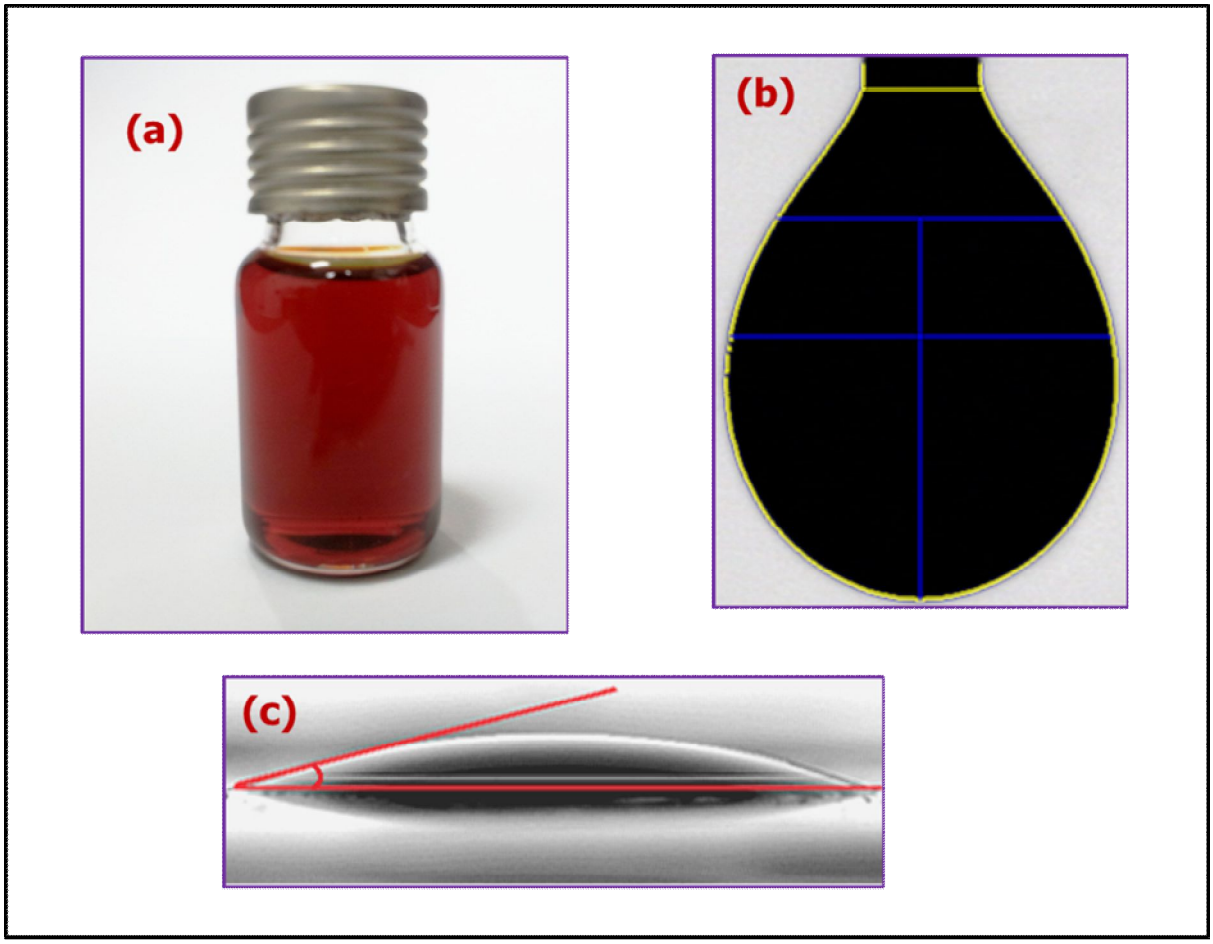

Figure 2-6 (a) Homogeneous mixture of composite P3HT:PCBM ink, (b) Surface tension of P3HT:PCBM ink, (c) Contact angle measurement of P3HT:PCBM on substrate

2.2.1.3 Fabrication process

The fabrication process consists of two steps, (i) deposition of PEDOT:PSS thin film on ITO coated PET substrate and (ii) deposition of P3HT:PCBM on PEDOT:PSS coated ITO/PET substrate.

(i) Deposition of PEDOT:PSS thin films using EHDA technique

The deposition of PEDOT:PSS films through EHDA technique discussed in our earlier report (Duraisamy et al. 2012)with little modifications due to the influence of substrate conductivity. In

EHDA technique, the process parameters (flow rate, applied potential, stand of distance and substrate velocity) have been varied with respect to substrates (copper, silicon, glass and flexible polymers) due to the influence of substrate nature (conductive or non-conductive nature). Briefly, we explained the electrospray deposition of PEDOT:PSS on ITO coated PET substrate. PEDOT:PSS ink was electrosprayed through metallic nozzle with internal diameter 430 µm. The substrate (ITO/PET) was kept at 13 mm stand-off distance from nozzle tip. Before the deposition, the ITO coated PET substrate was successively cleaned with acetone, isopropanol, water in bath sonication for 1200 sec and followed by UV-cleaning for 600 sec. The PEDOT:PSS ink was electrosprayed at flow rate of 700 µl/h and applied potential was 4.2 kV for achieving stable cone-jet mode for uniform thin film deposition. The deposited thin film was sintered at 120^{o}C for 45 min.

(ii) Deposition of P3HT:PCBM

The second step was deposition of P3HT:PCBM in which we used the as prepared P3HT:PCBM ink and is deposited by EHDA technique. In this case, the P3HT:PCBM ink was pump into a metallic nozzle with internal diameter of 150 µm. The substrate (PEDOT:PSS/ITO/PET) was mounted on to copper plate with stand-off distance was 12 mm from the nozzle orifice. During the spray process, a flow rate of 450 µl/h has been used throughout the experiments for thin film deposition. During the electrospray process, different atomization mode was appeared such as dripping, micro-dripping, un-stable cone-jet, stable-cone-jet and multi-jet (figure 2-7a). The flow rate and applied potential has been optimized through operating envelop of inks in EHDA process as shown in the figure 2-7b. At constant flow rate (450 µl/h), the dripping mode was appeared from 0 kV until to 1.1 kV, while micro-dripping was started to ejecting at 1.1 kV. The unstable-cone-jet mode was appeared at 3.1 kV. However at 4.2 kV, the most important

atomization mode of stable cone-jet was appeared and it was maintained until multi-jet was started. If further increase the applied potential, jet was discharged. The deposited thin films were annealed at 140 ^{o}C for 45 min under N_2 atm. The deposited layer was kept in glove box under N_2 atm.

In order to make electrical contacts from the top P3HT:PCBM and bottom ITO, we deposited the active material in the area 1.0 × 1.0 cm on the ITO substrates of area about 1.5 × 1.0 cm , thereby remaining uncoated area is used making electrical contacts.

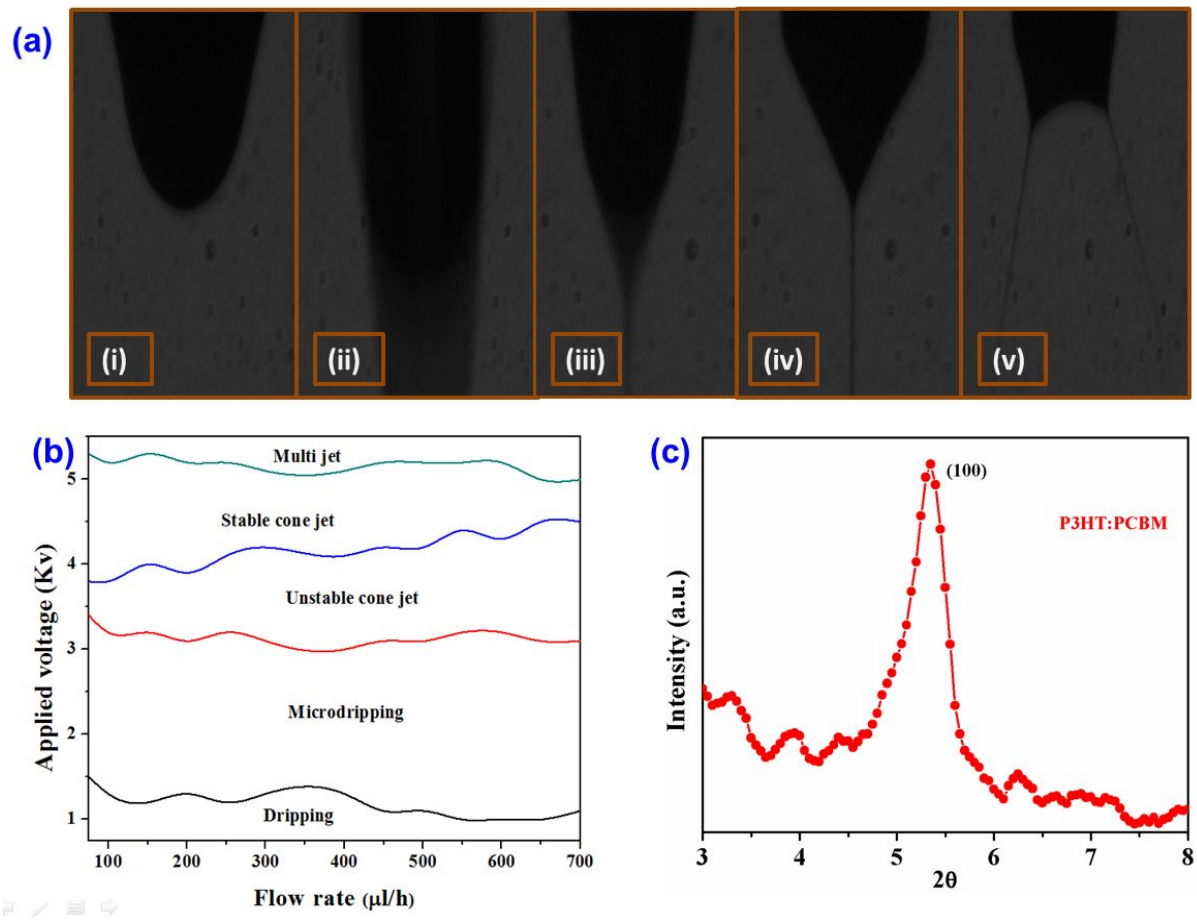

Figure 2-7 (a) Atomization modes of P3HT:PCBM : (i) dripping ,(ii) micro-dripping, (iii) unstable-cone jet, (iv) stable-cone-jet, (v) multi-jet, (b) Operating envelop of P3HT:PCBM, (c) X-ray diffraction of P3HT:PCBM layer

2.2.1.4 Characterization techniques

The electrical conductivity, viscosity and surface tension of the P3HT:PCBM ink was measured by a conductivity meter (EUTECH Instruments, ECOSCAN CON 6), viscometer (ARES, TA Instruments, USA), surface tension meter (SEO-Phoenix). The phase purity and crystallinity of the deposited P3HT:PCBM films were analyzed using an X-ray diffractometer (Rikagu D/MAX 2200H, Bede model 200). The XRD measurement was performed using a Cu κ_{α}radiation source of wavelength λ = 1.5406 Å. The surface morphology of deposited thin film was analyzed by

field emission scanning electron microscope (FESEM JEOL. Ltd., JEM 1200EX II). The presence of functional groups in the P3HT:PCBM film was investigated through FTIR analyzer (Bruker IFS 66/S, Germany). The absorbance of the film was recorded by a UV-vis spectrometer (Shimadzu UV-3150) with a range of 200–800 nm. The electrical characteristics of the thin film were measured by a semiconductor device (B1500A, Agilent, USA) parameter analyzer.

2.2.2 Results and discussion

2.2.2.1 Structural analysis

The X-ray diffraction pattern is used to investigate the structural characterization of a given material. Figure 2-7c shows the XRD pattern of deposited P3HT:PCBM film using EHDA technique. The XRD result shows a strong peak at 2θ value of 5.3^{o}, which is indicate the presence of (100) reflection plane corresponds to the thiophene rings in crystalline P3HT chain. The observed crystalline phase of P3HT is strongly interconnected with amorphous nature of PCBM (Yusli et al. 2009).

2.2.2.2 Surface morphology

The FE−SEM shows the surface morphology of P3HT:PCBM (figure 2-8a and b). Figure 2-8a reveals the homogeneous deposition of blended polymer. The high magnification image (figure 2-8b) shows the regular arrangement of blended polymer of P3HT:PCBM with less agglomerated polymeric chains due to the influence of mono-dispersed electrospray and also uniform mixture of polymeric ink. Due to the large inter−contact area of uniformly deposited blended polymer chain would permit a good charge transport between P3HT and PCBM (Lee et al. 2010).

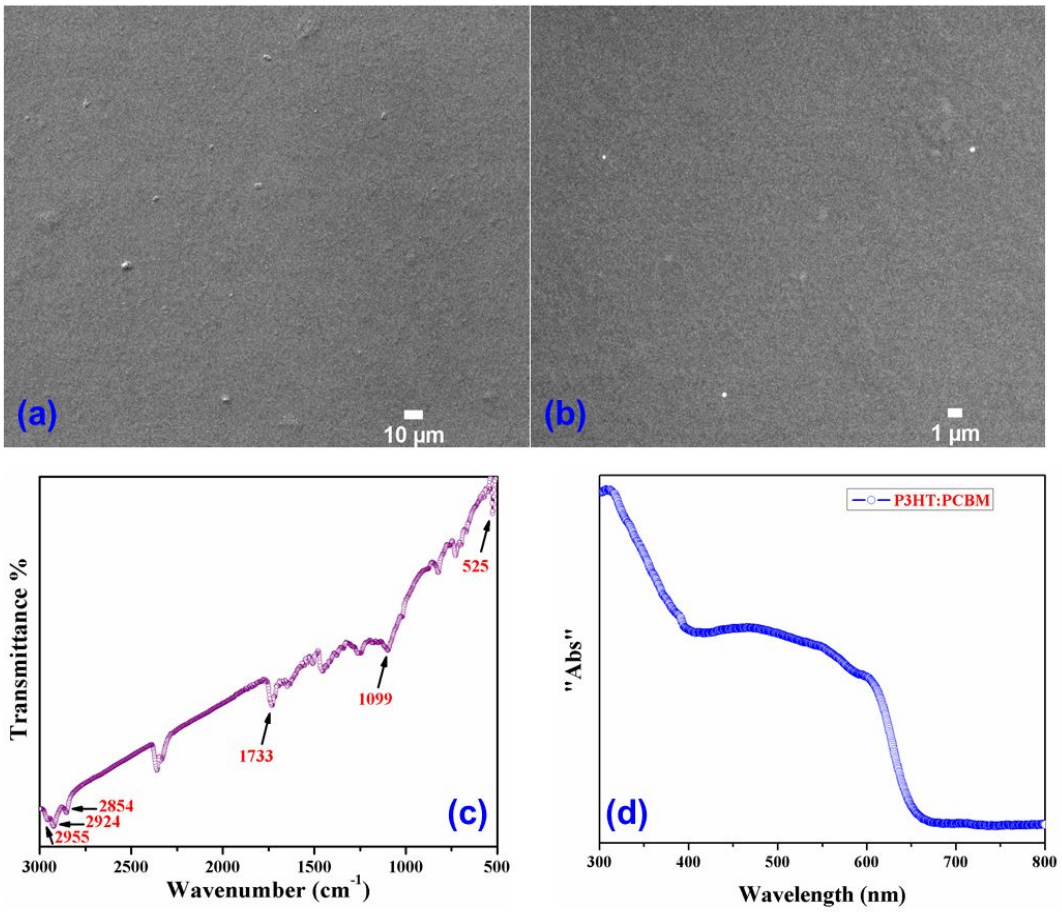

Figure 2-8 FE−SEM analysis of thin film, (c) low magnification surface morphology, (d) high magnification morphology of thin film, (c) FT-IR spectra of P3HT:PCBM film, and (d) absorption spectra of P3HT:PCBM film

2.2.2.3 Chemical composition

The FT−IR spectra of deposited P3HT:PCBM film is shown in figure 2-8c. The characteristic band at 820 $cm^{-1}$is assigned to the out of plane deformation of C−H group in aromatic ring (Kalita et al. 2010). The peak at 2955, 2924 and 2854 cm^{-1} correspond to the stretching vibration of aliphatic C−H group. Additionally the stretching mode around 1500−1452 cm^{-1} revealed that the aromatic ring represents. The P3HT:PCBM represents the stretching vibration of C=O and

C−O appeared around 1733 cm^{-1} and 1099 cm^{-1}. The most important characteristic peak appeared at 525 cm^{-1} corresponding to the fullerene group (PCBM) in the polymer matrix.

2.2.2.4 Optical properties

The optical properties of thin film are used to examine by UV-vis spectra. Figure 2-8d shows the absorbance spectra of the as-deposited P3HT:PCBM thin film. The observed results indicate that the layer absorbance in the range of 400−600 nm which is due to presence of P3HT. The absorbance in the visible region can be attributed to the π−π* transition (Vishal et al. 2005). The small shoulder peaks are observed in the range of 515−575 nm, which is due to presence of PCBM. The optical absorbance confirmed that the deposited P3HT:PCBM based thin film is more suitable for organic solar cells applications (Vishal et al. 2005).

2.2.2.5 Electrical study

A schematic diagram of current−voltage (*I–V*) characteristic of the P3HT:PCBM deposited on PEDOT:PSS / ITO−PET substrates is shown in the inset in figure 2-9a. *I–V* analysis of figure 2-9a shows a rectifying behavior which confirms that the interface between the two layers in which the PEDOT:PSS is used as a blocking layer for the hole transport (Rider et al. 2010). In order to analyze the *I–V* characteristics, we plotted the semi-logarithmic curve as shown in figure 2-9b. It shows that an exponential behavior in low voltage region and non-linear behavior in high voltage region.

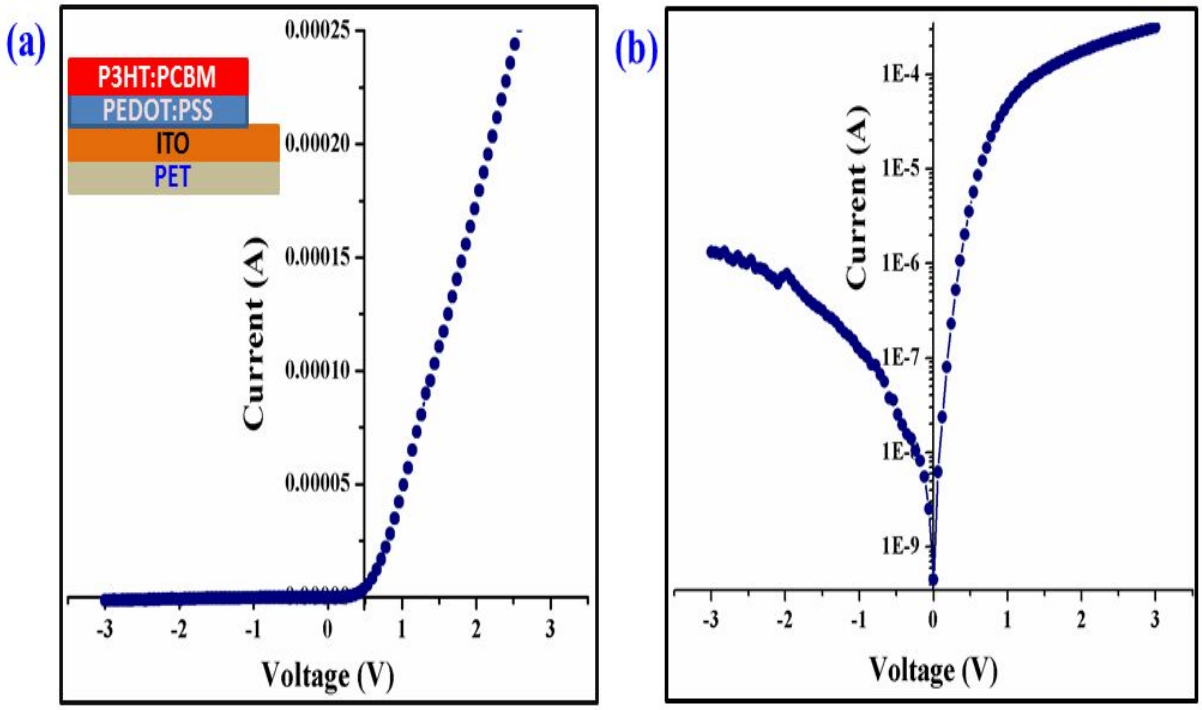

Figure 2-9 (a) *I–V* analysis of P3HT:PCBM / PEDOT:PSS, the inset shows schematic diagram of fabricated multilayers, and (b) semi-logarithmic scale of thin films

In order to study the charge-storage mechanism in the as fabricated thin films, we examined the *C–V* characteristics of the P3HT:PCBM/PEDOT:PSS thin films at different input ac frequencies. Figure 2-10a shows the *C–V* characteristics of P3HT:PCBM/PEDOT:PSS layers measured at input frequency of about 1 kHz. It shows the ideal capacitive behavior of the films and the maximum capacitance is found to be 0.7 V. The observed capacitance dispersion is due to the presence of interfacial states in the organic semiconductor (Aydog et al. 2005). The peak capacitance of the device is attributed to the presence of series resistance, bulk resistance and capacitance dispersion (Tugluoglu et al. 2012). Further, the *C–V* characteristics with various frequencies are presented in figure 2-10b. It shows that the capacitance is decreased with increase in the input frequency levels. At lower frequencies, there is no significant change in the

maximum capacitance is observed in the *C–V* characteristics. However, when the input frequency is increased to higher levels (> 50 kHz), the sharp peak representing the maximum capacitance becomes broadened. At applied input frequency of about 100 kHz, the *C–V* characteristic is completely broadened. This drastic change in the *C–V* behavior is due to the fact that the interfacial states cannot follow the ac signal at higher frequencies which results in the broadening of the *C–V* peaks at higher frequencies (Ocak et al. 2009). These characteristics ensure that the as fabricated thin films structure with excellent charge storage properties can be utilized for their future applications in solar cell devices.

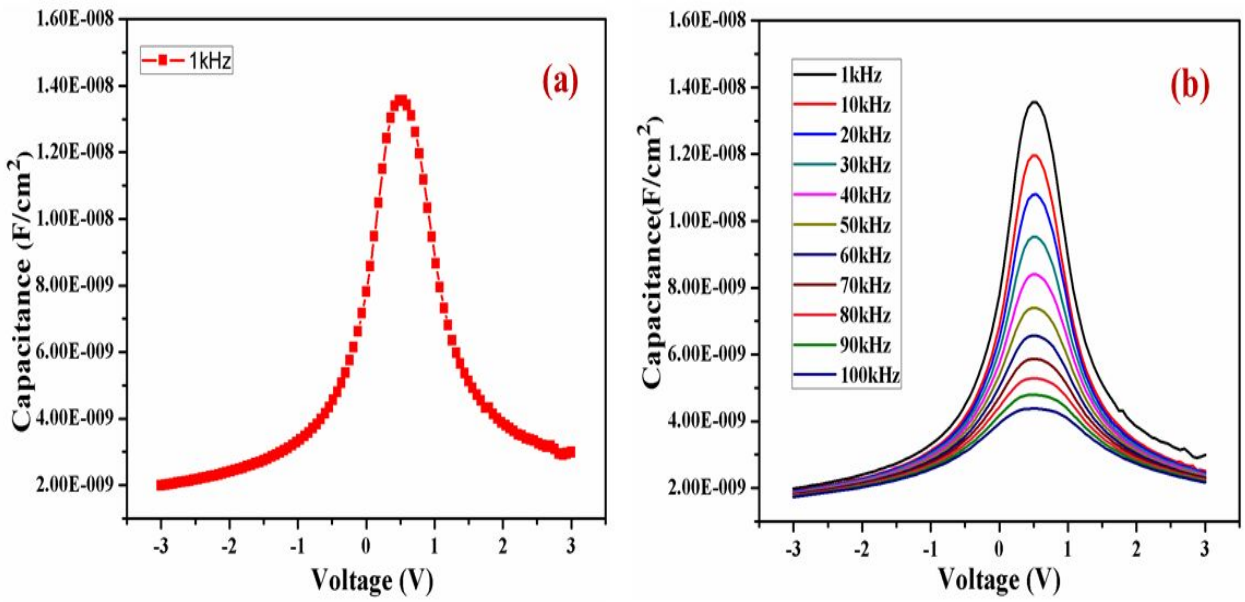

Figure 2-10 (a) *C–V* analysis of multilayer thin films, and (b) *C–V* analysis of film with different frequencies

3. Inorganic thin films

This chapter provides the deposition of nanostructured inorganic functional thin films using EHDA process. The structural, optical, electrical and their possible applications are discussed in detail.

3.1 Deposition of nanostructured Titanium (IV) oxide thin film

The unique and intriguing properties of nanostructured thin films have prompted tremendous motivation among researchers to explore the possibilities of using them in technological applications. In particular, the optical and electronic properties of nanostructured thin films have been of very high interest due to their potential applications in the fabrication of microelectronics and optoelectronic devices (Monat et al. 2006 and Krunks et al. 2008). The performance of the thin films for device applications are highly influenced by the crystallite size, morphology, phase and impurity type concentrations (Narashimha Rao et al. 1990). There is always an increasing demand for new technology for the fabrication of nanostructured thin films for functional devices in order to control the phase purity, morphology and the surface properties at the nanoscale which is of great interest to deliver distinctive properties. In this regard, many studies have been recently carried out to produce surfaces and films by tailoring nanostructure.

Nanostructured thin films of titanium dioxide (TiO_2) have been regarded as subject of great deal of research due to its exceptional chemical, electrical, optical properties and its potential applications diverse field such as (i) optoelectronic, (ii) photocatalytic (iii) solar cell (iv) photovoltaic, (v) self-cleaning coating (vi) antibacterial activity etc. (Hofmann et al. 1995, Fuyuki et al. 1986 and Linsebigler et al. 1995) Generally, TiO_2 nanostructured films exist in two

phases viz. a) anatase and b) rutile. Depending of the phase structure of TiO_2, it can be employed for diverging applications. The TiO_2 in anatase phase could accomplish the degradation of organic pollutants and photovoltaic devices (Jung et al. 2003 and Takeda et al. 2001). The rutile TiO_2 being a biocompatible material for blood and also can be used as an artificial heart valves (Zhang et al. 1996). The fabrication of nanostructured TiO_2 thin films has been achieved by several methods such as sol-gel, dip and spin coating, chemical vapor deposition (CVD), sputtering, pulsed laser deposition etc. (Kim et al. 2009, Voudouris et al. 1999 and Vahlas et al. 2006) In case of sol-gel and dip coating, controlling the morphology and thickness of the film is one of the biggest challenges until now (Kim et al. 2006 and Jaworek and Krupa. 1999) The other methods such as PVD and CVD are capable of producing highly transparent films but they are expensive and also need high vacuum system (Ganan-Calvo et al. 1997).

The development of new cost effective techniques and methods for fabrication of thin film devices with high purity and large area transparent films has attracted many researchers recently. With this motivation, we employed the electrohydrodynamic atomization (EHDA) technique for the fabrication of nanostructured TiO_2 thin films. EHDA is one of the innovative techniques to produce thin films at a high deposition rate and moreover it is cost effective (Luo et al. 2011). EHDA works on the principle of applying electric and mechanical energy to the liquid jet containing the precursor and allowing that to disintegrate into small nano sized droplets which deposit on the substrate (Jayasinghe and Edirisinghe. 2002 and Jayasinghe and Edirisinghe. 2002).

The electrospray deposition of TiO_2 thin films has already been reported in the literature by Mahalingam and Edirisinghe (Mahalingam and Edirisinghe. 2007). In their study, a higher voltage, 4.5 kV, was utilized for the electrospray deposition while in the present study the

electrospray deposition has been carried out at almost half of the voltage requirements. Also their field emission scanning electron microscope (FE-SEM) analysis revealed that the morphology of as deposited film was homogeneous and particle size was ~1μm while in this paper the morphology of as deposited TiO_2 thin films has been reported where particle size of < 80 nm was achieved by using PVP as stabilizer and 40 ± 5 nm was achieved at annealing temperature of 450 ^oC with very good film morphology. Furthermore a comparable transmittance in the visible region has been achieved at 450 ^oC. Some more characterizations have been discussed in this study where FT-IR and XPS analysis of the deposited films have been carried out to complete the functional group and chemical state, electronic state of the TiO_2 and electrical characterization has been done to check the applicability of electrohydrodynamically deposited TiO_2 films as functional material in optoelectronic and microelectronic applications.

3.1.1 Materials and methods

3.1.1.1 Materials used

Titanium (IV) isopropoxide ($Ti(OCH(CH_3)_2)_4$) and polyvinyl pyrrolidone (PVP) were purchased from Sigma-Aldrich, South Korea. Ethanol was obtained from Daejung Chemicals and Metals Ltd, South Korea. Silver nanoparticle ink was received from Harima Chemicals Inc, Japan.

3.1.1.2 Preparation of precursor solution

The preparation of optimum precursor solution for the EHDA deposition is an important criterion for achieving the uniform deposition. The formation of stable cone jet from the precursor solution is one of the key issues that need to be addressed in EHDA deposition (Hartman et al. 2000). The stable cone jet can be achieved by optimizing the following parameters of the precursor solution viz. (i) surface tension, (ii) electrical conductivity and (iii) viscosity of theprecursor solution (Chen et al. 1995). The precursor solution for the TiO_2 thin

films was prepared by dissolving titanium (IV) isopropoxide (0.96 g/mL) in ethanol and allowed vigorous stirring for 1 h at a rate of 1000 rpm. It results in the formation of a white colored precipitate of titanium hydroxide. Then, a solution containing 5 ml of freshly prepared PVP (0.01 g/ml) in ethanol was pipetted out into the above solution and allowed stirring vigorously for 20 min at 1300 rpm. We employed the experiment with various concentrations of the titanium isopropoxide in the precursor solution and measured the formation of stable cone jet. The details regarding the optimization process are given in Table 3-1. With various compositions of the precursor solution examined, composition No. 4 resulted in the formation of stable cone jet and resulted in uniform deposition of TiO_2.

No	Titanium isopropoxide (0.96 g /ml)	Stability of the sol	Viscosity (mPa.s)	Surface tension (mN/m)	Electrical conductivity (μS/cm)	Formation of stable cone jet
1	1	Stable	1.10	27	1.89	Stable Cone jet
2	2	Stable	1.17	28	1.72	Stable Cone jet
3	3	Stable	1.29	27	1.60	Stable Cone jet
4	**4**	**Stable**	**1.40**	**28**	**1.49**	**Stable Cone jet**
5	5	Unstable (Precipitation occurs)	1.58	28	1.31	Unstable Cone jet
6	6	Unstable (Immediate Precipitation)	×	×	×	×

Table 3-1various concentration of titanium isopropoxide in ethanol with 5 ml of PVP (0.01 g/ml in ethanol) as stabilizer. The total volume of the precursor solution is kept as 20 ml

3.1.1.3 Thin film deposition

The TiO_2 thin film was prepared on a corning glass (Corning 7059) substrate through EHDA at room conditions with a substrate speed of 0.30 mm/sec. The distance between the capillary and the substrate (standoff distance) was 6 mm. Before the deposition process, the glass substrate was sonicated with acetone, ethanol and rinsed with deionized water and then irradiated under UV light in the UV cleaner for 20 minutes and plasma treatment to convert nature of surface of the glass to be hydrophilic. The deposited films were annealed at 450 ^{o}C for 2 h before the characterization process.

3.1.2 Results and discussion

3.1.2.1 Taylor cone and spray formation

The EHDA experiment usually start from a minimum flow rate and continue to a maximum flow rate (50 µl/h to 450 µl/h in this case) with various voltages order to obtain different atomization modes such as dripping, micro-dripping, pulsating cone-jet, stable cone-jet and multi-jet. This process is used to optimize the flow rate and applied voltage for the stable cone-jet mode of spray. The possible operating envelop has been shown in figure 3-1a. Figure 3-1b shows the different modes of atomization captured by a high-speed CCD camera with a constant flow rate of 200 µl/h at different voltages. The dripping and micro-dripping modes appeared from zero voltage until to 2.1 kV, while the spindle mode started appearing at 2.1 kV. The pulsating cone-jet appeared at 2.5 kV. The stable cone-jet formed at 2.7 kV and it remained until the multi-jet formed at 3.2 kV. Increasing the applied voltage after 3.2 kV led to jet discharge. A flow rate of 200 µl/h was used throughout the experiment. If the flow rate had been too small, the cone-jet would not have remained stable for a long period of time.

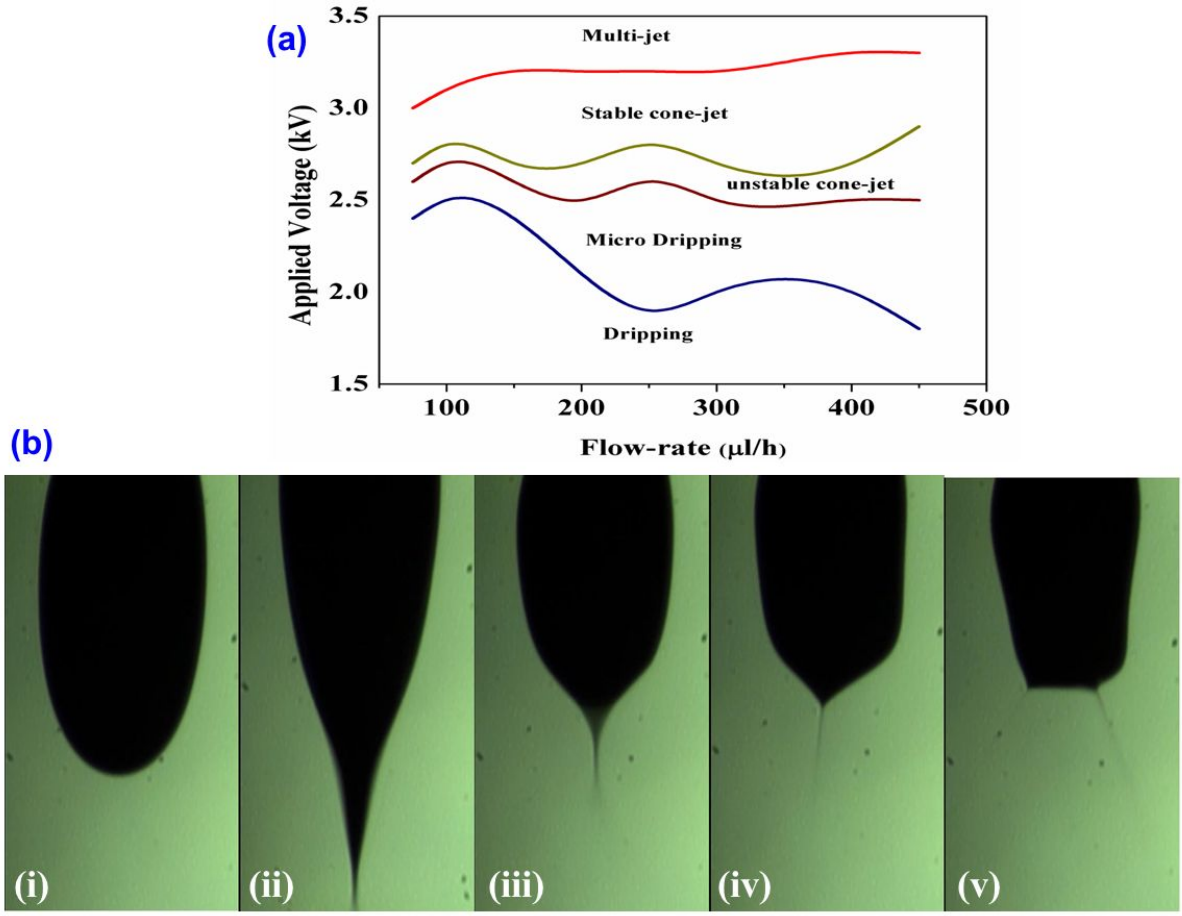

Figure 3-1 (a) Operating envelop of precursor solution, and (b) Mode of atomization (i) micro dripping, (ii) spindle mode, (iii) pulsating cone jet, (iv) stable cone jet, (v) multi-jet mode

According to the classical electrohydrodynamic atomization of stable cone jet mode, the electrical relaxation time, T_e, must be very much smaller than the hydrodynamic time T_h (Ganan-Calvo et al. 1997).It is established by the inequality

$$\frac{\beta\varepsilon_o}{K} << \frac{LD}{Q} \quad \text{..... [1]}$$

where, β is the relative permittivity, K is the electrical conductivity, L is the axial length of the jet, D is the jet diameter, Q is the given flow rate and $\varepsilon_o$is the permittivity of vacuum (8.85×10^{-12} Fm^{-}

[1]). The following values were substituted in the above equation, Q is 5.556×10^{-11} m^3/s, D is 16.236 μm, L is 241.3 μm, K is 0.00049 S/m and β is 15, which gives T_e 2.70×10^{-7} s and T_h 1.15×10^{15} s. Therefore $T_e << T_h$ and the classical electrohydrodynamic atomization criteria are fulfilled.

3.1.2.2Structural analysis

The XRD patterns of TiO_2 thin films annealed at 450 ^oC were presented in figure 3-2. The presence of peaks revealed the formation of nanocrystalline TiO_2 film. It showed Bragg's reflection at 2θ values of 25.4 ^{o}, 37.6 ^{o}, 48 ^{o}, 53.6 ^{o}, 54.9 ^{o}, 62.7 ^{o}, 68.6 ^{o}, 69.8 ^{o}, and 75^o indicating the characteristic peak of tetragonal crystal planes of anatase phase TiO_2 (Wang et al. 2006), suggesting the high quality of TiO_2 thin films. No peak corresponding to the rutile phase of TiO_2 was seen in the diffractogram, suggesting clearly that only anatase phase has been formed. Moreover, the average crystallite size was estimated by using Debye−Scherer's equation (Karthikeyan et al. JNPN) as shown below

$$D = \frac{k\lambda}{\beta \cos\theta} \quad \text{..... [2]}$$

Where D is crystalline size, λ is the radiation wavelength (1.5406 Å), β is the peak full width at half maximum (FWHM), θ is the diffraction angle and k = 0.94 for spherical shape particles.The average crystallite size was calculated by employing the DS equation as ~ 25 nm.

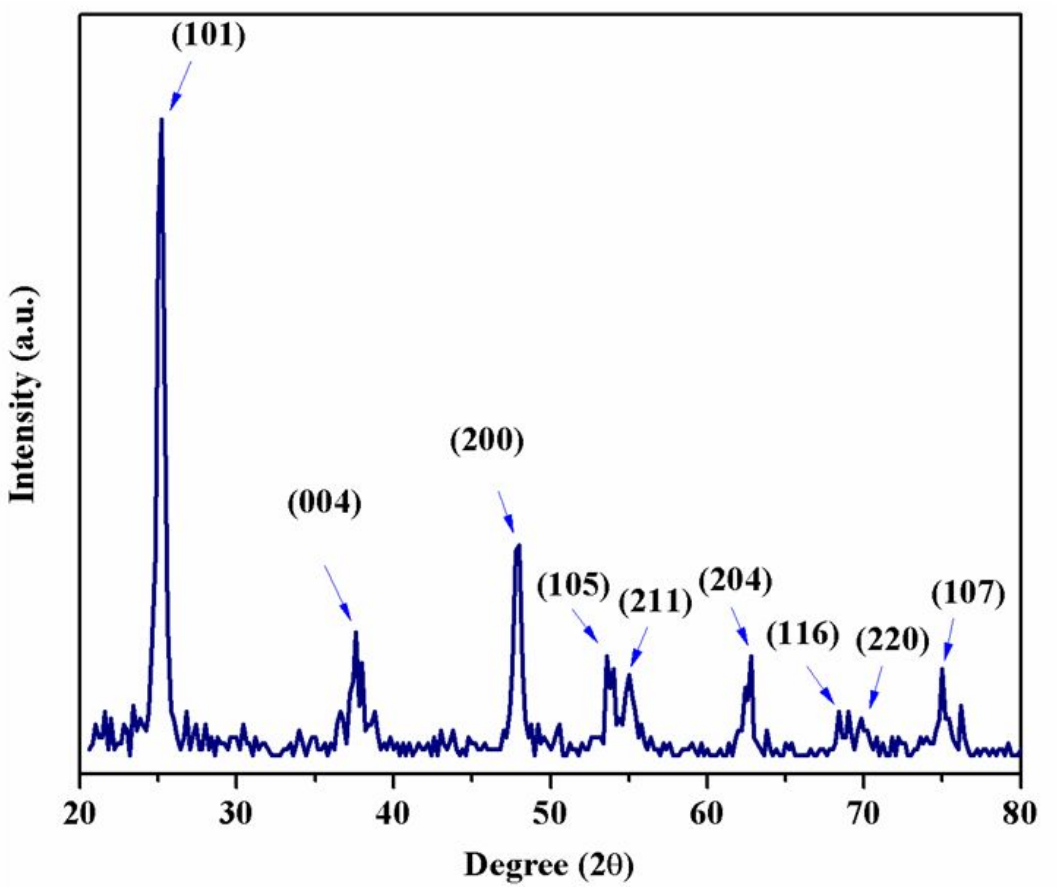

Figure 3-2 X-ray diffraction pattern of TiO_2thin films

3.1.2.3 Surface morphology

The surface morphology of the TiO_2 thin films is measured by using FE-SEM. As shown in figure 3-3 (a-b). FE-SEM image reveals that the as deposited TiO_2 thin film is very homogeneous with very less agglomeration of particles due to using PVP, which leads to prevent the particle agglomeration. Figure 3-3 (c-d) showed the uniform morphology of the annealed TiO_2 thin film. The grain size is measured as 40 ± 5 nm with spherical morphology as shown. The grain size from the FE-SEM studies is in accords with the XRD results shown in the previous section.

At 450 ^{o}C deposited particle rearrangement takes place and the nature of the film becomes good crystalline nature. The main advantage of EHDA lies in the fact that the deposition process is very simple and is carried out at room temperature. Achievement of the presented results at room conditions and open environment is an achievement.

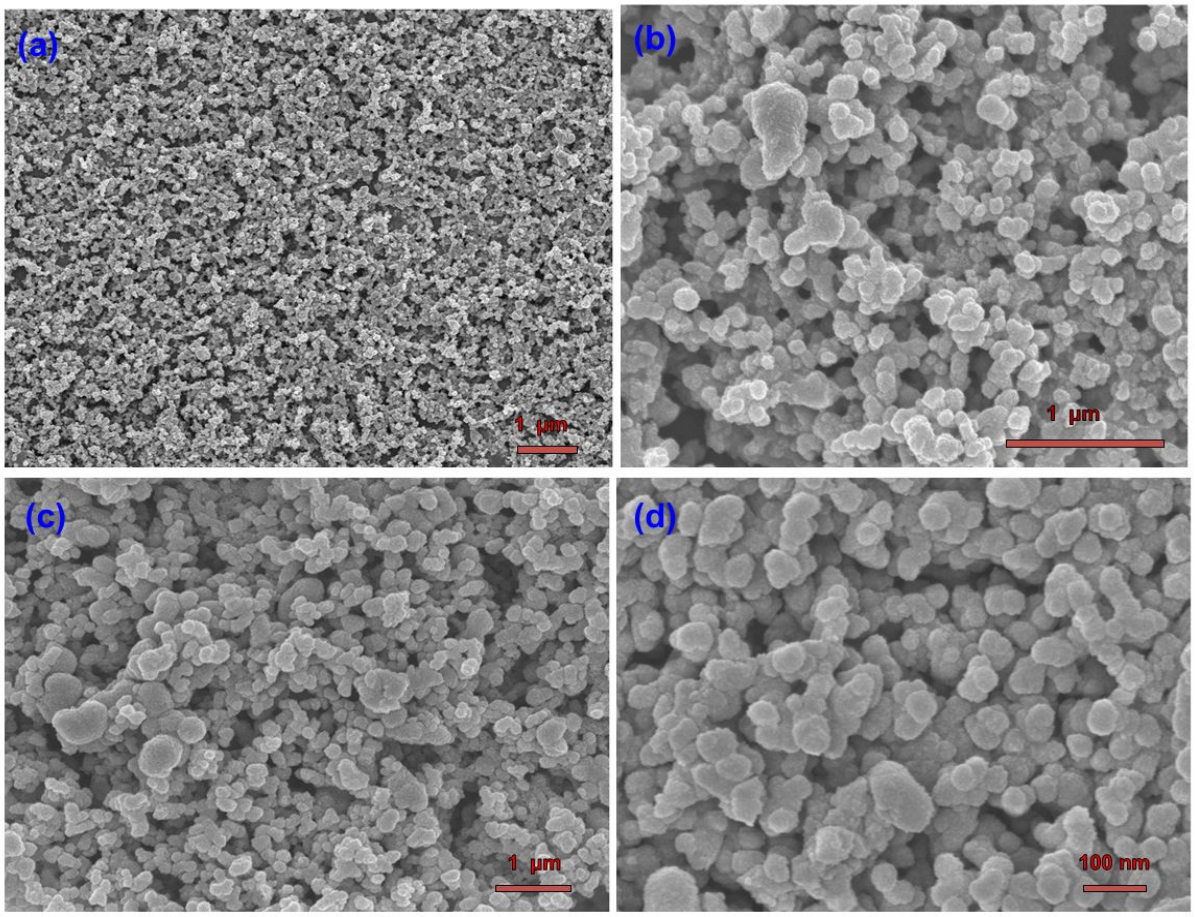

Figure 3-3 FE-SEM observation of TiO_2 thin films: (a), (b) as-deposited and (c), (d) annealed at 450°C

3.1.2.4 Chemical composition and film purity

(i) FT-IR analysis

The FT-IR spectra of TiO_2 thin films (as deposited and annealed at 450 ^oC) are shown in figure 3-4 (a-b). The spectra of as-deposited film show the presence of Ti−O stretching around 500 to 800 cm^{-1} (Zhang et al. 2002). It also shows the peaks corresponding to the organic components present in the PVP stabilizer in the region 1000 cm^{-1} to 1400 cm^{-1} corresponding to the pyridine ring (C_4H_8N-) in the PVP (Khanna et al. 2004). It also exhibited the peak corresponding to hydroxyl groups (O−H stretching) or water content in the region 1620 and 3500 cm^{-1} (Zhang et al. 2002). After annealing the thin film at 450 ^oC for 3 h, the Ti−O peak becomes narrowed in the region 450 to 600 cm^{-1} which is due to the transformation of $Ti(OH)_2$ into TiO_2 (Zhu et al. 1999). Here, that the presence of organic residues due to the stabilizer PVP in the as-deposited film removed completely in the spectra of the films annealed at 450 ^oC.

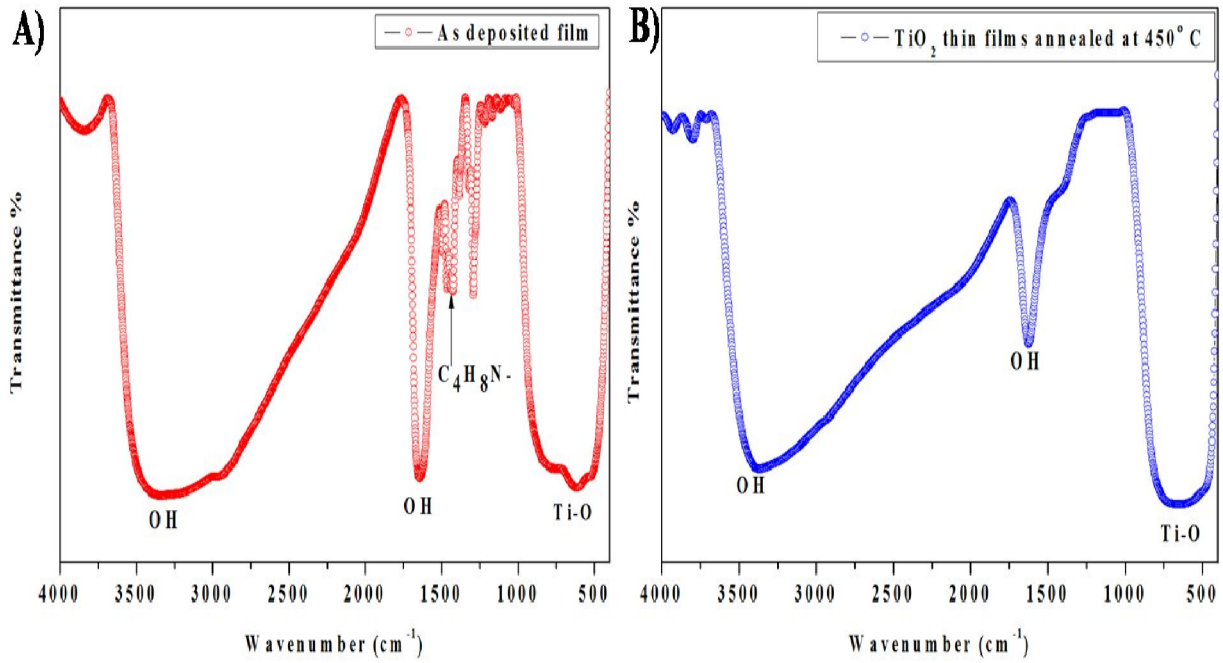

Figure 3-4 FT-IR spectra of TiO_2 thin films (a) as deposited and (b) annealed at 450 ^oC

(ii) XPS analysis

The X-ray photoelectron spectrum of the TiO_2 thin films deposited by EHDA technique is shown in figure 3- 5a showing the presence of Ti2p and O1s (Zhang et al. 2004). The deconvoluted spectrum of Ti2p (as shown in figure 3-5b) exhibited the characteristics peaks of $Ti2p_{3/2}$ and $Ti2p_{1/2}$ with the corresponding binding energies $E_b(Ti2p_{1/2})$ = 464.05 eV and $E_b(Ti2p_{3/2})$ = 458.4 eV respectively. In the case of oxygen, the high resolution spectrum of O1s had a peak in 529.5 eV that corresponds to the TiO_2 binding energy, as shown in figure 3-5c**.** No characteristic peaks of any impurities were detected in the XPS analysis, suggesting that high quality of TiO_2 thin films were obtained.

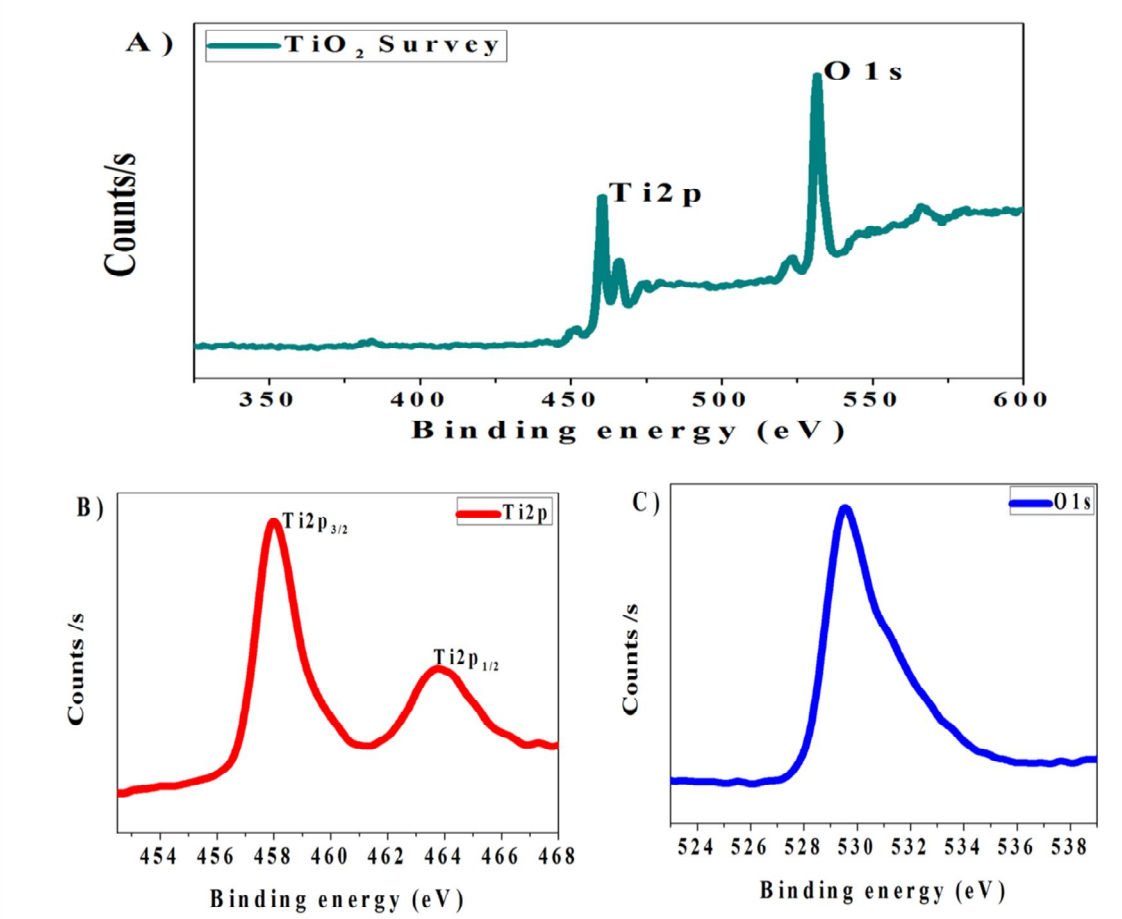

Figure 3-5 XPS spectra of TiO_2thin films deposited using EHDA

3.1.2.5 Optical analysis

The optical properties of the TiO_2 thin films annealed at 450 ^oC were characterized by UV-vis spectroscopy as shown in figure 3-6a. The absorption spectrum shows that the absorption onset around edge of TiO_2 was found at 330 nm. The absorption spectra revealed that TiO_2 film has low absorbance in the visible region which is a characteristic of TiO_2. The transmittance spectrum of the TiO_2 film showed that it has 85 % transmittance in the visible region. The optical band gap energy from the UV-vis spectra can be estimated by using the following equation (Krishnamoorthy et al. 2011).

$$\alpha = \frac{A(E_g - hv)^n}{hv} \quad \text{..... [3]}$$

Where, α is the absorption coefficient, A is a constant, E_g is the band gap and n is equal to 1/2 for an indirect transition. The band gap is estimated from a plot of $(\alpha h\nu)^{1/2}$ versus photon energy ($\alpha h\nu$). The intercept of the tangent to the plot gave a good approximation to the band gap energy for this indirect band gap material. Figure 3-6b shows optical band gap calculation scheme of the deposited film was found as 3.45 eV and the absorption edge was red shifted. The average value of the band gap of the bulk anatase is 3.2 eV (Lei et al. 2001). The band gap widening in the TiO_2 films is mainly attributed to the contribution of crystallite size effects (Mogyorosi et al. 2003 and Lei et al. 2006). Moreover, it can be said that the TiO_2 thin films are more suitable for solar cell applications due to the fact that the recombination processes are decrease in semiconductors with wide band gap.

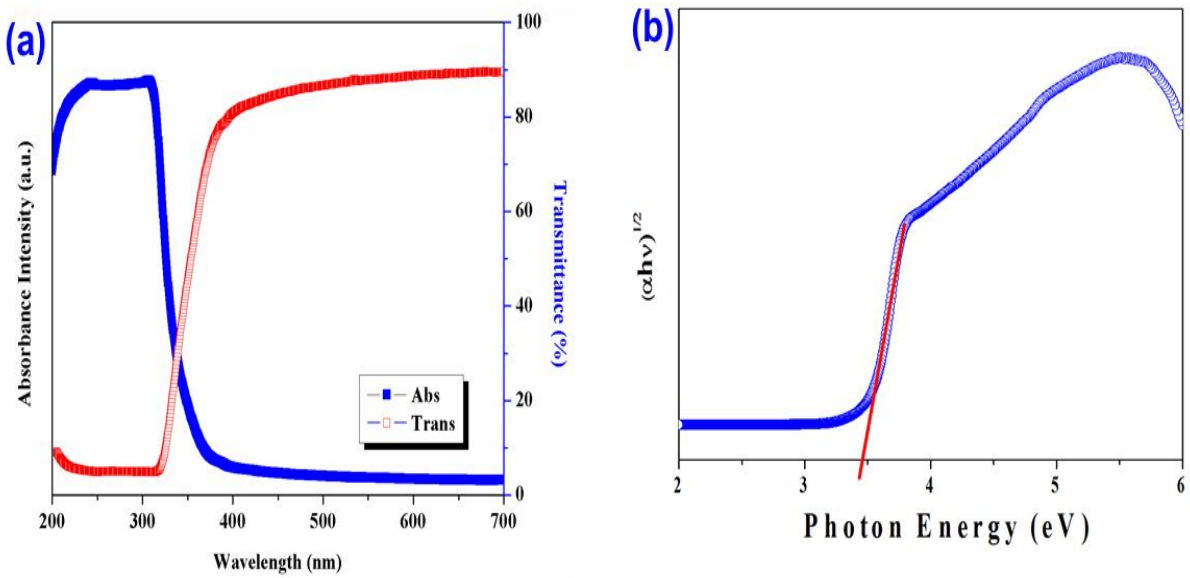

Figure 3-6 (a) UV-vis spectra of TiO_2 thin films showing the absorbance and transmittance curve, and (b) Tauc plot of determining the optical band gap of TiO_2 thin films

3.1.2.6 Electrical Characterization

Figure 3-7 shows *I-V* measurement characteristic of TiO_2 thin film. The electrodes were made by silver (Ag) using silver ink (NPK ink Ltd) deposited by EHD method (Khan et al. 2011). The *I-V* curve shows a nearly linear behavior indicating the good ohmic contact between metal electrode and TiO_2 thin film. Our result finds support with the previous results (Bearzotti et al. 1994). The important parameter for the observation of good ohmic contact in the *I-V* characteristic is due to the proper matching of the work function between the silver electrode and the TiO_2 thin film. The TiO_2 thin film has a work function of around 4.4 eV (Orendorz et al. 2005). Meanwhile work function of Ag is 4.3 eV (Kim and Rhee. 2009). The resistivity was calculated from the slopes of the linear *I-V* plot and using the sheet resistivity formula (Muhammad et al. 2011) for a thin film:

$$\rho = \frac{\pi t}{ln2}\left(\frac{V}{I}\right) \quad \text{[4]}$$

where t is the film thickness, while V and I are voltage (V) and current (I) from the *I-V* curve. The resistivity was found out to be 45 mΩ.cm.

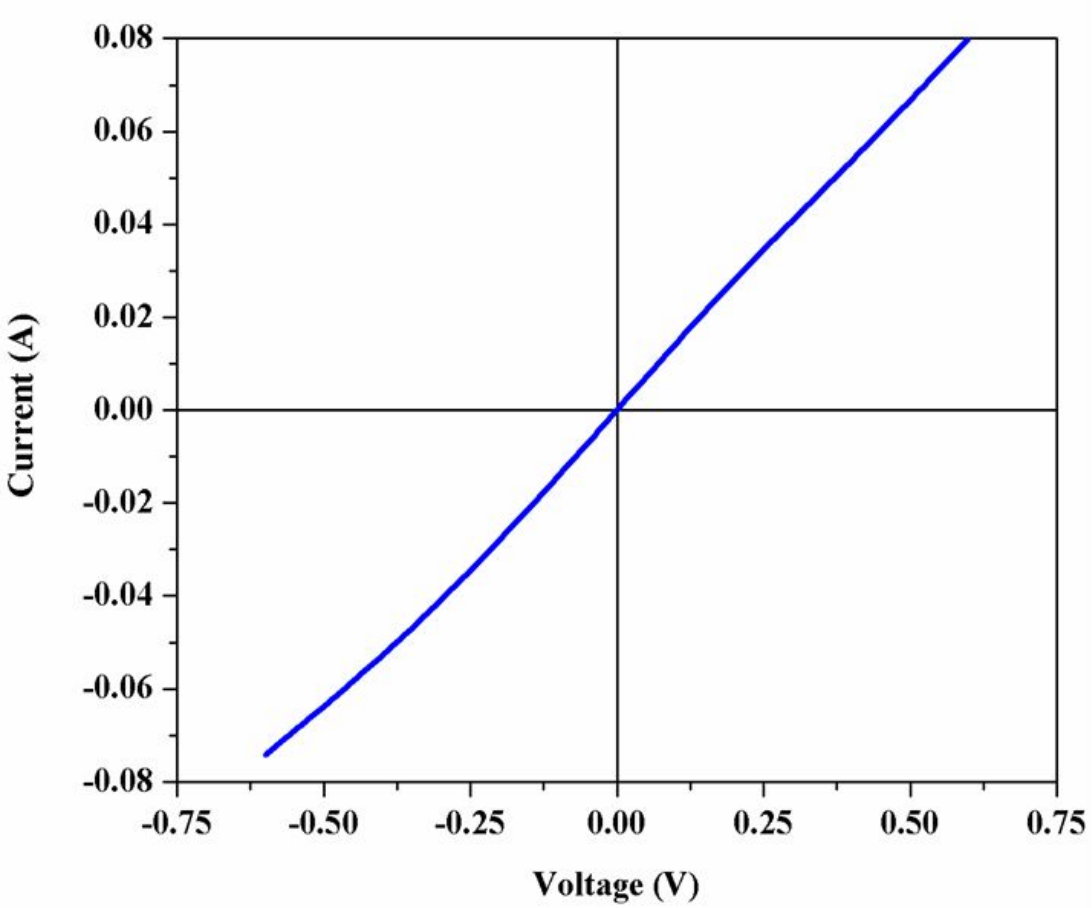

Figure 3-7*I*−*V* characteristic curve of TiO_2 thin films

3.2Fabrication of nanostructured Zinc oxide thin film

Zinc oxide (ZnO) has been great interesting functional semiconducting metal oxide with wide range of industrial applications such as gas sensors, solar cells, light emitting diodes, photodetectors, nanogenerators, medicines and photodegradation of environmental pollutants (Wang et al. 2008, Longyue et al. 2006, Xu et al. 2010, Lee et al. 2011 and Premanathan et al. 2011). ZnO is an II-IV division of semiconductor with various nanostructured configurations (Mohan et al. 2012 and Mohan et al. 2012). ZnO materials have broad attention due to its wide energy band gap, good UV photosensitivity, chemical stability, nontoxicity and resistance to radiation hardness, etc. (Wang. 2004, Raoufi and Raoufi. 2009 and Guo et al. 2013). The unique and fabulous photoconductivity properties of nanostructured ZnO thin film has also been considered as an alternative to titanium oxide due to wide band gap, low cost and easy to synthesis. (Mohan et al. 2012).n-type semiconducting property of ZnO occurs due to oxygen vacancies and native defects (Mishra et al. 2012). Generally, a surface related photoconduction is slow process than that of bulk related process. Photoconduction can occur by the adsorption and desorption of oxidizing molecules. However, the oxide materials tend to create the electron depletion region under the influence of adsorbed oxidizing molecule in the absence of light irradiation. In case of light irradiation, the generation of holes moves into the surface of oxide layers and neutralized the charged molecules, which leads to increase the surface conductivity. Whereas, the irradiation is turn off, the surface conductivity has reduced due to the lack of oxidizing molecules desorption (Mishra et al. 2012 and Jun et al. 2009). The ZnO thin film is not only for the conductivity changes but also has quick response in presence of photons. The surface defects in the ZnO lead to reduce the charge conduction process, which may be

controlled by introducing suitable thin film deposition process (Jun et al. 2009 and Dwivedi et al. 2013). Nowadays, the solution based process techniques is one of the good technique for the fabrication of nanostructured ZnO thin film due to good physico-chemical flexibility, large area film deposition, high quality of nano/micro structured thin films and low cost (Nayak et al. 2010 and Dai et al. 2011).

The development of unique advantage of solution based thin film deposition is offered by electrohydrodynamic atomization (EHDA) technique. The selection of EHDA techniques is due to low cost, easy to fabricate nanostructured thin film over large area at room atmosphere (Shigeta et al. 2012 and Poon. 2002). In this technique, to overcome the surface tension of host liquid by the influence of electric potential, lead to achieve a Taylor cone or stable cone-jet, which is further disintegrate into fine droplets and uniformly deposited on the substrates (Choi et al. 2012 and Ellis et al.2012). In EHDA process, droplet congelation does not exist due to the influence of strong repulsive force of charged droplets. The size of the droplets is in the range of several hundred of micron to tens of nanometer scale (Vishlaghi et al. 2012). The physico-chemical properties of colloidal liquids or precursor solution such as viscosity, surface tension, and conductivity are plays a significant role for stabilizing the stable cone-jet. The stability of cone-jet is influence the surface interface of deposited thin films on substrates (Duraisamy et al. 2012). Therefore, the Further, surface charged droplets. The deposition of ZnO thin film thickness and spray area has easily controlled by concentration of precursor solution, stand-off distance, flow rates, charge of liquid droplet size, substrate velocity (Ellis et al.2012 and Duraisamy et al. 2012).

Herein, we report a solution based nanostructure ZnO thin film deposition by using EHDA technique. The structural and surface morphology of thin films are investigated through XRD

and FE-SEM. The film purity and chemical composition of deposited layer are investigated by FT-IR and XPS analysis. The optical film transparency and photocurrent properties are discussed.

3.2.1 Material and methods

3.2.1.1Materials used

Zinc acetate dihydrate ($Zn(COOCH_3)_2.2H_2O$, and monoethanolamine ($OH\text{-}CH_2\text{-}CH_2\text{-}NH_2$) were purchased from Sigma-Aldrich and ethanol from Dang Chemicals. Silver nanoparticle ink was received from Harima Chemicals Inc, Japan. All the materials have been used without further purification

3.2.1.2 Preparation of precursor solution

The zinc acetate dihydrate (4 g) was dissolved in ethanol medium and the solution was vigorously stirred at 50 ^oC for 30 min. Then, few drops of monoethanolamine solution were added into that solution and the stirring was continued for 2 h at 1500 rpm. Finally, a homogeneous and clear solution was obtained and used for ZnO thin film deposition using EHDA technique.

The liquid with high surface tension (e.g. H_2O) tend to prevent the Taylor cone or stable cone-jet, which lead to significantly affect the film uniformity. Based upon this phenomenon precursor solution was prepared by using ethanol, which have high dielectric constant with low surface tension and also more suitable solvent medium for preparation of precursor solution. In order to achieve a homogeneous solution, $OH\text{-}CH_2\text{-}CH_2\text{-}NH_2$ was used as a surfactant to provide the stable and clear solution. The physical properties of prepared solution were given in the Table.3-2.

Physical Properties	Values
Viscosity	2.33 mPa S
Surface tension	26mN m^{-1}
Electrical conductivity	562 µS cm^{-1}

Table 3-2 Physical properties of precursor solution

3.2.1.3 Spray formation and thin film fabrication

The nanostructured ZnO thin film was deposit on glass substrate through atomization process. The main tool in this process is micron size metallic capillary, which can eject the micron /nano sized liquid droplets under the influence of applied potential to achieve a uniform thin film. The experimental setup of EHDA has been clearly discussed in our previous work (Muhammad et al. 2013 and Duraisamy et al. 2012). Herein, the optimum flow rate of 100 µl/h has been selected for thin film deposition on pre-cleaned glass substrate. Initially, the dripping mode was appeared and it was maintained until 2.2 kV. At 2.2 kV, the micro dripping was observed. The pulsating cone –jet or unstable cone-jet was observed at 2.8 kV but when the voltage was increased, the Taylor cone or stable cone-jet was observed at 4.7 kV, which is most important atomization mode for achieving nanostructured ZnO thin film. The achieving stable jet was maintained up to 4.9 kV. At 4.9 kV multi jet was observed. Further increase the applied voltage, jet led to discharge. However, the mode of atomization with respect to voltage at constant flow rate (100µl/h) is shown in figure 3-8. The deposited thin film was sintered at 500 ^{o}C for 4 h.

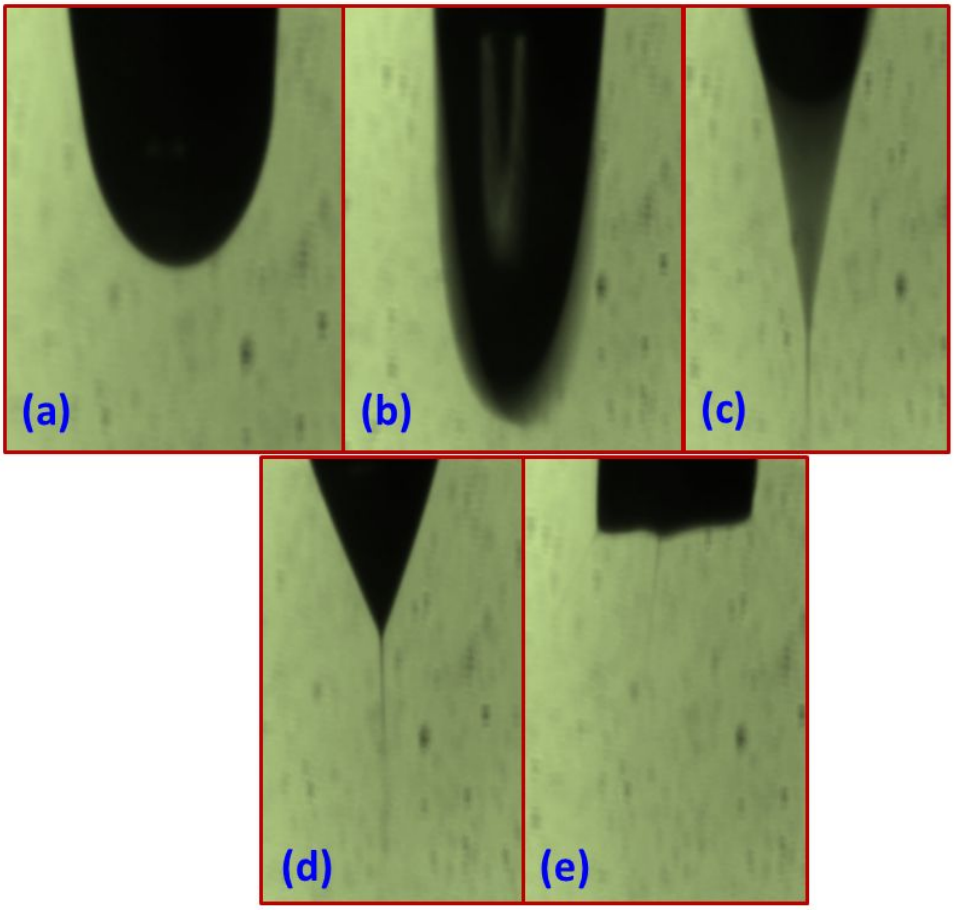

Figure 3-8Atomization mode with respect to voltage at constant flow rate

3.2.2Results and discussion

3.2.2.1 Structural analysis

The XRD analysis was acquired in the grazing incidence mode to determine the crystallinity, phase purity and average crystallite size of deposited ZnO thin film using EHDA process. Figure 3-9a shows the XRD pattern of ZnO thin film. The XRD pattern of 500 ^{o}C annealed ZnO film exhibit the diffraction peaks at 2θ values of 32.31^{o}, 35.06 ^{o}, 36.94 ^{o}, 47.85 ^{o}, 57.33 ^{o}, 63.46 ^{o} and 68.61 ^{o} are corresponds to the crystalline planes such as (100), (002), (101), (102), (110), (103)

and (112) respectively. This observation can be indexed to wurtzite structure of ZnO thin film (JCPDS card no: 36-1451), suggesting the high purity of the ZnO thin film. Moreover the average the crystalline size was estimated using Debye−Scherer's method (Krishnamoorthy et al. 2012) as given below

$$D = \frac{k\lambda}{\beta \cos\theta} \quad \text{..... [5]}$$

Where D is crystalline size, λ is the radiation wavelength (1.5406 Å), β is the peak full width at half maximum (FWHM), θ is the diffraction angle and $k = 0.94$ for spherical shape particles. The average crystallite size was estimated and was found to be ~ 28 nm.

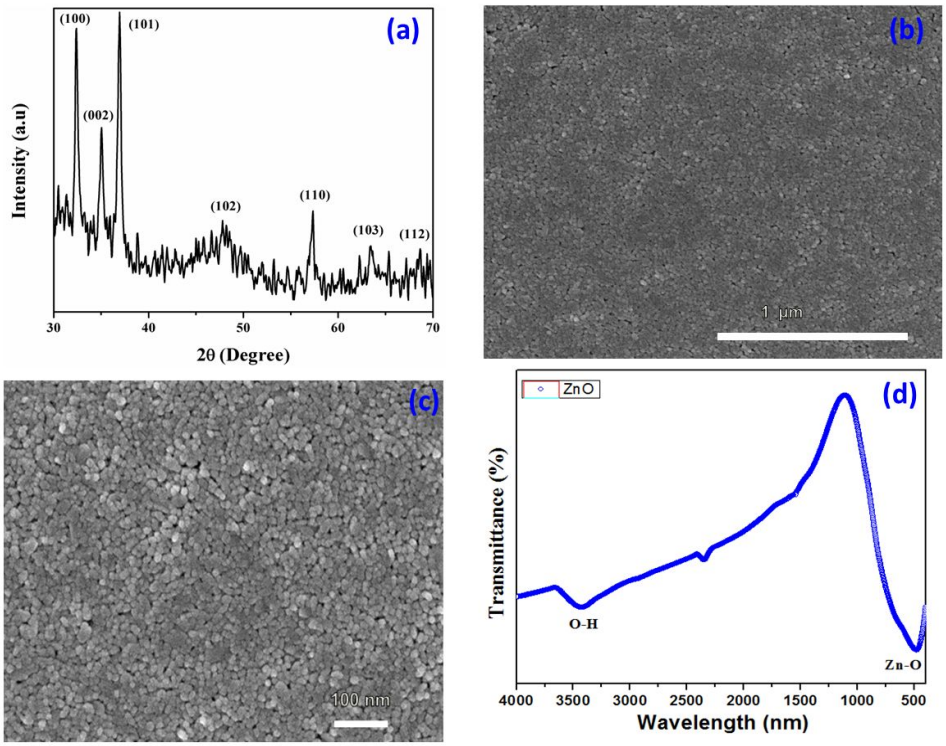

Figure 3-9 (a) X-ray diffraction of nanostructured ZnO thin film, Surface morphology, (b) low magnification FE-SEM, (c) high magnification FE-SEM, and (d) FT-IR analysis

3.2.2.2 Surface morphology

FE-SEM analysis was used to investigate the surface morphology of nanostructured thin film. Figure 3-9 (b-c) shows the FE-SEM micrograph of annealed ZnO film prepared by EHDA technique. The low magnification image revealed the homogeneous deposition of ZnO with less agglomeration due to influence of jet based coating technique (Duraisamy et al. 2012) and also enhance the ability of film adhesion on substrate. The high magnification FE-SEM shows the non-porous with spherical morphology of nanostructured ZnO film was achieved and the grain size was measured as 40 ± 5 nm. However, an ordered nanostructured thin film was achieved using EHDA process at room atmosphere.

3.2.2.3 Chemical composition and film purity

(i) FT-IR analysis

The FT-IR spectra ware mainly used to analyze the functional group and chemical composition of deposited ZnO thin film. Figure3-9d shows the spectra of annealed ZnO thin film. The observed significant peak at 475 cm^{-1} for Zn−O stretching mode, which was confirmed the presence of nanostructured ZnO thin film. However, the broad absorption in ~ 3340 cm^{-1} was observed because of the adsorption of water molecules on the surface of the thin film (Gayen 2011). No other characteristic peaks of organic moieties were observed, which was confirmed that the achieved high quality of nanostructured ZnO thin film annealed at 500 ^{o}C.

(ii) XPS analysis

The XPS analysis was investigate the ZnO thin film deposited through EHDA technique. Figure 3-10a shows the survey spectrum of nanostructured ZnO thin film, which was shows the presence of Zn2p and O1s (Nayak et al. 2010 and Smirnov et al. 2010). Figure 3-10b shows the deconvoluted spectrum of Zn2p, which is exhibited the characteristic peaks of E_b *(*Zn2p1*/*2*)* = 1045 eV and E_b *(*Zn2p3*/*2*)* = 1022 eV, respectively. The observed peaks confirm the presence of Zn in a +2 oxidation state in the matrix (Wei. 2007). The binding energy of oxygen peaks corresponds to 530.8 eV as shown in figure 3-10c No other characteristic peaks of any other organic residues were observed, which was confirmed in the survey spectrum, suggesting the high purity of thin film was obtained through EHDA technique.

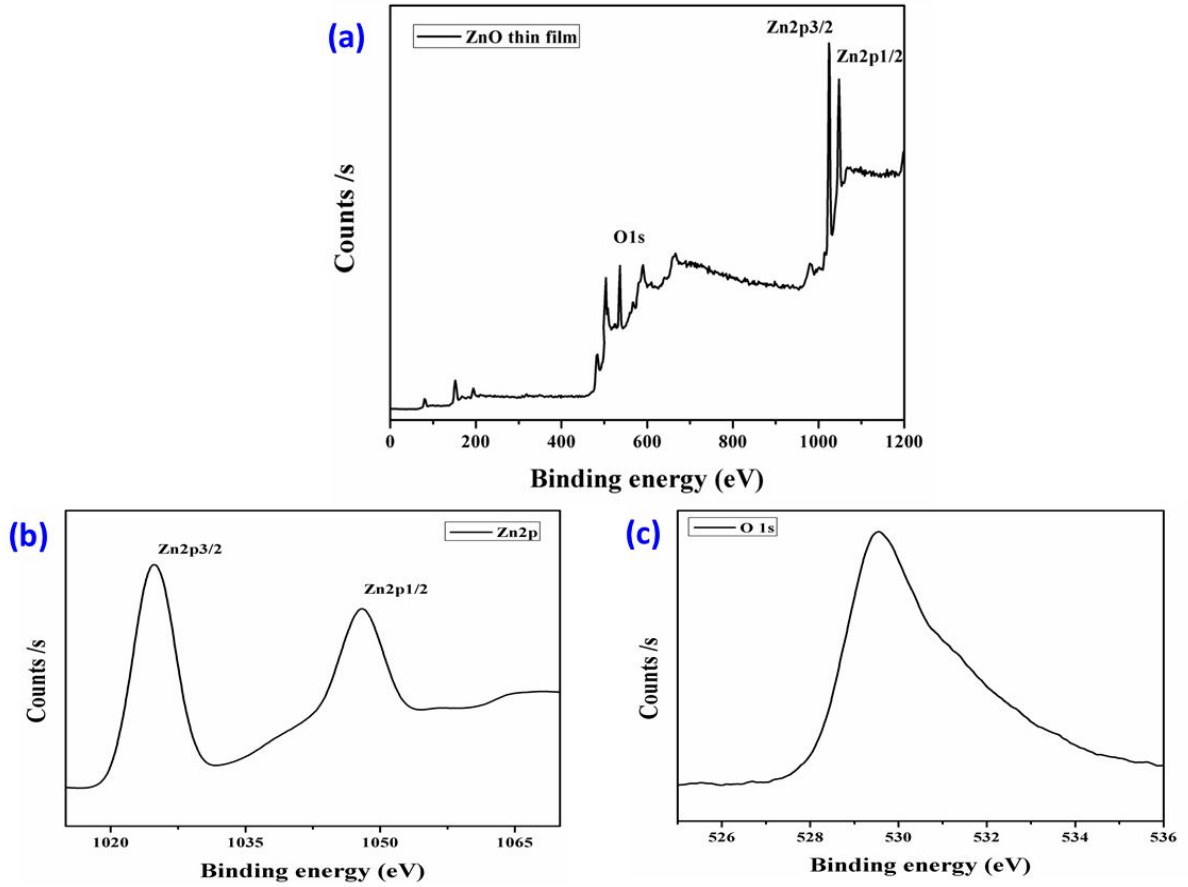

Figure 3-10 X-ray photoelectron spectroscopy of ZnO thin film deposited through EHDA process

3.2.2.4 Optical study

The optical properties of deposited ZnO thin film were analyzed through UV-vis spectrum in the wavelength range 300−750 nm. Figure 3-11a shows the optical transmittance of annealed thin film. The deposited thin film exhibit an average optical transmittance was nearly ~ 90 % in the visible region. The good optical transmittance was achieved may be due to densification of film crystallites (Smirnov et al. 2010). The optical energy band gap of thin film can be estimated by using Tauc model equation (Krishnamoorthy et al. 2011) as given below:

$$\alpha = \frac{A(E_g - hv)^n}{hv} \quad \text{..... [6]}$$

Where α is the absorption coefficient, A is a constant, $E_g$is the energy band gap and n is direct transition (n =1/2 or 3/2). However, the energy band gap was calculated from the relationship between $(\alpha hv)^2$ and hv is plotted. The energy band gap (E_g) was obtained by extrapolating the linear portion to the photon energy (eV) axis as shown in figure 3-11b. The band gap was found to be 3.17eV. The obtained value was in good agreement with the bulk ZnO (Smirnov et al. 2010). Moreover, the deposited nanostructured ZnO thin film is more suitable for electronic applications due to good transmittance with wide band gap.

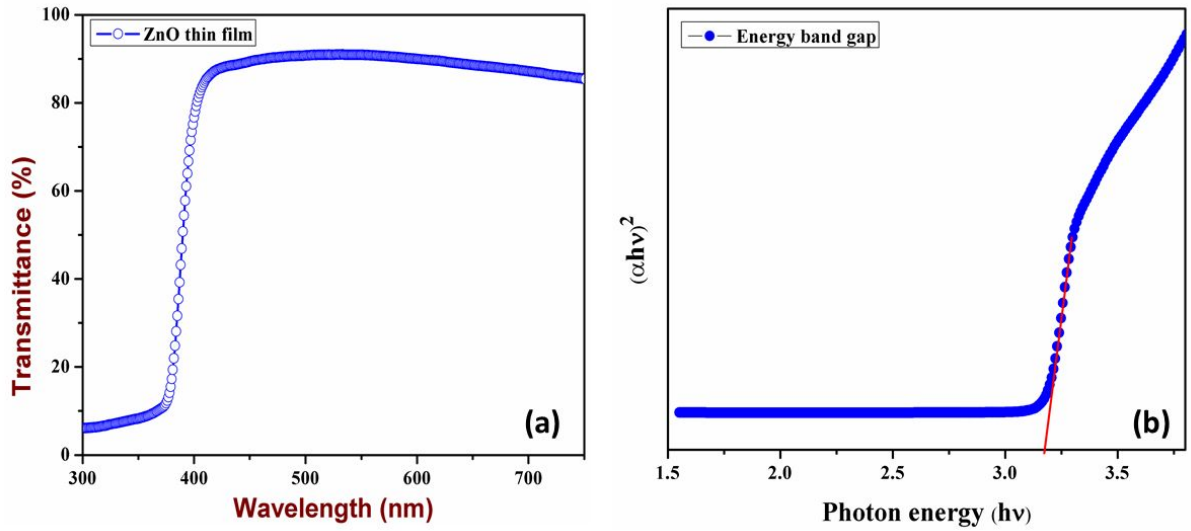

Figure 3-11 (a) UV-vis spectra of ZnO thin film shows transmittance curve, (b) Tauc plot of determining the optical band gap ZnO thin film

3.2.2.5 Photocurrent study

The *I–V* characteristics of the fabricated device consists of nanostructured ZnO thin film and the electrodes are made by the silver using silver nanoparticles ink, which is deposited through electrohydrodynamic printing (Arshad et al. 2011). The I–*V* analysis was measured at fixed level

of UV light illumination (λ=365 nm) in room atmosphere. Figure.3-12a shows the *I−V* curve measure in the presence of light illumination with wavelengths of 365 nm and compared with absence of UV light or dark. The *I−V* analysis exhibit the semiconducting behavior of ZnO thin film. The device exhibits the tremendous change in the conductivity under UV illumination as shown in figure 3-12a which is confirmed that the nanostructured ZnO is very quickly responding to UV illumination. Figure 3-12b shows the time dependence of the photocurrent under periodic UV light illumination, it is most important to study the temporal response of fabricated ZnO thin film based device. The photoresponse of nanostructured ZnO measured at 1V. In presence of UV illumination, the conductivity is raised suddenly from off-state to on−state and attains saturation. The photoconductivity remains in saturation until removal of UV illumination. On removal of UV light, the conductivity dropped and back to off− state.

The photoconductivity phenomena in ZnO are mainly related either surface or bulk related process. In surface related process are occurred due to adsorption and desorption of oxygen (O_2) on the surface of ZnO. Generally, three types of photocurrent process are expected during photo excitation such as (i) chemisorption of O_2, (ii) desorption of O_2 and (iii) recombination of electron−hole pair. In the absence of UV illumination or dark condition, the O_2 molecules are easily chemisorbed on the surface of nanostructured ZnO from atmosphere due to presence of trap level and oxygen vacancy. The adsorbed O_2 molecules can easily trap the free electron from the surface near the Zn lattice as $O_2\,(g) + e^- \rightarrow O_2^-$ (adsorbed species). This process leads to decrease the conductivity of ZnO due tolarge number of ionized oxygen (O_2^-) molecules (Dwivedi et al. 2013 and Dhara and Giri. 2011). Under the UV illumination, the electron-hole pairs are generated ($h\nu \rightarrow e^- + h^+$) by absorption of light radiation, which is significantly

contribute to the conductivity raise due to free charge carriers. The holes eventually involved in the oxidization of ionized oxygen molecule and release the O_2 gas ($O_2^- + h^+ \rightarrow O_2(g)$ (desorption species)). The photoconductivity is attributed due to presence of crystalline quality, oxygen defects on the surface of ZnO thin film, which is occurred from fabrication process and annealing atmosphere. Hence, the result suggests that the photocurrent response could be related with its structural and surface properties of nanostructured ZnO thin film.

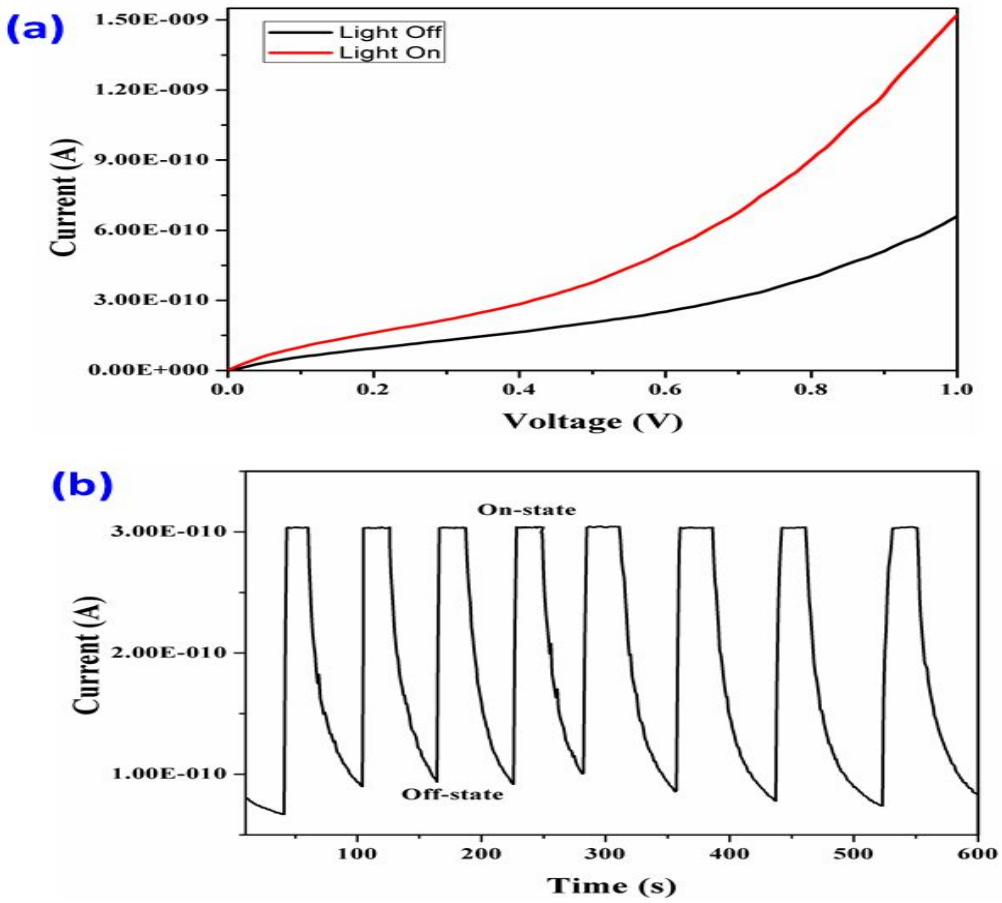

Figure 3-12 (a) Current−voltage measurement of ZnO thin film with and without UV-light illumination, (b) The curve exhibits photoresponse of ZnO thin film with respect to time under presence and absence of UV illumination

3.3 Nickel oxide thin film deposition and characterization

The nanostructured thin films are wide range of applications in electronic industries due to their unique physico-chemical properties. In particular, the anomalous electrical, surface electrochemical activity and mechanical properties of thin films are varied with respect to surface morphology, phase crystallinity and chemical nature of the deposited materials. Therefore nanostructured thin films are always considered as significant building blocks for fabrication of micro/nano devices such as solar cells, diodes, supercapacitors and memristors, etc. (Schubert et al. 2012, Wang et al. 2012, Gwinner et al. 2010 and Duraisamy et al. 2012). In these aspects, a tremendous amount of research has been directed to study the functional thin films in the field of science and technology (Tang et al. 2011, Li et al. 2009 and Shua et al. 2010).

Nanostructured metal oxides have received a great deal of research on functional thin films due to its physico-chemical properties and its potential applications. There are numerous metal oxides (TiO_2, ZnO, NiO, CuO, MnO_2, and V_2O_5 etc) with different structural morphology are used to develop the nanostructured functional thin films(Choi et al. 2012, Awais et al. 2013, Wei et al. 2009 and Song et al. 2012). All metal oxides have their own merits and demerits. In this aspect, nickel oxide (NiO) attracts particular interests due to its excellent properties and importance in many applications. Generally, NiO with NaCl type structure is good antiferromagnetic properties. A wide band gap NiO, being a buffer layer for solar cells and light emitting diode applications (Sato et al. 1993 and Steirer et al. 2011). The NiO with high specific capacitance, thermal/chemical stability and low cost can be used as electrodes in the electrochemical supercapacitors and battery applications (Wang et al. 2013, Srinivasan and Weidner 2000 and Zhong et al. 2011). The fabrication of NiO thin film has been achieved by

various techniques such as spray pyrolysis, CVD, reactive sputtering, sol-gel process and dip coating, etc (Ghamdi et al. 2009 and Muecke et al. 2009). However, CVD and sputtering techniques are capable of fabricating uniform thin layers but they are very expensive and difficult to handle (Ganan-Calvo et al. 1997). Other processes are easy to handle for solution based thin film deposition but achieving uniform layer with desired area and large scale deposition are very difficult aspects until now (Choi et al. 2012 and Kim and Kim 2006).

In order to develop a new technique for the fabrication of high purity and large area thin film deposition with low cost has recently attracted many researchers. With this motivation, we employed the solution based electrohydrodynamic atomization (EHDA) technique. EHDA is one of the advanced techniques for nanostructured NiO thin film deposition on glass substrate. In this technique, electric potential is applied onto a liquid jet and the jet is further dispersed into fine droplets due to the influence of repulsive forces between the charged droplets. The presence of similar polarity of charged droplets are preventing the coalescence in the range of micron to nano scale. Finally, uniform sized droplets are deposited on the substrate without any irregular arrangement of the layers morphology. Recently, Mahalingam et al and Choi et al reported the deposition of TiO_2 thin film through EHDA technique (Mahalingam et al. 2007 and Choi et al. 2012). In EHDA, the surface morphology of deposited thin films has been controlled by concentration of precursor solution, flow rate, applied potential, standoff distance (from nozzle tip to substrate) and substrate velocity (Rietveld et al. 2008 and Muhammad et al. 2011).

In this work, we report the deposition of NiO thin film through EHDA technique, which can be investigate as an electrode for supercapacitor application. The film uniformity and surface morphology controlled via atomization process is elucidated in detail. The phase crystallinity, surface morphology and film purity of thin films were investigated by X-ray diffraction, FE-

SEM and FT-IR analysis. Optical and electrical characterization of NiO thin film was characterized through UV-vis analysis. The electrochemical properties of NiO were explored in details using the cyclic voltammetry.

3.3.1 Materials and methods

3.3.1.1 Materials used

Nickel (II) acetate tetrahydrate (Ni $(CH_3COO)_2 \cdot 4H_2O$) and Tritont X100 were received from Sigma Aldrich, South Korea. Ethanol was purchased from Dang Chemicals. All chemicals were used without further purifications.

3.3.1.2 Preparation of precursor ink and its properties

0.5 M of nickel (II) acetate tetrahydrate (Ni $(CH_3COO)_2 \cdot 4H_2O$) was added into 5 ml of ethanol and vigorously stirred at 45 ^oC for 30 min. Then 1.5 ml of non-ionic surfactant (triton X100) was added drop by drop within 2 min into the above solution and the stirring was continued for 2 h at 60 ^oC. Finally, the homogeneous dispersion of nickel oxide precursor solution was obtained and used for further experiment. The physical properties of precursor solution were given in Table. 33.

Parameters	Values
Viscosity	2.57 mPa S
Electrical conductivity	32×10^{-6} S cm^{-1}
Surface tension	26 mN m^{-1}

Table 3-3. Physical properties of precursor solution

The precursor solution was prepared from nickel (II) acetate terahydrate, ethanol and non-ionic surfactant (Triton X100). Ethanol was used as a solvent medium due to high dielectric with low surface tension, which is more suitable for EHDA (Choi et al. 2012). However, water could not be used as a solvent due to high surface tension and high electrical conductivity, which prevents the stability of Taylor cone (Ijsebaert et al. 2001 and Duraisamy et al. 2012). In order to achieve a stable and non-agglomerated uniform dispersion of precursor solution, triton X100 was used as a surfactant.

3.3.1.3 Deposition of NiO thin film

In EHDA, thin film deposition of NiO was achieved at a stand-off distance of 16 mm with substrate velocity of 3 mm/s. Prior to film deposition, the substrate was cleaned via acetone, isopropanol, DI-water to remove all adsorbed impurities and further dried under UV light for 300 s. Finally, the glass substrate was subjected to O_2 plasma treatment to enhance the surface hydrophilic nature, which indirectly plays a key role to promote the film adhesion. The deposited thin film was sintered at 450^{o}C for 2 h and the film was used for further characterization.

3.3.2 Results and discussion

3.3.2.1 Taylor cone and spray formation

In EHDA technique, to achieve a Taylor cone or stable cone-jet mode is the most important atomization mode for uniform thin film deposition. However, the stability of Taylor cone mainly depends upon the physical properties of precursor solution, flow rate and applied potential. In EHDA, the precursor flow rate starts from a minimum value and reaches to a maximum with respect to the applied potential in order to find the optimum flow rate and applied potential for stable Taylor cone formation (figure 3-13a). Based on this procedure a flow rate of 250µl/h has been used throughout the experiment for thin film deposition. At initial voltage, the dripping mode was appeared and it was maintained until micro dripping was initiated. When the applied potential was increased, unstable cone jet was observed at 4.1 kV and it was maintained until 5.1 kV. Finally at 5.1 kV, the most important atomization mode of stable cone jet or Taylor cone was observed. Further, increasing the voltage beyond 5.8 kV, multi-jet was observed. These different atomization modes were captured and they are shown in figure 3-13b. The uniform deposition of NiO thin film was achieved via Taylor cone at 5.1 kV and it was sintered at 450 ^{o}Cto achieve a NiO thin film on glass substrate.

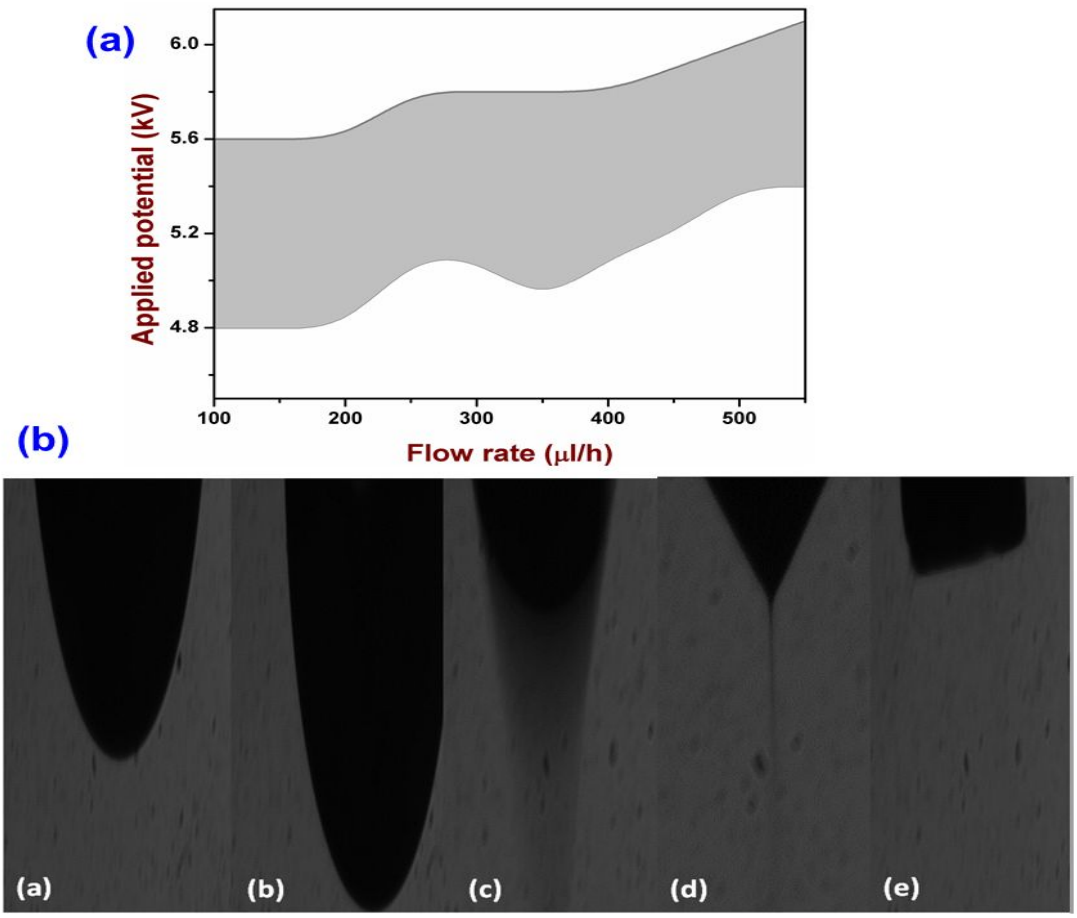

Figure 3-13 (a) Operating envelop of NiO precursor solution, (b) Atomization mode: (a) dripping, (b) micro-dripping, (c) unstable cone-jet, (d) stable-cone-jet, (e) multi-jet

3.3.2.2 Structural analysis

X-ray diffraction was used to examine the phase purity and crystallinity of deposited thin film. figure 3-14 revealed the XRD pattern of as deposited NiO thin film by EHDA method. The diffraction peaks appearing at $2\theta = 37.28^{o}$, 43.28^{o}, 62.88^{o}, 75.28^{o} and 79.48^{o} respectively, which was indexed as (111), (200), (220), (311) and (222) plane. The observed crystalline planes correspond to face centered cubic structure of NiO thin film (JCPDS No. 78-0643). No other peaks corresponding to $Ni(OH)_2$ was observed indicating the purity of the fabricated NiO thin film.

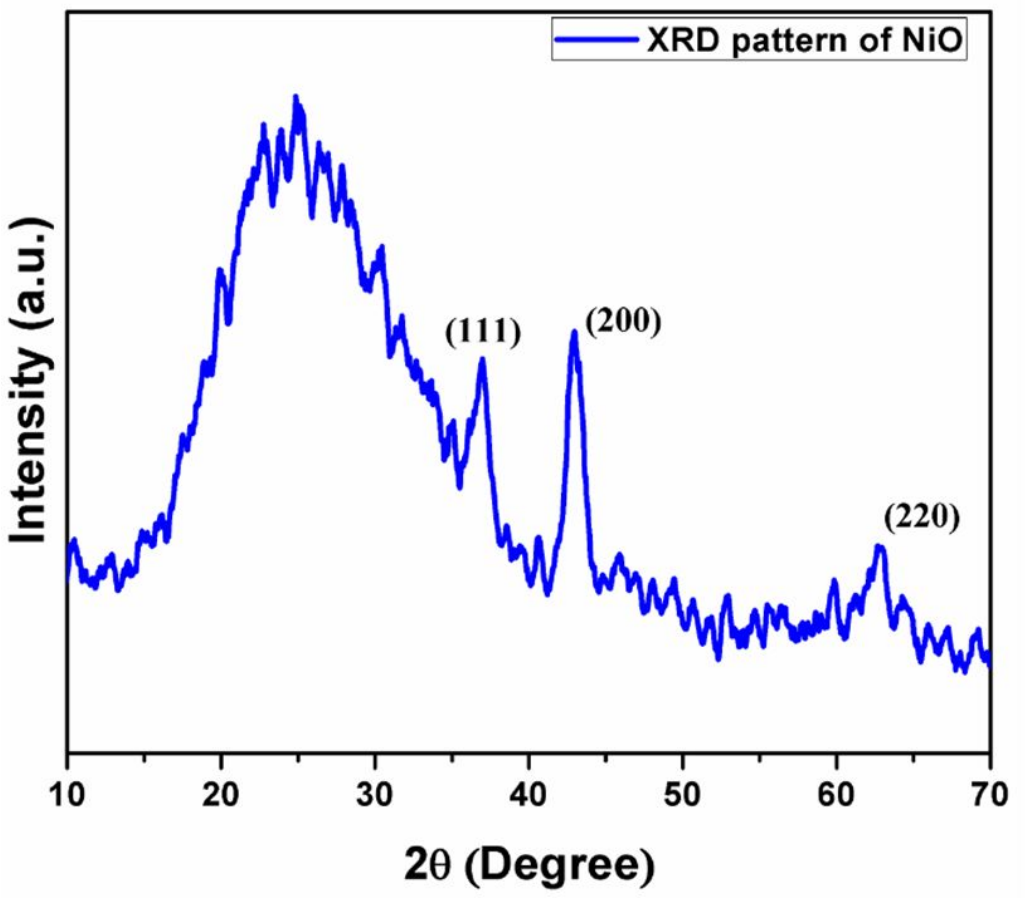

Figure 3-14 X-ray diffraction pattern of NiO thin film

3.3.2.3 Surface analysis

The surface morphology of thin film was studied by FE-SEM analysis. Figure 3-15 revealed the morphological study of deposited NiO thin film. The low magnification FE-SEM shows the uniform deposition of nanostructured NiO with void free surface morphology. The grain boundary of deposited NiO interacted with each other, which is significantly reducing the surface roughness of thin films. Figure 3-15b reveals the high magnification FE-SEM image of NiO thin film. It shows that the deposited NiO is in plate like surface morphology and uniform interconnection of grain boundaries.

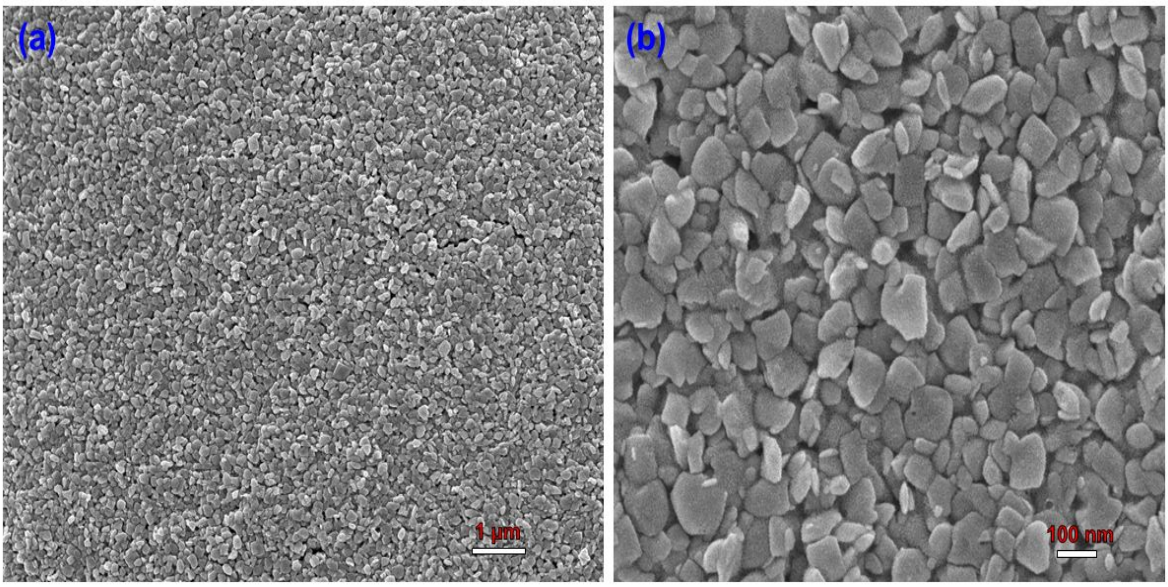

Figure 3-15 FE-SEM analysis of NiO thin film

The topographical image and surface roughness of deposited thin film was investigated by optical profiler (Aal et al. 2009). Figure 3-16shows optical image of deposited NiO thin film through EHDA technique. The topographical image revealed the nanostructured thin film has smooth surface on glass substrate due to stable Taylor cone process. However, the 3D image shows that the fabricated NiO film has pin-hole free surface and the surface roughness was found to be ~ 2 nm. The optical profiler analysis confirmed that the uniform deposition of the nanostructured NiO thin film was achieved (FE-SEM image). The uniformity and low surface roughness of deposited NiO thin film through EHDA technique play a significant role in thin film applications.

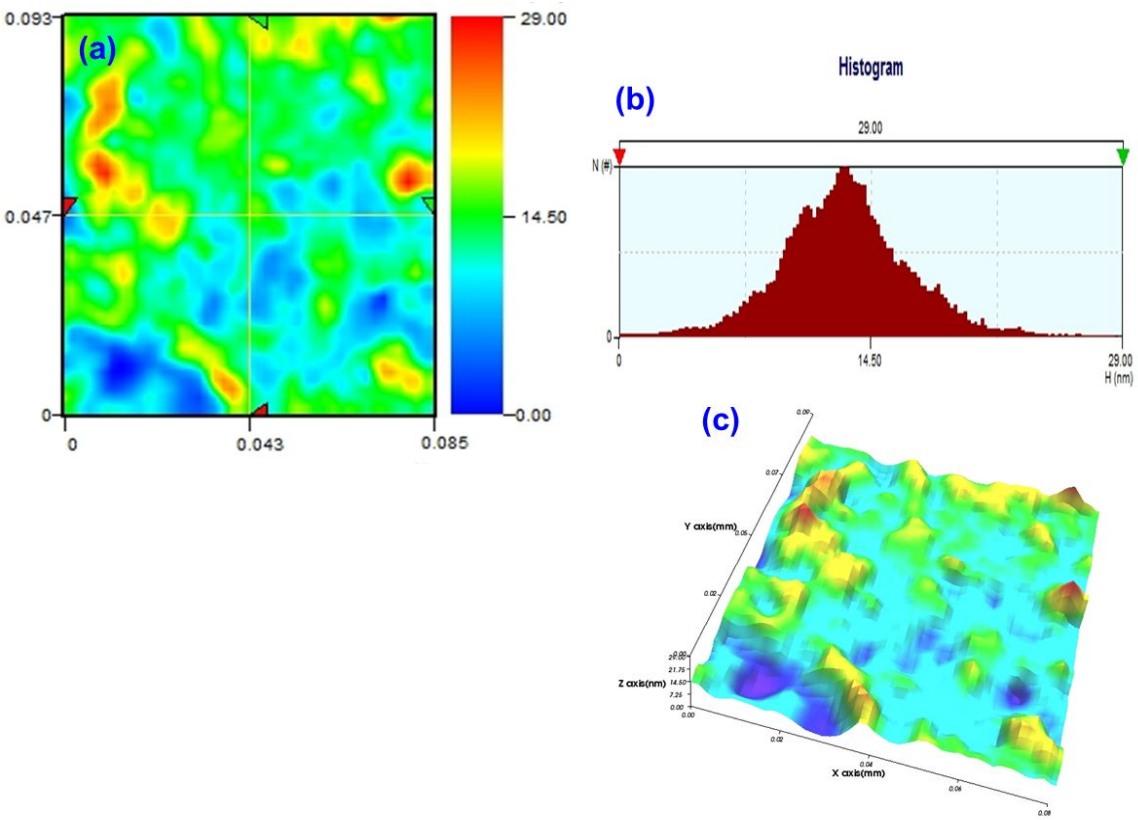

Figure 3-16 Optical surface profiler, (a) 2D surface image of NiO thin film, (b) Histogram of thin film, (c) 3D image of thin film

3.3.2.4 Chemical composition and surface purity

XPS analysis is widely used to investigate the surface chemistry and purity of deposited thin film. Figure 3-17shows the survey spectrum of NiO thin film deposited through EHDA technique. In survey spectrum, the peaks of Ni2p and O1s were recorded as deposited thin film (Wruk et al. 1993). The deconvoluted spectrum of Ni2p revealed the binding energy peaks at 854.8 and 873.6 eV which corresponds to NiO 2p3/2 and 2p1/2, respectively (Zhou et al. 2006) whereas, O1s peaks was observed at 530 eV (Shu et al. 2010). However, no other characteristic peaks from $Ni(OH)_2$ was observed, suggesting the purity of NiO thin film.

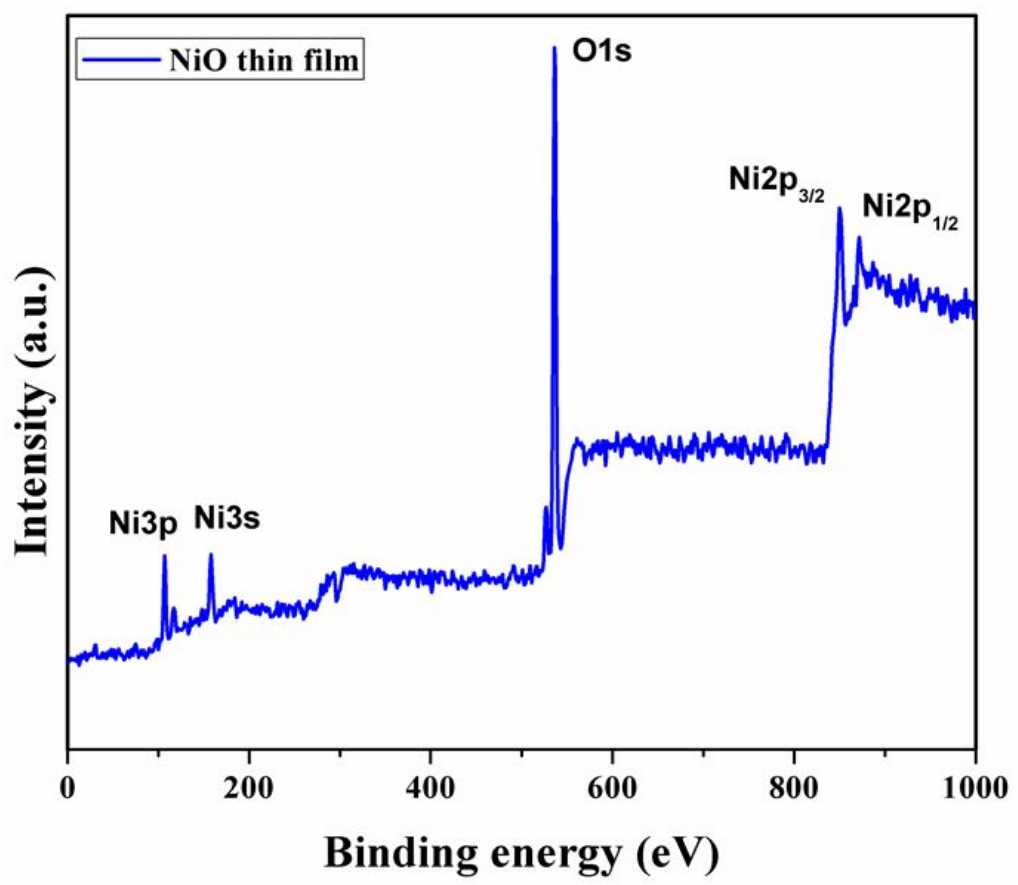

Figure 3-17 X-ray photoelectron spectroscopy of deposited NiO thin film

3.3.2.5 Optical analysis

The optical property of deposited NiO thin film is measured by UV-vis analysis. The transmittance of thin film was observed in the range of 300−700 nm wavelengths as shown in figure 3-18a. NiO thin film shows the transmittance value of 80~ 83% in the visible region (Das et al. 2010). In contrast the absorption spectrum showed the absorbance onset edge at 360 nm, which confirms that the NiO has low absorbance in the visible region. The optical band gap energy from the UV-vis spectra can be estimated by using the following equation.

$$\alpha = \frac{A(E_g - h\nu)^n}{h\nu} \quad \text{..... [7]}$$

Where, α is the absorption coefficient, A is a constant, E_g is the band gap and n is equal to 1/2 for an indirect transition. The band gap was estimated from a plot of $(\alpha h\nu)^{1/2}$ versus photon energy ($\alpha h\nu$). In figure 3-18b, the intercept of the tangent to the plot gave a good approximation to the band gap energy for this indirect band gap material. The optical energy band gap of NiO thin film was calculated and found to be E_g= 3.7 eV (Awais et al. 2010). The wide band gap was observed in NiO thin film. However, the deposited NiO thin film was more applicable as an electron blocking or hole transport layer in solar cells application (Park et al. 2010), which significantly controls the electron-hole recombination process.

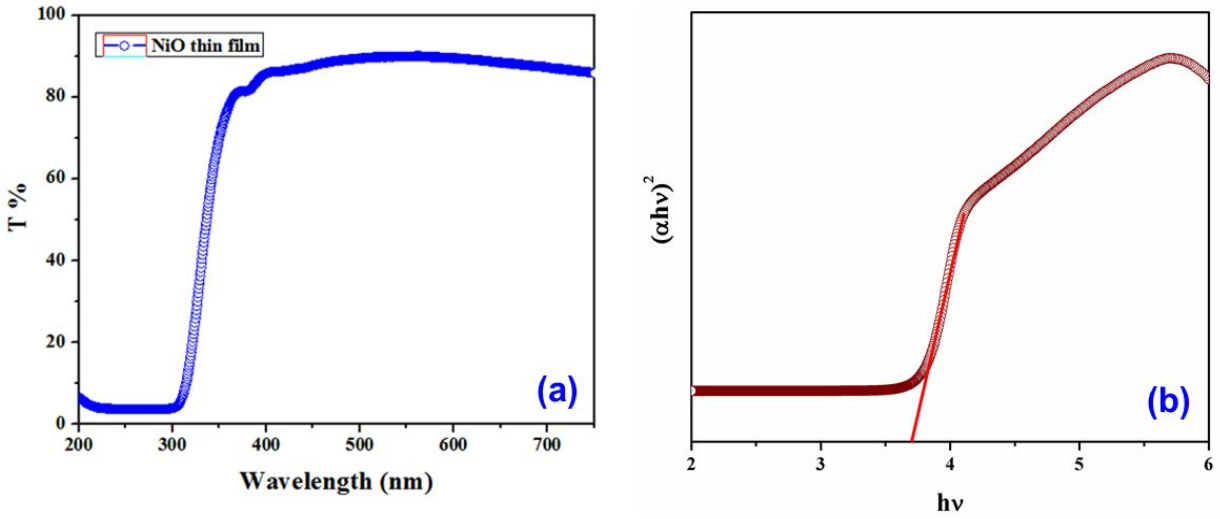

Figure 3-18 Optical properties of NiO thin film, (a) Transmittance curve of thin film, (b) Energy band analysis of thin film

3.3.2.6Electrochemical measurements

Electrochemical properties of NiO thin film is examined through electrochemical workstation in a three-electrode mode, including platinum as counter electrode and a standard Ag/AgCl electrode as reference electrode. Herein, the NiO thin film is deposited on nickel foam via EHDA technique, which acts as a working electrode. The electrochemical properties are studied

using 1M solution of NaOH as electrolyte. Figure. 3-19 displays the CV curves of the NiO nanostructures measured at different scan rates at the potential range 0 to 0.7 V.

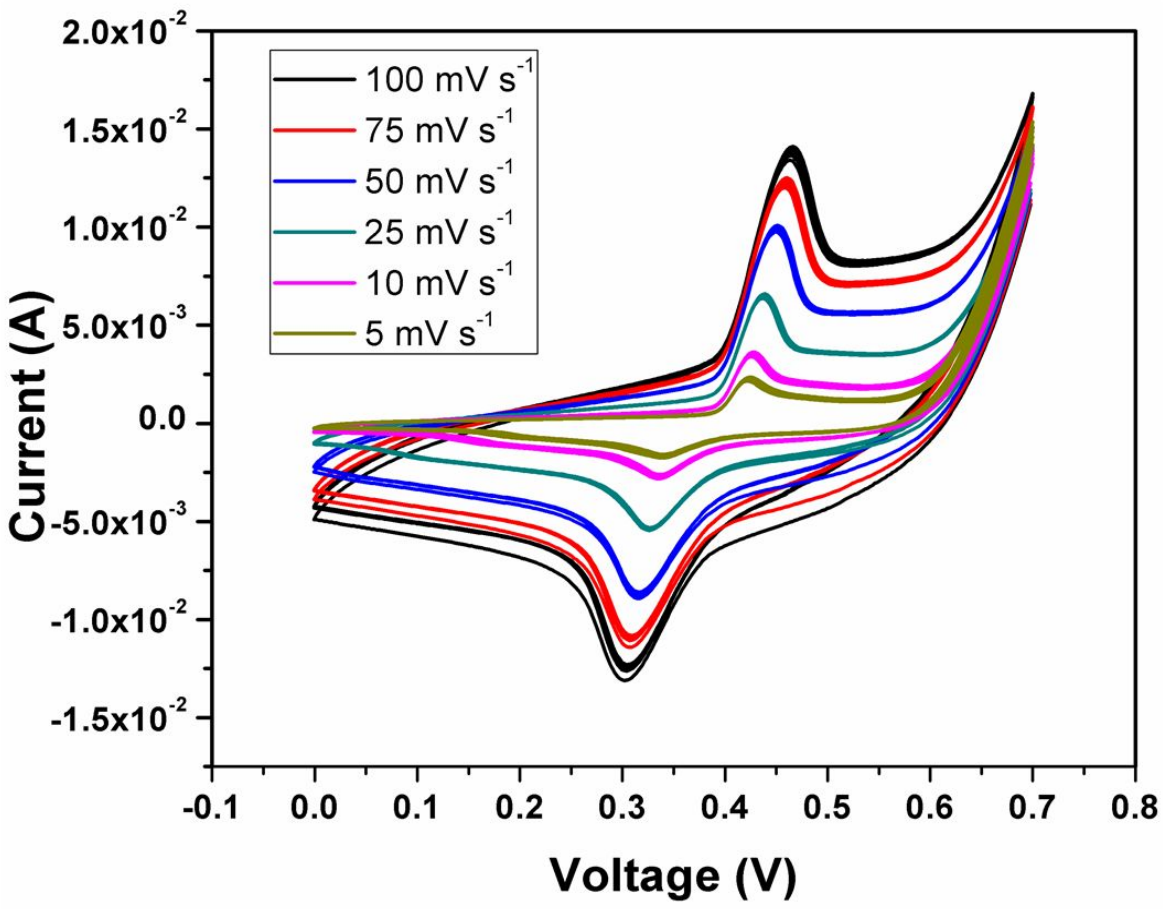

Figure 3-19 Cyclic voltammetry curves of NiO thin film measured in 1M NaOH electrolyte

It shows that NiO nanostructures exhibit symmetric CV curves in forward and reverse sweeps. It is clear from the CV curves which show a pair of redox peak due to the transition between +2 and +3 oxidation state of NiO. During this process, NiO converts into NiOOH by changing its oxidation state from +2 to +3 and vice versa. The reaction occurs at the surface layer of the NiO with respect to OH ions in the electrolyte, which are shown in the equation:

$$NiO + OH^- \rightarrow NiOOH + e^-$$

The CV curves of NiO nanostructures with different scan rate shows that the current under the curve was slowly increased with respect to the increase in scan rate. This confirms that the voltammetric currents are directly proportional to the scan rate, signifying an ideal capacitive behavior. The specific capacitance (Csp) can be calculated from the CV curves according to the given equation [24]:

C_{sp} ……..... [8]

where "*I*" is the current, "*S*" is the specific capacitance, "∫ *V*" is the potential window and "*w*" is the mass of the active material. With the increase in scan rate, the area of the CV loop increases and shows a decrease in specific capacitance as observed from figure. 3-19 and Table.3-3. This may be due to the fact that during faster scan rate, the active material (NiO) is not fully utilized because of slow diffusion rates of ions at relatively faster scan rates (Guo et al. 2011 and Veerapandian et al. 2012). The maximum specific capacitance (28F/g) was achieved with a scan rate of 5 mV/s. This is attributed to the deposited nanostructured NiO thin film via EHDA are significant interest in the energy storage application.

Scan rate (mV/s)	**C_{sp} (F/g)**
5	28

10	16
25	10
50	7
75	6
100	5

Table 3-4 Specific capacitance of NiO electrodes with different scan rates

4. One dimensional silver nanostructures embedded PEDOT:PSS thin film

Engineering one dimensional nanostructure with organic polymers will produce enhanced properties in the resulting hybrid material, which is mainly due to the physico-chemical properties of nanostructured materials. Nowadays, organic conducting polymers gained significant interests in the electronic industry due to its good optical and electrical properties, low cost, environmentally stable and easy processability on flexible/non-flexible substrates (Timpanaro et al. 2004). The presence of π-orbitals in the conductive polymers plays a vital role in their charge transport mechanism (Friend et al. 1999, Sariciftci et al. 1992 and Hüttner et al. 2008). Among the widely used conducting polymers, polyaniline based derivatives are documented as an environmentally toxic due to the presence of benzidine moieties (Groenendaal et al. 2000). The other hetero-aromatic polymers and their derivatives such as polyphenylenes, polypyrroles, polythiophenes are shown to be environmentally non-toxic and possess good physico-chemical properties. In particular, thiophene based derivatives such as poly(3,4-ethylenedioxythiophene) (PEDOT) has received much attention in optoelectronics such as solar cells, light emitting diodes, light emitting transistors (Ahlswede et al. 2008, Hong et al. 2008 and Burroughes et al. 1990). The major drawback of PEDOT which limits their usage in the above mentioned applications as it lacks from solubility in different solvents (Groenendaal et al. 2000). This can be overcome by incorporating some functional derivatives such as poly(styrene sulfonic acid) (PSS) (Nardes et al. 2008). The PSS doped PEDOT has good optical properties but less conductivity due to the presence of insulating PSS in the PEDOT matrix (Yun et al. 2011). The conductivity of PEDOT:PSS can be significantly increased by introducing some conductive

materials such as organic conducting solvents, metallic grids, MWCNT/SWCNT, metallic nanowires (Yun et al. 2011 and Gaynor et al. 2011). Metallic nanowires such as silver will be of better choice for using as an additive for PEDOT:PSS in order to improve electrical conductivity, optical properties, air stability with mechanical flexibility and often cost effective (Hu et al. 2010 and Sun et al. 2002).

The most important criteria for the development of the metal incorporated polymer nanocomposition thin films are achieving uniform deposition. Up-to-date, there are several types of deposition process are available for the fabrication of nanostructure thin films such as spin coating, dip coating, sputtering, chemical vapor deposition (CVD), physical vapor deposition (PVD), and pulsed laser deposition (PLD) (Kim et al. 2011 and Molina et al. 2012). The spin coating and dip coating method possess the advantage of being solution processed thin film deposition, however, controlling the film thickness and large area production for commercial application is limited in these method (Ramadoss et al. 2012 and Sriwong et al. 2012). On the other hand, the CVD and PVD based techniques require high vacuum system and also more expensive (Sriwong et al. 2012 and Jaworek and Krupa. 1999). Hence, the development of new cost effective methods for the fabrication of nanostructured thin films is highly encouraged due to their widespread applications. Being a non-vacuum technique with cost effective and also solution processability, electrohydrodynamic atomization (EHDA) becomes an ideal choice for overcoming the above mentioned demerits of the conventional coating methods. Moreover, this method also promising for the large-scale fabrication of nanostructured thin films with controlled film thickness and also can be used for different variety of substrates either flexible/non-flexible (Duraisamy et al. 2012, Ellis et al. 2012 and He et al. 2011).

Being solution processable, EHDA technique relies on proper chemical engineering for the preparation of precursor ink solution which is mainly due to the basic principle of EHDA as follows: in a typical EHDA process, the surface tension of a liquid has been overcome by tangential electric filed to achieve a Taylor cone or stable cone-jet. The Taylor cone has further disintegrated into small droplets in the range from micrometer to nanometer scale with narrow size, charge and velocity distributions (Duraisamy et al. 2012). Several parameters such as physical (viscosity, surface tension, electrical conductivity) and chemical properties (solvent nature, structure of the materials) of precursor solutions or inks are needs to optimize prior to EHDA deposition.

In this study, we report the deposition of AgNWs/PEDOT:PSS nanostructured thin films via EHDA technique and the optimization process are investigated. The as-deposited thin films are widely characterized using FE−SEM, XRDand XPS analysis. The optical and electrical properties of AgNWs/PEDOT:PSS thin film is examined by using UV−vis spectrum and current−voltage measurement. A detailed study on the changes in the optical transmittance, sheet resistance of the fabricated thin films with respect to various spraying time is discussed in detail.

4.1 Materials and methods

4.1.1 Materials used

PEDOT:PSS (2.3 wt.%) was received from Agfa Materials Japan Ltd, Japan. Ethanol was purchased from Dang Chemicals, South Korea. Silver nanowires (AgNWs) were synthesized as reported in literature (Korte et al. 2008 and Ramasamy et al. 2012).

4.1.2 Preparation of AgNWs/PEDOT:PSS ink and its properties

The precursor ink for the deposition of AgNWs/PEDOT:PSS nanocomposite films was prepared via ultrasonication method using two different solution of AgNWs and PEDOT:PSS as starting materials for the ink. Briefly, 5 mL of solution containing AgNWs (0.5 wt.%) in ethanol was added dropwise to aqueous solution PEDOT:PSS (0.5 wt.%) under ultrasonication for 5 min. Finally, a homogeneous dispersion of AgNWs embedded PEDOT:PSS matrix ink was achieved as shown in figure 4-1. The preparation of stable precursor ink is very important in the EHDA deposition of material in order to achieve uniform thin films. Herein, for the EHDA deposition of Ag NW/PEDOT:PSS deposition, a 1:1 mol ratio of AgNWs embedded PEDOT:PSS ink is prepared through ultrasonication. Ultrasonication is used for achieving the homogeneous dispersion of inorganic material in organic matrix (Karthikeyanet al. 2009 and Krishnamoorthy et al. 2013). In addition, the AgNWs are energetically embedded on polymer matrix through ultrasonic waves,which help the homogeneous dispersion of AgNWs/PEDOT:PSS without affecting their chemical structure as confirmed through UV−vis absorbance (figure 4-2).

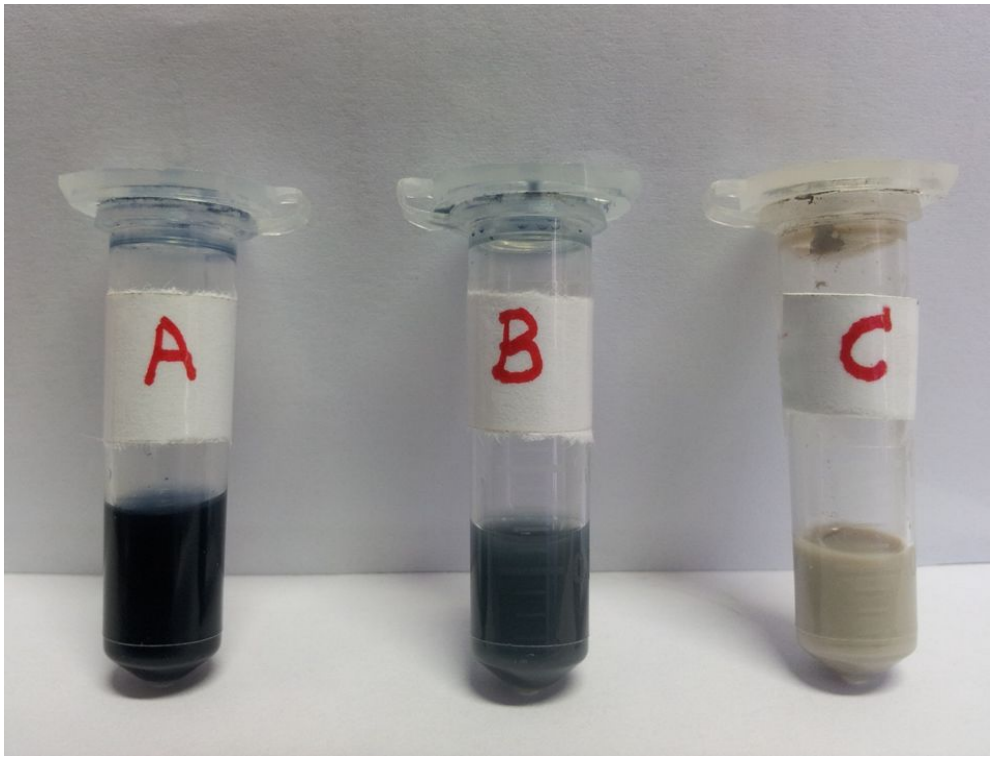

Figure 4-1 (a) Pure PEDOT:PSS ink, (b) Composite AgNWs embedded PEDOT:PSS ink, (c) Pure AgNWs ink

The UV-visible absorption spectra (figure 4-2) was used to elucidate the absorption peaks of AgNWs embedded PEDOT:PSS as compared with pure PEDOT:PSS and AgNWs. The pure AgNWs (spectrum (a)) were shown two absorption peaks at 390 nm and 350 nm corresponds to transverse plasmon resonance and transverse quadrupole resonance of AgNWs respectively (Ramasamy et al. 2012). The absorbance peaks confirmed that the presence of AgNWs without any other impurities. Figure 4-2 (spectrum (c)) revealed the sharp absorption peak at 225 nm due to the presence of PSS in polymer chain and the PEDOT absorbance in near-IR region (not shown here) (Memarzadeh et al. 2012 and Lin et al. 2009). However, the optical absorbance has been influenced by prepared composite (AgNWs@PEDOT:PSS) as shown in the spectrum (b). The peak intensity of pure PEDOT:PSS was reduced due to influence of AgNWs. Although, the absorbance peak of AgNWs was slightly shifted into lower wavelength as well as diminishes the

transverse plasmon resonance intensity peak. The intercalated AgNWs with PEDOT:PSS was play a key role to enhance the conductivity of PEDOT:PSS without affect the optical transmittance in the visible region. This result further confirmed that, no significant changes in the chemical structure of the PEDOT:PSS and silver nanowires during ultra-sonication process.

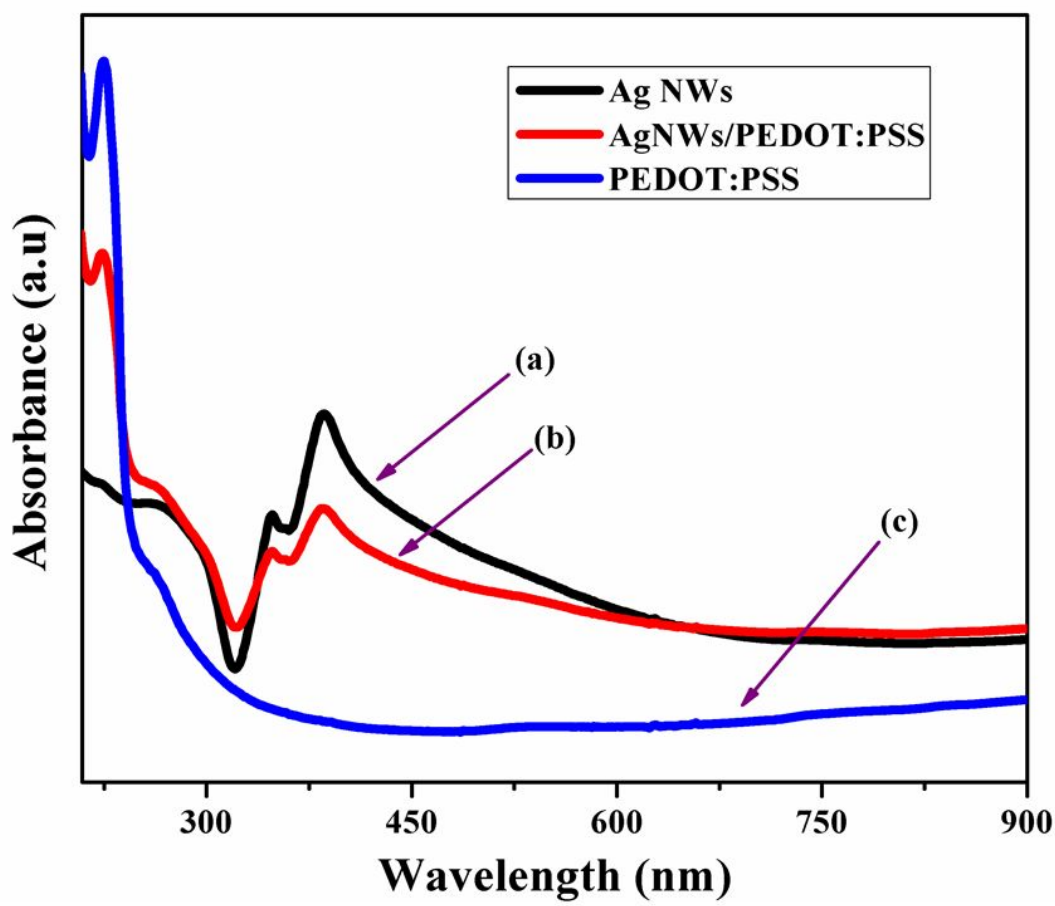

Figure 4-2 UV-visible absorbance spectra:(a)Pure AgNWs, (b)Composite of AgNWs/PEDOT:PSS, (c)Pure PEDOT:PSS

On the other hand, the preparation of suitable composite ink for EHDA process, the molar concentration of AgNWs and PEDOT:PSS is also very important. The ink prepared with this concentration about 1:1 ratio of AgNWs/PEDOT:PSS is stable more than 2 weeks and also

results in the deposition of uniform thin films, whereas, the decrease in the molar concentration of AgNWs with PEDOT:PSS significantly affected the surface morphology (figure 4-3) due to lower concentration of AgNWs embedded PEDOT:PSS matrix. Further, increase in the molar concentrations beyond the 1:1 mole ratio, adversely affect the ink stability. Hence, we used an optimum concentration of Ag NW/PEDOT:PSS in the ratio of 1:1 in the precursor ink for EHDA deposition and the phyico-chemical properties of the ink such as the viscosity, surface tension and electrical conductivity are given in Table 4-1.

Physical Properties	**Values**
Viscosity	2 mPa S
Surface tension	25mN m^{-1}
Electrical conductivity	6.4 μS cm^{-1}

Table 4-1 Physico−chemical properties of AgNW/PEDOT:PSS precursor ink for EHDA

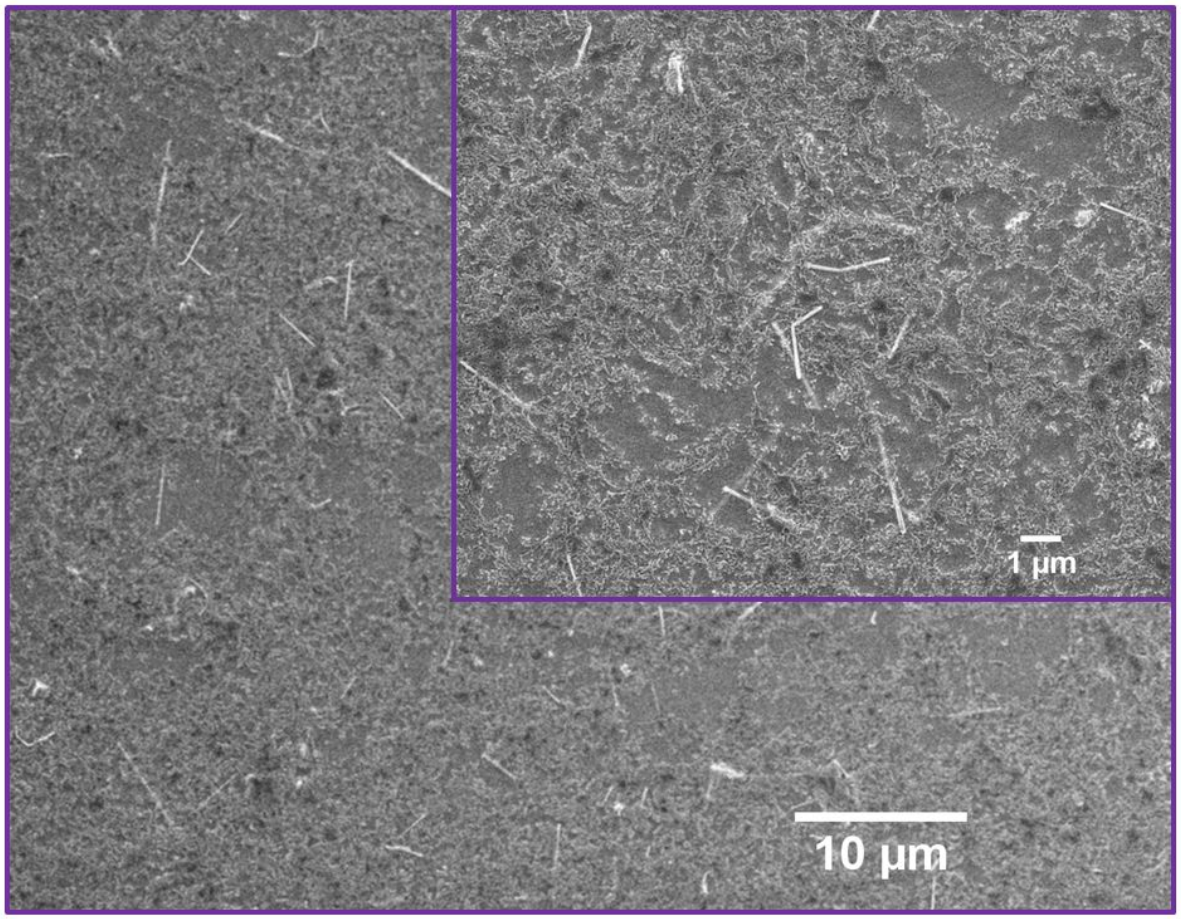

Figure 4-3 FE-SEM analysis: High magnification FE-SEM image of AgNWs embedded PEDOT:PSS thin film, the inset shows the low density of AgNWs embedded in a PEDOT:PSS matrix due to low concentration of AgNWs

4.1.3 Fabrication of composite thin film

Thin film deposition of AgNWs embedded PEDOT:PSS matrix was made on polyethylene terephthalate (PET) substrate through EHDA technique. Before the deposition process, the substrates are washed with solvents such as acetone, isopropanol and deionized water to remove the surface contaminations. Then, the cleaned substrate was irradiated with ultra violet light in a UV cleaner for 30 min. Finally, the substrate was subjected into O_2 plasma treatment to introduce the hydrophilic groups, which was enhancing the wetting and adhesion properties of

deposited thin film on PET substrate. During the atomization process, the substrate moving speed was maintained at 3 mm/s. Thin film deposition has been achieved by using 6 mm stand-off distance. Finally, the deposited film was annealed at 150 ^{o}C for 45 min. However, the deposited AgNWs embedded PEDOT:PSS thin film was compared with pure PEDOT:PSS thin film. The pure PEDOT:PSS thin film deposition through EHDA process with constant film thickness are achieved using metallic nozzle with internal diameter 410 µm and standoff distance between nozzle tip and substrate was 6 mm with substrate velocity 3 mm/s. Before the deposition process, the substrate was cleaned with acetone, ethanol and de-ionized water subsequently to remove the adsorbed impurities on the glass surface and followed by UV cleaning, plasma treatment to activate or enhance the surface adhesion. The ink has atomized with flow rate at a 250 µl/h throughout the experiment. The most important atomization mode of Taylor cone or stable cone-jet was achieved at an applied potential of 3.4 kV, which makes uniform deposition of PEDOT:PSS thin films. Further it was sintered at 150 $^{\circ}$C for 45 min.

4.2 Results and discussion

4.2.1 Characterization of silver nanowires

Figure 4-4a shows the XRD pattern of AgNWs which shows the four major peaks corresponds to the diffraction (111), (200), (220) and (311) planes of face centered cubic (fcc) silver (JCPDS card no. 04-0783). There are no other peaks corresponding to any such impurities or organic moieties were found in XRD pattern, suggesting a high quality of AgNWs were obtained. The absorbance spectra of pure AgNWs (as given in figure 4-2) show two absorption peaks at 390 nm and 350 nm corresponds to transverse plasmon resonance and transverse quadrupole resonance of AgNWs respectively. The surface morphology of the Ag NWs is studied using transmission electron microscopy (TEM) and the field emission scanning electron microscope

(FE-SEM) and the corresponding micrographs are given in figure 4-4(b-c). It shows the presence of nanowires with the diameters in the range of 70 ± 5 nm and lengths of tens of micrometers.

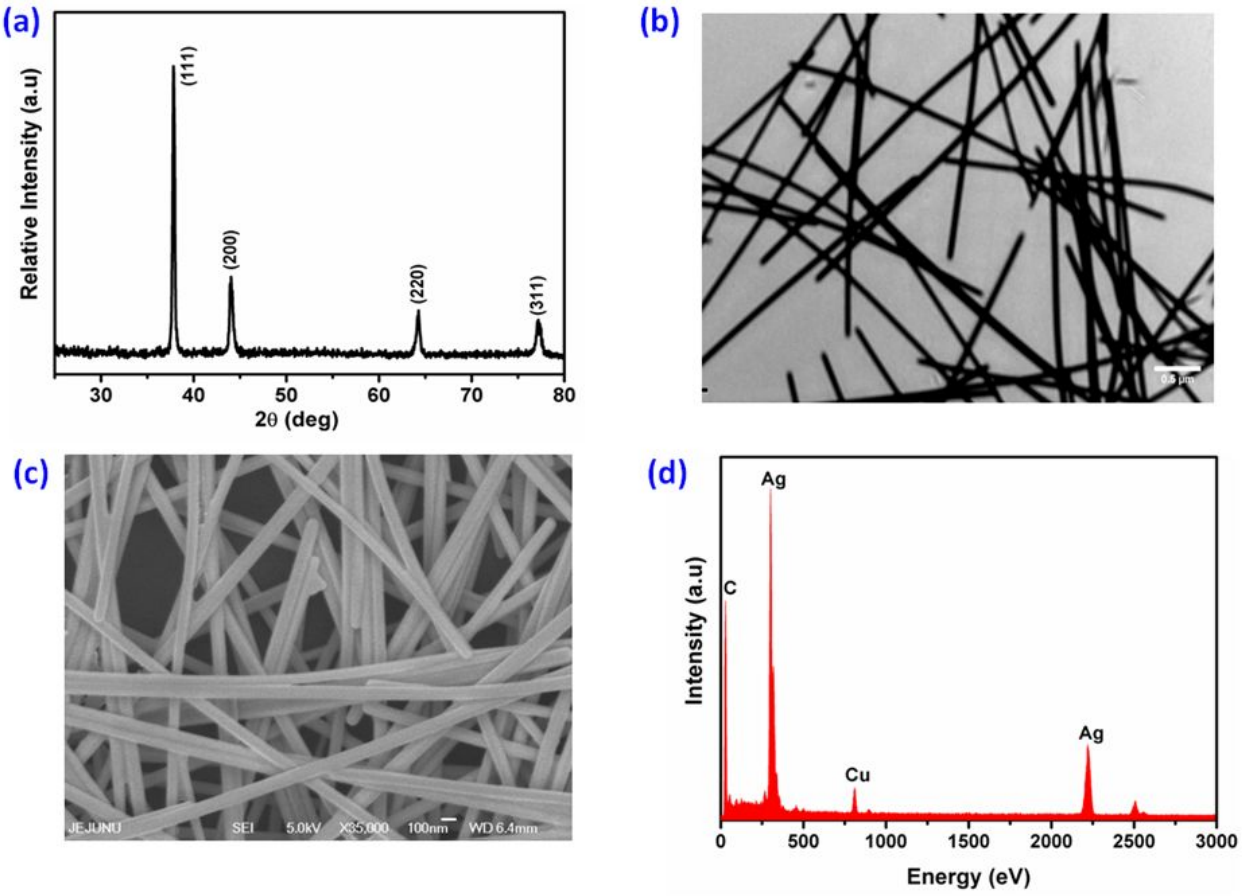

Figure 4-4 (a) X-ray diffraction pattern, (b) Transmission electron micrographs (c) Field emission scanning electron microscope and (d) Energy dispersive X-ray analysis of silver nanowires

In order to confirm the purity of the AgNWs, we also examined the energy dispersive X-ray spectroscopy (EDS) (figure 4-4d). Figure 4-4d shows the presence of only metallic Ag and no other elements such as oxide and other inorganic moieties in the AgNWs. This study demonstrates the synthesized AgNW possessing high degree of purity. Overall, the physico-

chemical characterizations illustrate that AgNWs is free of any impurities and it is used for further experiments in this study.

4.2.2 Taylor cone and spray formation

In EHDA technique, the precursor ink was sprayed using different flow rates (from minimum flow rate to maximum) with various applied potential (figure 4-5a) to determine the optimum flow rate and applied potential to achieve a Taylor cone or stable cone-jet. During the spray deposition, different atomization modes are observed such as dripping, micro-dripping, unstable-cone jet, stable cone-jet and multi-jet (Choi et al. 2012). However, at low flow rate, it is very difficult to achieve a continual spray whereas at high flow rate, irregular surface morphology is observed due to ejection of large droplet volume (Duraisamy et al. 2012 and Choi et al. 2012). However, in this experiment, the flow rate of 250 μl/h has been chosen for thin film deposition and the observed atomization modes are shown in figure 4-5b. The dripping is appeared from 0 kV to until micro-dripping is ejected (2.2 kV). The unstable-jet appeared at 3.0 kV and it is maintained until the voltage reaches 3.4 kV. At 3.4 kV, the Taylor cone or stable cone-jet is formed, which is the most important atomization mode for achieving uniform thin film. The multi-jet was appeared at 4.5 kV. If further increase in the applied potential, it led to jet discharge. Thickness of deposited thin film has been controlled by various factors such as ink concentration, flow rate, stand-off distance, and substrate moving speed or spray duration (Muhammad et al. 2011). This work is further deals with the influence of spray time on the structural, optical and electrical properties of AgNWs embedded PEDOT:PSS thin film.

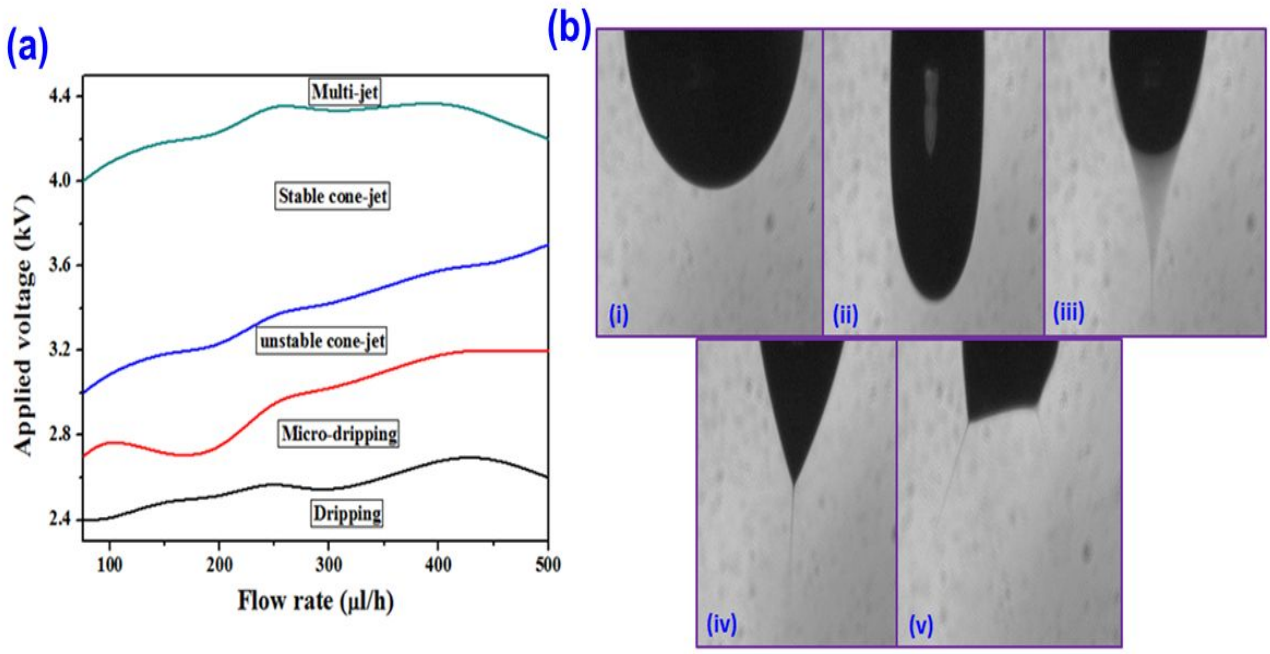

Figure 4-5 (a) Operating envelope of AgNW/PEDOT:PSS ink (b) Atomization mode during EHDA process, (i) dripping, (ii) micro-dripping, (iii) unstable cone-jet, (iv) stable cone-jet and (v) multi-jet

4.2.3 Structural analysis

The X-ray diffraction analysis is used to investigate the crystallinity of deposited thin films. Figure 4-6 shows the XRD pattern of deposited pure PEDOT:PSS and AgNWs embedded PEDOT:PSS thin film annealed at 150 °C. The XRD patterns of pure PEDOT:PSS thin film represents the amorphous nature of the polymer. However, there are significant changes in the XRD pattern were observed due to the addition of AgNWs in the PEDODT:PSS matrix. The XRD results of AgNW/PEDOT:PSS film exhibits strong crystalline peaks at 2θ = 38.3°, 44.5°, 64.4°, and 77.8° corresponds to the (111), (200), (220) and (311) planes of face centered cubic structure of silver nanowires (JCPDS card.no: 04-0783). This confirmed the presence of AgNWs in the PEDOT:PSS matrix in the as deposited films. Compared to the pure PEDOT:PSS thin films, which shows a broad diffraction peak corresponding to the amorphous polymer matrix, the

silver impregnated PEDOT:PSS thin films shows sharp diffraction peaks of silver which indicates the crystallinity of the films is improved due to the presence of silver in the polymer matrix.

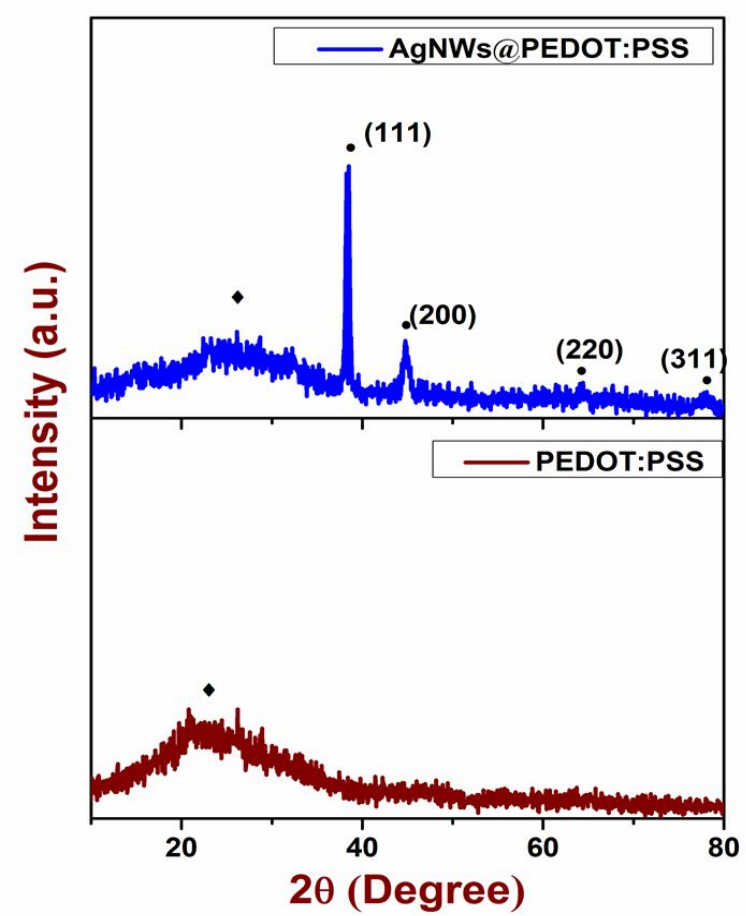

Figure 4-6 X-ray diffraction pattern of deposited pure PEDOT:PSS and AgNW/PEDOT:PSS thin film. The symbols (♦) and (●) represents the peaks corresponds to PEDOT:PSS and AgNWs respectively

4.2.4 Thickness of thin film

The thickness of the Ag NW/PEDOT:PSS thin films are measured by spectroscopic ellipsometry analysis (Venugopal et al. 2012 and Muhammad et al. 2012). The thickness is measured at 10 different points on the deposited film and the average value is taken as thickness. It is seen from

figure 4-7, the thickness of AgNW/PEDOT:PSS has been varied with respect to spray time. Similarly, a change in film thickness was observed due to variation in spray time at constant flow rate, stand-off distance, substrate velocity and material concentrations. The thickness of thin film plays a key role in the electrical and optical properties.

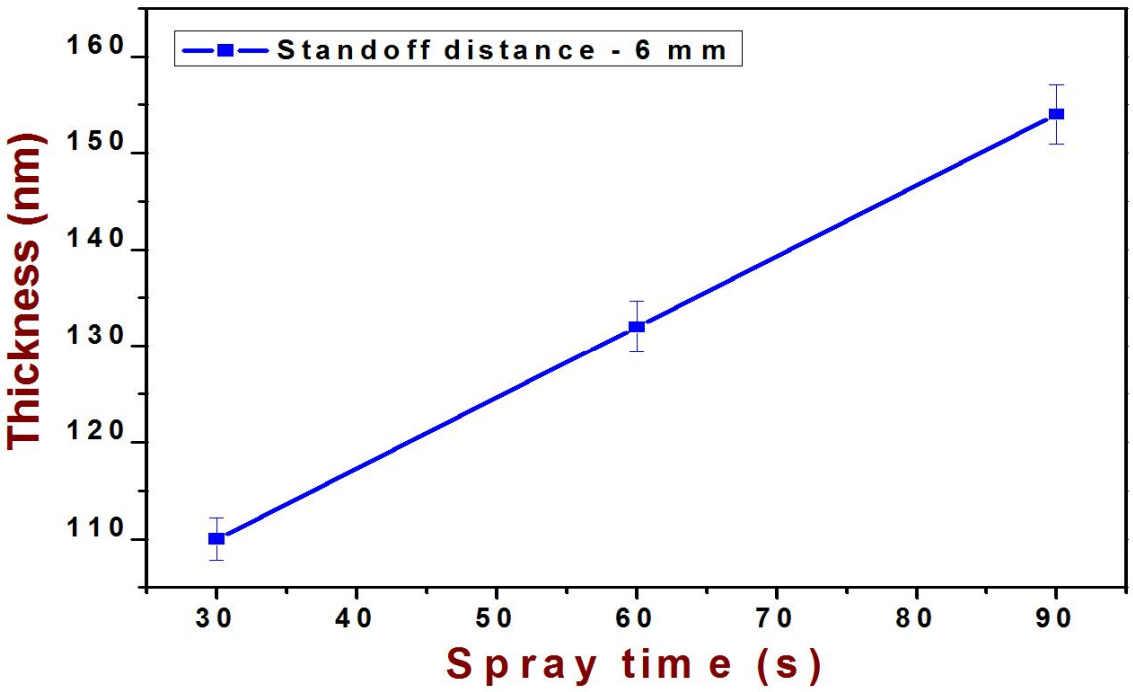

Figure 4-7 Variation of thickness as-deposited AgNW/PEDOT:PSS thin film with different spray time

4.2.5Surface Morphology

The surface morphology of the as deposited films is examined using the FE-SEM analysis. Figure 4-8(a-d) depicts the surface uniformity and homogeneous deposition of pure PEDOT:PSS and AgNW/PEDOT:PSS film. As compared with the morphology of the pure polymer film (figure 4-8a), the AgNW incorporated films shows changes in surface morphology due to the presence of inorganic material embedded in the organic matrix. FE-SEM micrograph reveals the

two distinct phases such as PEDOT (brighter region) and PSS (darker region) moiety on deposited thin film. Similarly, the uniformity of the thin films is high in the case of high spray time (figure 4-8d) compared to the films deposited in short spray time (figure 4-8 (b-c)). Herein, the use of ultrasonication during the preparation of precursor ink plays a crucial role in the deposition of films. A highly stable ink was prepared during the sonication process which results in the uniform deposition of thin films as shown in figure 4-8d. From the FE-SEM micrographs, it is evidenced that the AgNWs present in the organic matrix of PEDOT:PSS produces new conductive pathways which results in the improvements in the electrical conductivity. Overall, the surface analysis of thin film exhibiting the presence of highly interconnected AgNWs in the PEDOT:PSS matrix is in accordance with the XRD studies.

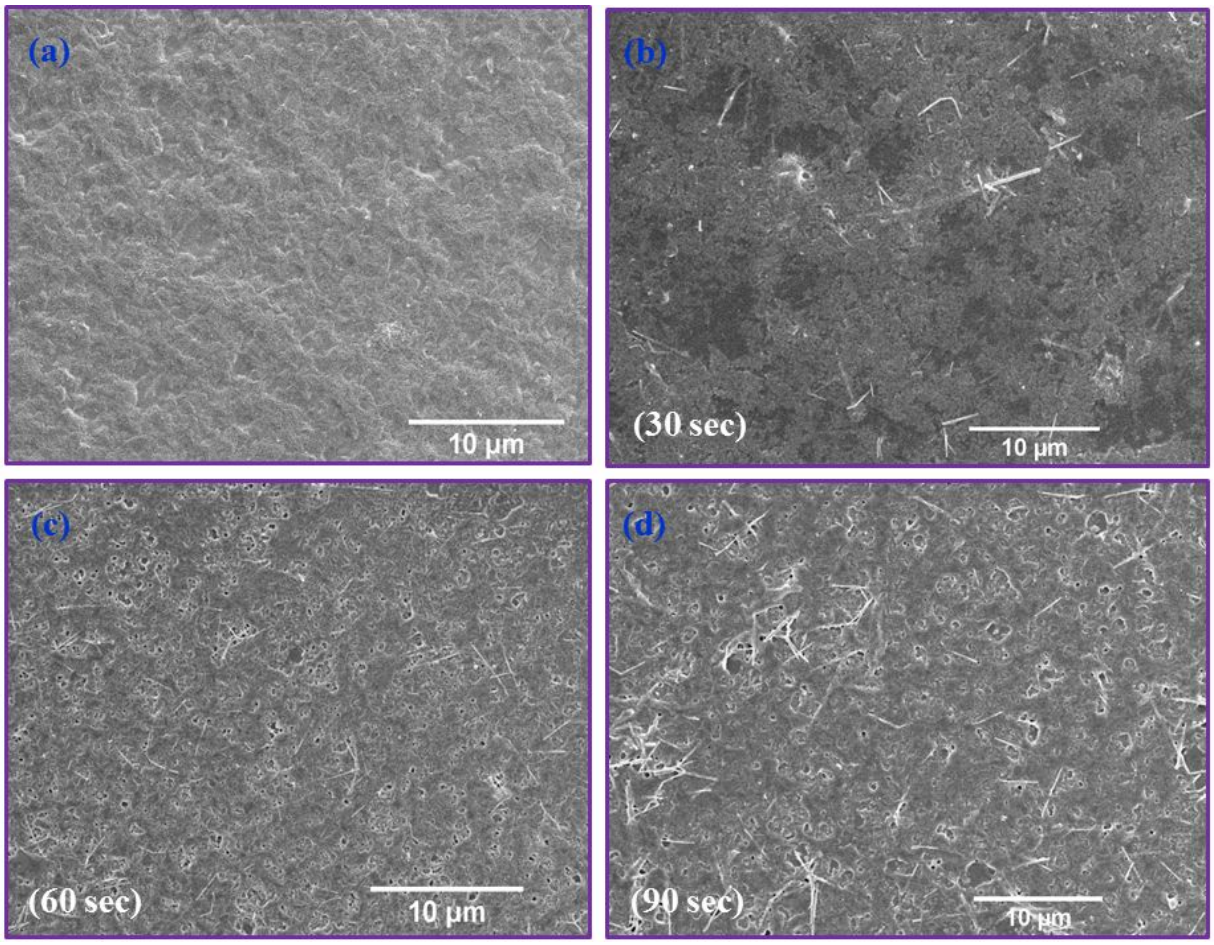

Figure 4-8 Field emission scanning electron microscopy, (a) surface morphology of pure PEDOT:PSS thin film, (b-d) AgNWs embedded PEDOT:PSS thin film corresponding to 30 s, 60 s and 90 s spraying time respectively

4.2.6 Chemical composition study

X-ray photoelectron spectroscopy (XPS) is one of the major techniques used to investigate the chemical states and purity of the nanostructured materials and thin films (Krishnamoorthy et al. 2013). In order to study the chemical states and purity of the as deposited film, we used the XPS analysis. The XPS survey scan of the AgNW/PEDOT:PSS films is shown in figure 4-9 which confirms the presence of binding energies corresponding to the metallic Ag, sulfur, carbon and oxygen. The binding energy corresponding to the Ag arises due to the presence of AgNWs whereas the presence of carbon, sulfur and oxygen corresponds to the PEDOT:PSS matrix in the films, respectively. In order to better understanding the chemical state of the elements present in the thin films, the deconvoluted spectra is shown in figure 4-10. Figure 4-10a shows the Ag 3d deconvoluted spectra with peaks at 367.6 eV and 373.6 eV corresponds to Ag $3d_{5/2}$ and Ag $3d_{3/2}$(Ramasamy et al. 2012) respectively. The deconvoluted S2p peaks is given in figure 4-10b shows two peaks at 164.0 eV and 168.2 eV which is ascribed to S2p of PEDOT and PSS moiety due to spin-split doublet of sulfur (Wang et al. 2009). The C1s deconvoluted spectra of the films is shown in figure 4-10c which shows three peaks at binding energies 284.9 eV, and 285.8 eV, corresponds to C−H/C−C, and C−C−O of the PEDOT:PSS present in the thin films (Farah et al. 2012). Fig. 7d represents the deconvoluted O1s spectra of the thin films shows a major peak at binding energies 531 eV which corresponds to the C−O−C groups in the PEDOT. Finally, the XPS analysis confirms that no characteristic peak of any impurities are identified, suggesting the purity of deposited AgNW/PEDOT:PSS thin film.

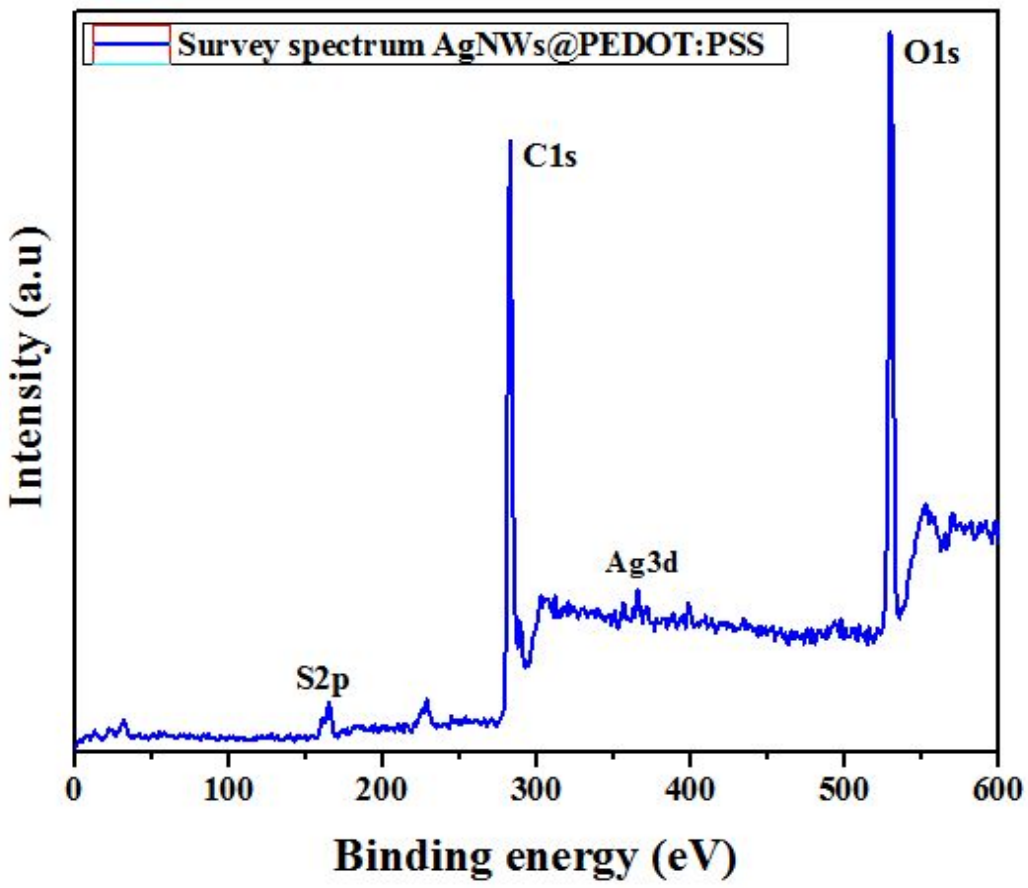

Figure 4-9 Typical survey scan of AgNW/PEDOT:PSS thin film thin film examined by X-ray photoelectron spectroscopy

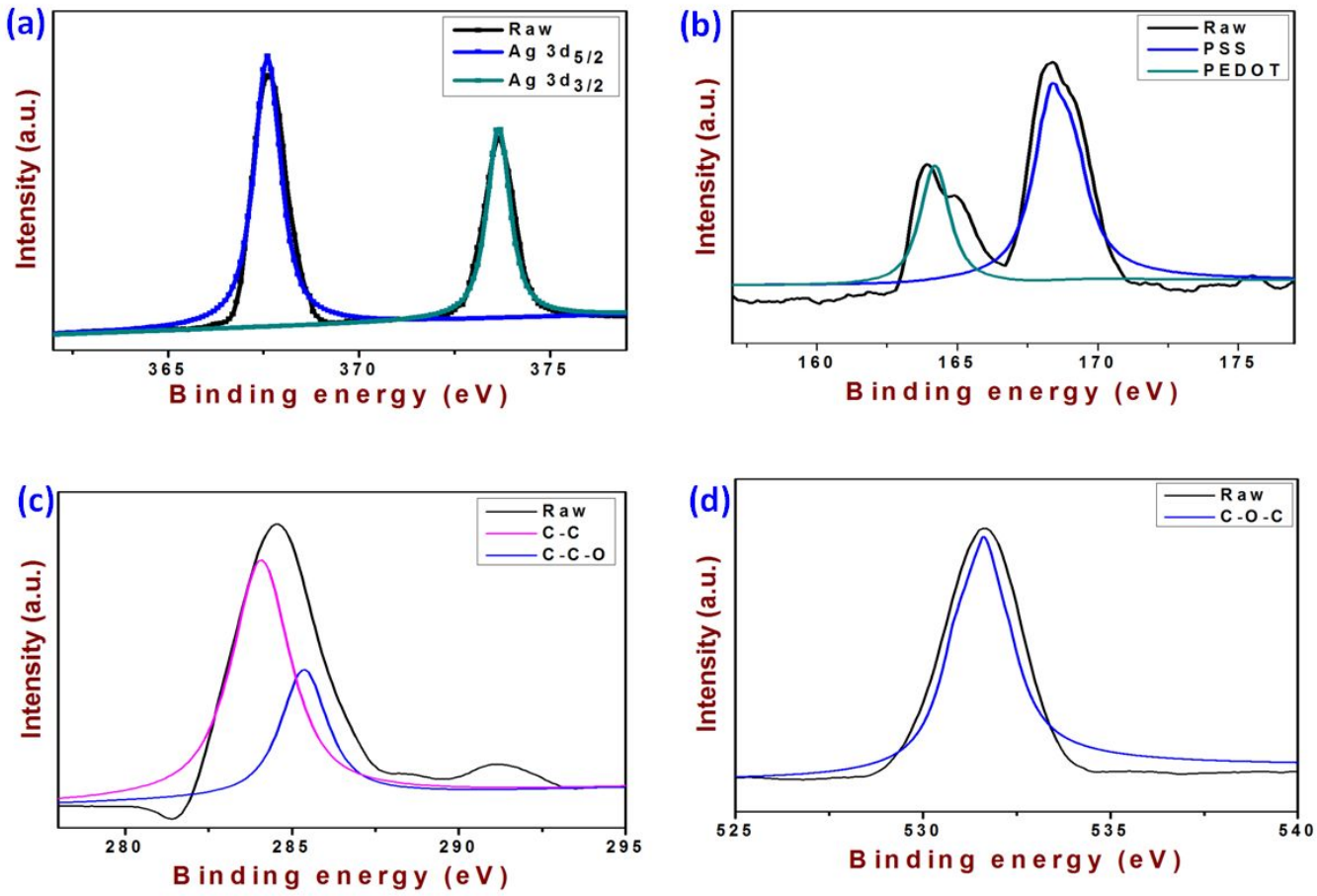

Figure 4-10 Deconvoluted XPS spectra of as deposited films: (a) AgNWs (Ag 3d), (b) sulfur (S2p), (c) carbon (C1s) and (d) oxygen (O1s) peaks

4.2.7 Optical Properties

The optical transmittance spectra of deposited film are analyzed through UV−vis spectrum. Figure 4-11 shows the transmittance spectrum of PEDOT:PSS thin film at 6 mm stand-off distance. The AgNWs embedded PEDOT:PSS film (spray time 30 s) exhibited transmittance nearly 77 %, which slightly less than pure PEDOT:PSS thin film (spray time 30 s) transmittance in the visible region, whereas the films deposited for 60 and 90 s have the transmittance of 74 % and 72 %, respectively. This is mainly due to the increase in film thickness. On the other hand, the sheet resistance of deposited thin film has decreased due to influence of densely intercalated

AgNWs into the polymer matrix (Yun et al. 2012), which is confirmed by FE-SEM. The UV−visible spectra results confirm that the deposited AgNWs/PEDOT:PSS composite has optimum transmittance in the visible region, which is more suitable for optoelectronic applications.

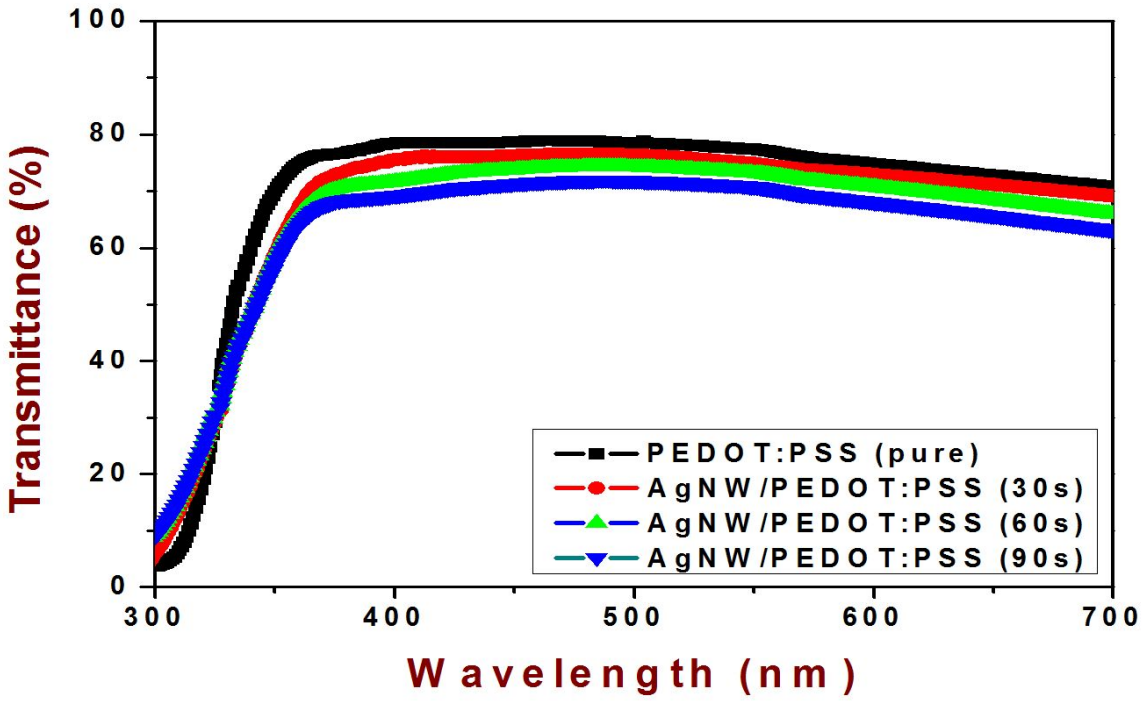

Figure 4-11 UV−visible transmittance spectra of pure PEDOT:PSS and AgNW/PEDOT:PSS thin films with different spray time

4.2.8 Electrical study

A two point probe with hemispherical is used to measure the electrical measurement of thin film. The current−voltage (*I−V*) measurement are carried out for AgNWs/PEDOT:PSS film. The top electrode contact using silver patterns are printed through EHDA technique on deposited thin film (Arshad et al. 2011). In *I−V* analysis, the electric current flows through the thin film in between the two probe. Figure 4-12 shows the *I−V* measurement of pure polymer films and the

AgNW/PEDOT:PSS thin films. The *I*−*V* measurement revealed the ohmic behavior which is due to the presence of AgNWs in the PEDOT:PSS matrix and also the Ag electrodes. The increase in electrical conductivity in the as deposited films due to increase in spraying time (thickness) is observed which is due to the presence of AgNWs which produces a new conducting pathways due to interconnected nanowires in the organic polymer matrix. The maximum thickness of thin films possesses high electrical conductivity due to the influence of high AgNW concentration in the as deposited film (as evidenced from figure 4-13). This is in agreement with the FE-SEM studies which show that the interconnection between the Ag NWs is less in the short sprayed sample whereas the long sprayed sample possesses high interconnection between the Ag NWs in the organic matrix, which drastically improves the electrical conductivity (figure 4-12).

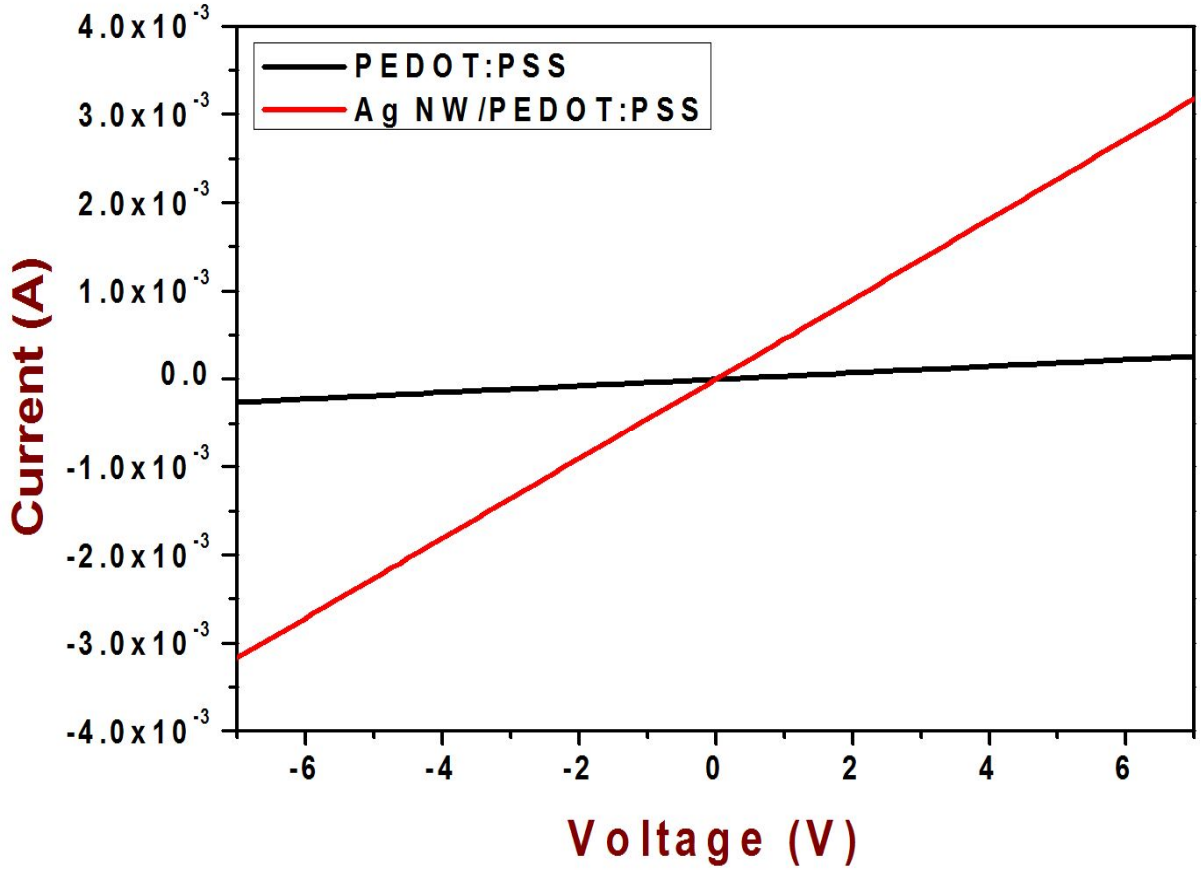

Figure 4-12 Current –Voltage (*I*−*V*) measurement of pure PEDOT:PSS and AgNW/PEDOT:PSS thin film

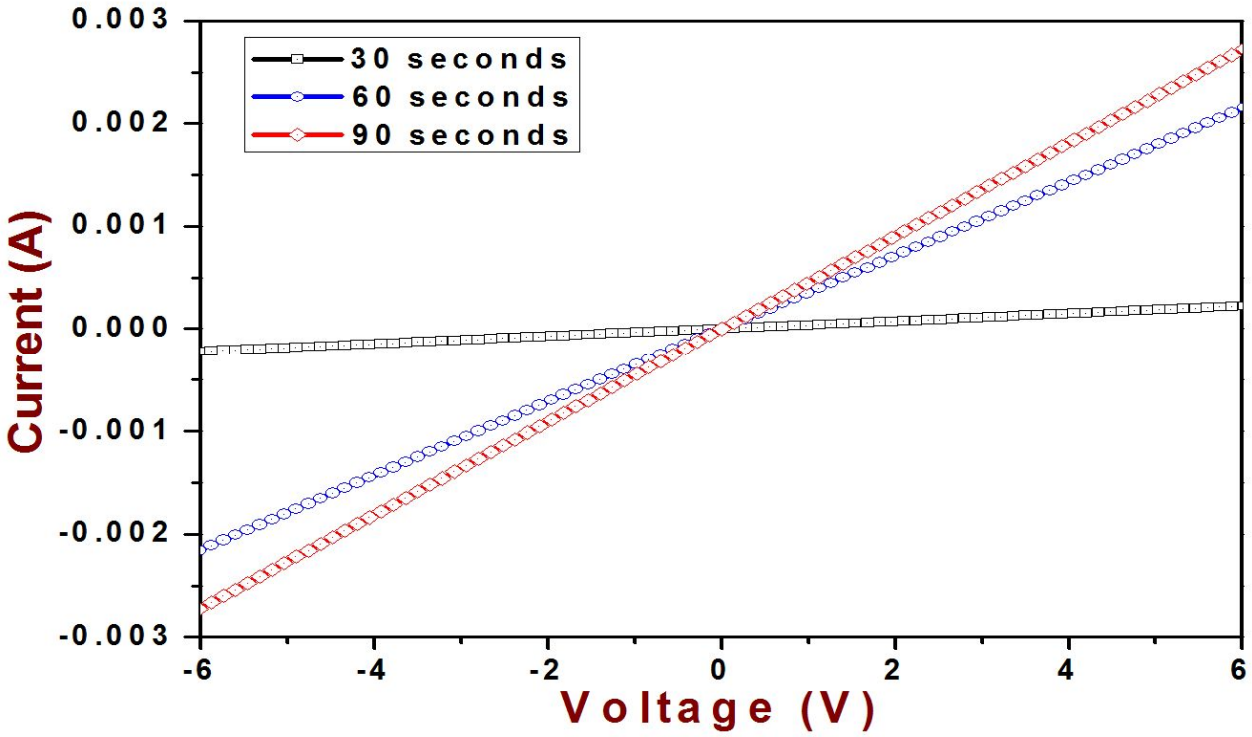

Figure 4-13 Current –Voltage (*I-V*) measurement of AgNWs/PEDOT:PSS thin film with different spray time

The optical transmittance and electrical conductivity are the two important features for any electrode material for its potential usage as transparent conducting electrodes (TCEs). Table 4-2 shows the obtained optical transmittance and the sheet resistance of the as deposited thin films. The observed sheet resistance of the PEDOT:PSS thin films are in agreement with the previous study by Chen et al. 2012. It clearly shows that the sheet resistance of the pure PEDOT:PSS thin films are decreased nearly one order after AgNW incorporation and only little change in the transmittance in the visible region. This illustrates the potential usage of AgNWs as filler in the organic transparent conducting electrodes. Another important parameter in the TCE applications

is the figure of merit of the semiconductor which is depends on the transmittance and sheet resistance of the thin films. An optimal consideration between optical transmission and electrical sheet resistance was achieved by Haacke et al. 1999, who defined the figure of merit as $\phi_{TC} = T^{10}/R_{s,}$ where T is the optical transmittance and R_s is the sheet resistance. The observed figure of merit of the pure PEDOT:PSS and AgNW/PEDOT:PSS (90 sec) thin films are found to be $6.17\times10^{-6}\Omega^{-1}$ and $3.49\times10^{-5}\Omega^{-1}$, respectively. It is observed that the changes in one order were achieved in the figure of merit of the electrodes after AgNW addition in the polymer matrix. The achieved figure of merit is less than that of the ITO electrode ($39.5\times10^{-3}\Omega^{-1}$) (Haacke et al. 1999). Collectively, in the view of solution processability and flexibility for commercial applications, this work highlights the importance of AgNWs as filler in the conducting polymers for enhanced properties in the TCE applications via EHDA technique.

Sample	**Optical transmittance (%)**	**Sheet resistance (Ω/□)**	**Figure of merit (Ω^{-1})** (ϕ_{TC})
PEDOT:PSS	78	1.35×10^{4}	6.17×10^{-6}
AgNWs/PEDOT:PSS	72	1.07×10^{3}	3.49×10^{-5}

Table 4-2 Comparison of properties of pure PEDOT:PSS and AgNW/PEDOT:PSS thin films

5. Summary

This chapter summarizes the entire results and over all achievements in this thesis. Concluding, this dissertation presented the basic understanding of electrohydrodynamic atomization technique and deposition of nanostructured functional thin films with detailed spectroscopic characterizations. Our experimental results suggesting that the deposition of functional thin films can be controlled by the physico-chemical properties of precursor solution or ink and the atomization process of EHDA. On this basis, we have presented different types of functional thin films (organic, inorganic and composites) for wide range of multifunctional applications.

Initially, we have discussed the merits and demerits of conventional techniques for thin film deposition and then motivation and importance of alternative technique of electrohydrodynamic atomization for large scale thin film deposition on different substrates (flexible and non-flexible). This chapter clearly discussed the working principle, importance of atomization modes such as dripping, micro-dripping, unstable cone-jet, stable-jet and multi-jet and also significant influence of process parameters (flow rate, applied potential, stand-off distance, etc.) along with physico-chemical properties of precursor solution or ink.

With the understanding the basic principle of EHDA, We used to deposition of functional organic thin films such as PEDOT:PSS and multi-layered thin films. The PEDOT:PSS thin film deposited on flexible PET substrate. Optimum flow rate and applied potential for stable cone jet mode has been confirmed through operating envelope. The uniformity and film thickness has been investigated by a field emission scanning electron microscope. The thin film shows nearly 75-82 % transmittance in visible region. The electrical study shows good ohmic behavior of

PEDOT:PSS thin film with the resistivity of approximately 49.6 mΩ cm. However, multi-layered P3HT:PCBM/ PEDOT:PSS deposited on ITO coated flexible substrate. Deposition conditions such as stable cone jet formation, flow rate and applied potential have been investigated. X-ray diffraction analysis revealed the presence of P3HT polymer in the as deposited film. Surface morphology of the films are investigated using a field emission-scanning electron microscope confirms that a uniform deposition of thin films was achieved. The current−voltage characteristics of the as deposited films show a rectifying behavior. The capacitance−voltage study indicated that the frequency dependent capacitance of the as deposited thin films depended on the frequency.

We also demonstratedthat the deposition of nanostructured metal oxide thin films using EHDA process. Herein, the deposition of nanostructured TiO_2 ZnO and NiO thin films using the EHDA technique with organic polymers as a stabilizer. The required parameters for achieving the uniform films using EHDA are also discussed in detail. X-ray diffraction results confirmed that the TiO_2 ZnO and NiO films were oriented in the anatase, wurtzite and cubic phases. Field emission scanning electron microscope studies revealed the uniform deposition of the nanostructured metal oxides thin films. The purity of the films are characterized using Fourier transform infra-red (FTIR) and X-ray photoelectron (XPS) spectroscopy confirming the presence of Ti−O, Zn−O and Ni−O bonding in the films without any organic residues. The optical properties of the thin films were measured by the UV-visible spectroscopy which shows the transparency of the films is in the visible region. The current-voltage (*I-V*) curve of the TiO_2 thin films shows a nearly linear behavior with 45 mΩ.cm of electrical resistivity. The photocurrent measurement of ZnO thin film is investigated under the UV light illumination. Finally, the

electrochemical analysis of NiO thin film demonstrated that the electrode behavior and storage capacity for energy storage application.

Finally, Silver nanowires (AgNWs) embedded PEDOT:PSS nanocomposite thin films was deposited on flexible substrate through EHDA. The optimization of flow rate and applied potential for achieving uniform thin film via Taylor cone formation has been discussed in detail. The crystallinity and surface morphology of the as-deposited thin films was investigated by X-ray diffraction and field emission scanning electron microscope. The X-ray photoelectron spectroscopy results showed that the nature of chemical bonding and film purity of intercalated AgNWs in PEDOT:PSS matrix. The optical and electrical studies revealed high transparency in the visible region and lower sheet resistance of the AgNWs/PEDOT:PSSthin films. These results indicate that the AgNWs embedded PEDOT:PSS is a key factor to enhance the film conductivity without any loss of optical properties which may create new horizon in their potential applications in optoelectronics. The unique advantage of EHDA technique play a significant role for the manufacture of functional thin films based printed devices at room atmospheric conditions and this thesis is used to further illuminates the EHDA process as an alternative to conventional techniques.

6. Conclusions and Future work

The PEDOT:PSS thin film has been deposited through EHDA. The deposited thin film shows nearly 75-82 % average transmittance in visible region. Field emission scanning electron microscopy images reveal uniform deposition with less agglomerated polymeric chains and the film thickness was ~180 nm with good adherence to the substrate. *I–V* characteristics of thin film show good ohmic behavior with the electrical resistivity of 49.6 mΩ cm. The successful deposition of PEDOT:PSS thin film through the EHDA technique indicates its promising application in the field of optoelectronic printed devices. On the other hand, P3HT:PCBM has been successfully deposited by EHDA technique. The XRD and FT−IR revealed the crystallinity and chemical composition of blended polymer. The surface morphology of deposited film showed the uniform deposition without any agglomeration of blended polymer. The optical absorbance of P3HT:PCBM was observed in the visible region with peak shift into lower wavelength due to the influence of PCBM. The *I–V* analysis showed rectifying behavior of fabricated organic device. The *C–V* measurement showed that the capacitance strongly depends on the applied bias and frequency. The fabrication of organic polymers through EHDA process ensures their potential application in micro/nano electronic printed energy devices.

Nanostructured TiO_2 thin films on glass substrates were prepared using EHDA technique. The process parameters of the EHDA spray for the achievement of uniform film was discussed. The XRD results indicated that TiO_2 films were oriented in the anatase phase. SEM studies revealed the uniform morphology of TiO_2 thin films due to the influence of PVP as a stabilizer. The FTIR and XPS spectroscopy confirmed that the TiO_2 was present in the film without any organic residues suggesting the high purity of the method. The EHDA deposited TiO_2 films exhibited more than 85 % transparency and the optical band gap of the TiO_2 film was found to be 3.45 eV.

The band gap widening in the TiO_2 films is mainly attributed to the contribution of crystallite size effects. The *I-V* characteristics of the deposited films show good ohmic-behavior with a sheet resistance of 45 mΩ.cm. However, nanostructured ZnO thin films have been deposited on glass substrate through electrohydrodynamic atomization technique. The XRD results indicated that deposited ZnO thin films are oriented in the wurtzite structure. The film uniformity and void free surface are analyzed using FE-SEM. The FT-IR and XPS analysis confirmed that the deposited ZnO film suggests film purity without any organic residue. The film transparency observed nearly ~ 90% in the visible region with energy band gap of 3.17 eV. The photocurrent analysis of nanostructured ZnO thin film shows good photoresponse in UV region with wavelength of 365 nm. The observed results suggest new positive features in the deposition of nanostructured thin films using EHDA techniques for future electronic device applications. Further, the solution based EHDA technique is used to deposit the nanostructured NiO thin film on glass substrate. In EHDA, the processes parameters for achieving homogeneous thin film are discussed. The XRD pattern and FE-SEM image indicated that the deposited NiO thin film is oriented in the cubic phase with plate-like morphology. The measured surface roughness was ~ 2nm due to influence of non-ionic surfactant. The deposited thin film shows the presence of Ni-O bonding without any impurities, suggesting the high crystalline purity of NiO thin film via EHDA technique. Thin film an exhibit the optical transparency is more than 80~83 % in the visible region and the energy band gap was found out to be 3.7eV. The electrochemical measurement reveals that that deposited NiO thin film used as electrodes in energy storage supercapacitor applications. These results can be considered as potential findings regarding nanostructured NiO thin film deposition through EHDA technique which has versatile role in the future printed device applications.

Electrohydrodynamic atomization of AgNW/PEDOT:PSS thin film has been achieved via Taylor cone formation. The chemical engineering of the preparation of stable precursor ink and the optimization process in the EHDA deposition of AgNW/PEDOT:PSS are discussed in detail. The formation of uniform thin films via EHDA deposition and the influence of AgNWs in the as deposited films are widely analyzed using XRD, UV−vis, XPS and FE-SEM analysis. The interconnected AgNWs networks inside the polymer matrix create new conductive pathways which further result in the enhancement of the electrical conductivity of the as deposited films. The optical transmittance, sheet resistance and the figure of merit of the as-deposited films revealed the potential utility of the AgNWs as an additive in the conducting polymers for TCE applications. With the advantage of being solution processability, flexibility, cost-effective and easy chemical functionalization of precursors, the EHDA technique and the enhanced properties of as-deposited AgNW/PEDOT:PSS thin films, we believe that it will create new developments in the field of printed electronics.

The work in this thesis demonstrated that the deposition of functional thin films on various substrates. Here, we have investigated the deposition and characterization of organic polymers, inorganic metal oxide and one dimensional metals intercalated with polymer matrix through EHDA and its electronic applications. In future, the research areas are concerned the fabrication of nanowires/nanorods, nanosheets, core cells, quantum dots and its composite materials on flexible and stretchable substrates through solution based EHDA. Thin film deposition is not only carried out using single step nozzle but also try to use multi nozzle systems to achieve a large area deposition with quick time period. However, there are certain issues can occur using multi nozzle setup and also solution based one, two dimensional and quantum dots materials. In case of multi nozzle setup, the most important challenging task is system design and cross talk

between the adjacent nozzle under the influence of electric filed, leads to damage the cone stability and film uniformity. On the other hand, physico-chemical properties of respective precursor solution or inks such as electrical conductivity, surface tension, viscosity, dielectric constant, non-agglomeration nature and ink stability. The development of one or two dimensional and quantum dots based nanostructured functional thin films via EHDA process play a vital role in the field of future printed electronics and bioelectronics application.

References

Jørgensen et al., Adv. Mater. 24(5), 580 (2011)

Paul et al.,Appl. Phy. Lett. 96, 082116 (2010)

Nagashima et al.,Appl. Phy. Lett.94, 242902 (2009)

Yao et al.,Sens. Actuators, B. 16, 1053 (2012)

Hyeong et al.,Science, 333, 838 (2011)

Hyeong et al.,Annu. Rev. Biomed. Eng. 14, 113 (2012)

Mannoor et al.,Nat. commun. 3, 1 (2012)

Fortunato et al., Adv. Mater. 24, 2945 (2012)

Kim et al., Adv. Mater. 24, 5565 (2012)

Cheng et al., Adv. Mater. 17, 2753 (2005)

Madaria et al.,Nanotechnology 22, 245201(2011)

Radisavljevic et al., Nat. Nanotechnol. 6, 147 (2011)

Kaempgen et al., Nano Lett.9 (5),1872 (2009)

Wang et al.,Adv. Mater.23, 1630 (2011)

Christos et al.,Adv. Mater. 14, 99 (2002)

Yu et al.,Adv. Mater.23, 4453 (2011)

Boucle et al.,J. Mater. Chem. 17, 3141 (2007)

Kim et al.,Phys.Chem. Chem. Phys.14, 3530(2012)

Gupta et al.,Bull. Mater. Sci. 27, 445 (2004)

Penga et al.,J. Appl. Phys. 93, 7975 (2003)

Teixeira et al.,J. Nanosci. Nanotechnol. 9(7), 4061 (2009)

Choi et al.,J. Appl. Phys. 98, 033715 (2005)

He et al., Nucl. Instr. Meth. Phys. Res. B. 135, 512 (1998)

Kelly et al., Surf. Coat. Tech. 86-87, 28 (1996)

Hayati et al.,Nature 319, 41 (1986)

Choi et al.,Nanoscale5, 977 (2013)

Cloupeau and Prunet-Foch, J. Aerosol Sci. 24 (6), 1021 (1994)

Samarasinghe et. al. Appl. Phys. A 91, 141 (2008)

Jaworek and Krupa, J. Aerosol Sci. 30 873 (1999)

Hartman, PhD Thesis, Technische Universiteit Delft, 1998.

Shigeta et alAnal. Chem.84 (22), 10012 (2012)

Burroughes et al., Nature 347(6293), 539 (1990)

Yong et al., Adv. Mater. 2, 1076 (2011)

Stephan et al., J. Mater. Chem. 15, 2077 (2005)

Marcus et al., Appl. Phys. Lett. 81, 289 (2002)

Nardes et al., Org. Electron. 9, 727 (2008)

Youn et al., Mater. Lett. 65, 3055 (2011)

Marin et al., Electrochem. Commun. 11, 2060 (2009)

Ganan-Calvo et al., J. Aerosol. Sci. 28, 249 (1997)

Hartman et al., J. Aerosol. Sci. 31, 65 (2000)

Choi et al., Appl. Phys. A 107, 715 (2012)

Ijsebaert et al., J. Appl. Physiol. 91, 2735 (2001)

Erika et al., Proceedings of IS&T Digital Fabrication, Denver. 107 (2006)

Muhammad et al., Curr. Appl. Phys. 11, S68 (2011)

Jaworek et al., J. Mater. Sci. 42, 266 (2007)

Lapkowski and Pron, Synth. Met. 110, 79 (2000)

Garreau et al., Synth. Met. 125, 325 (2002)

Kim et al., Adv. Mater. 14, 206 (2002)

Arshad et al., Appl. Phys. A. 104, 1113 (2011)

Currie et al., Science 321, 226 (2008)

Sekitani et al., Science 326,1516 (2009)

Forrest et al., Nature 428, 911 (2004)

Haddon et al., Acc. Chem. Res. 25 (3), 127 (1992)

Shah et al., Science 285, 692 (1999)

Muhammad et al., Curr. Appl. Phys. 13, 90 (2013)

Duraisamy et al., Mater. Lett. 83, 80 (2012)

Yusli et al., Mater. Lett. 63, 2691 (2009)

Lee et al., J. Mater. Chem. 20, 3287 (2010)

Kalita et al., Solid. State. Electron. 54, 447 (2010)

Vishal et al., Chem. Phys. Lett. 411, 138 (2005)

Rider et al., Adv. Funct. Mater. 20, 2404 (2010)

Aydog et al., Vacuum 77, 269 (2005)

Tugluoglu et al., Curr. Appl. Phys.12,1529 (2012)

Ocak et al., Synthet. Met. 159, 1603 (2009)

Monat et al., Nano. Lett. 6, 1464 (2006)

Krunks et al., Sol. Energ. Mater. Sol. Cell. 92, 1016 (2008)

Narashimha Rao et al., J. Vac. Sci. Technol. A: Vac. Surf. Films. 8, 3260 (1990)

Hofmann et al., Chem. Rev. 95, 69 (1995)

Fuyuki et al., Jpn. J. Appl. Phys. 25, 1288 (1986)

Linsebigler et al., Chem. Rev. 95, 735 (1995)

Jung et al., Surf. Coat. Technol. 174-175, 296 (2003)

Takeda et al., Thin Solid Films. 392, 338 (2001)

Zhang et al., Surf. Coat. Technol. 84, 476 (1996)

Kim et al., J. Nanosci. Nanotechnol. 9, 4285 (2009)

Voudouris et al., Surf. Coat. Technol. 115, 38 (1999)

Vahlas et al., Mater. Sci. Eng. R.53, 1 (2006)

Kim et al., J. Aerosol Sci.37, 1532 (2006)

Luo et al., Food Bioprocess Technol. 5, 2285 (2011).

Jayasinghe and Edirisinghe, J. Aerosol Sci. 33, 1379 (2002)

Jayasinghe and Edirisinghe, J. Mater. Sci. Lett. 37, 1987 (2002)

Mahalingam and Edirisinghe,Appl. Phys. A. 89, 987 (2007)

Chen et al, J. Aerosol Sci. 26, 963 (1995)

Wang et al., Mater. Lett. 60, 77 (2006)

Karthikeyan et al., J. Nanostruct. Polym. Nanocompos. 5, 83 (2009)

Zhang et al., J. Non-Cryst. Solid 303**,** 134 (2002)

Khanna et al., J. Mater. Sci. 39, 5956 (2004)

Zhang et al., Key Eng. Mater. 224–226**,** 573 (2002)

Zhu et al., J. Mater. Res. 14 (2), 444 (1999)

Zhang et al., J. Mater. Sci. Technol. 20**,** 31 (2004)

Krishnamoorthy et al., Appl. Phys. Lett. 98, 244101 (2011)

Lei et al., Chem. Phys. Lett. 338**,** 231 (2001)

Mogyorosi et al., Langmuir 19**,** 2938 (2003)

Lei et al., Appl. Surf. Sci. 253**,** 720 (2006)

Khan et al., Appl. Phys. A. 104, 1113 (2011)

Bearzotti et al., Sensor Actuat. B-Chem.19**,**525 (1994)

Orendorz et al., Appl. Surf. Sci.252, 85 (2005)

Kim and Rhee, Microelectron. Eng. 86, 2153 (2009)

Muhammad et al, Thin Solid Films, 520, 1751(2011)

Wang et al., Appl. Phys. Lett. 92, 112101(2008)

Longyue et al., Plasma Sci. Technol. 8, 172 (2006)

Xu et al., Nat. Nanotechnol. 5, 366 (2010)

Lee et al., Sensor. Lett. 9, 132 (2011)

Premanathan et al., Nanomedicine: NBM, 7, 184 (2011)

Mohan et al., Solid. State. Commun. 152, 375 (2012)

Mohan et al., Chem. Phys. Lett. 539, 83 (2012)

Wang, J. Phys.: Condens. Matter.16, R829 (2004)

Raoufi and Raoufi, Appl. Surf. Sci. 255, 5812 (2009)

Guo et al., J. Alloys. Compd. 552, 70 (2013)

Mishra et al., J. Alloys. Compd, 539, 1(2012)

Jun et al.,Ceram. Int. 35, 2797 (2009)

Dwivedi et al., J. Semicond, 34(3), 033001 (2013)

Nayak et al., Phys. Status. Solidi, A. 207, 1664 (2010)

Dai et al., J. Sol-Gel Sci. Technol. 60, 17 (2011)

Poon, PhD. Thesis, Princeton University, United Kingdom, 2002

Ellis et al., Chem. Eng. J. 181– 182, 798 (2012)

Vishlaghi et al., Mater. Res. Bull. 47, 1666 (2012)

Duraisamy et al., Thin Solid Films. 520,5070 (2012)

Krishnamoorthy et al., J. Mater. Chem. 22,24610 (2012)

Gayen, Indian J. Pure Appl. Phys, 49, 470 (2011)

Smirnov et al.,Appl. Surf. Sci, 256, 2405 (2010)

Wei, Physica B, 388, 145 (2007)

Dhara and Giri, Nanoscale. Res. Lett. 6, 1(2011)

Schubert et al., Adv. Funct. Mater. 22, 4993 (2012)

Wang et al., Adv. Mater. 24, 1903 (2012)

Gwinner et al., Adv. Funct. Mater. 20, 3457 (2010)

Tang et al., Nat. Nanotechnol. 6,568 (2011)

Li et al., Science, 324, 1312 (2009)

Shua et al., J. Alloy. Compd. 496, 633 (2010)

Awais et al., Microelectron. Eng. 103, 167 (2013)

Wei et al., J. Alloy. Compd. 479, 855 (2009)

Song et al., J. Nanopart. Res. 14, 698 (2012)

Sato et al., Thin solid films. 236, 27 (1993)

Steirer et al., Adv. Energy Mater. 1, 813 (2011)

Wang et al., Int. J. Electrochem. Sci., 8, 4785 (2013)

Srinivasan and Weidner, J. Electrochem. Soc. 147 (3), 880 (2000)

Zhong et al., J. Alloy. Compd. 509, 3889 (2011)

Ghamdi et al., J. Alloy. Compd. 486, 9 (2009)

Muecke et al., Thin Solid Films. 517, 1522 (2009)

Kim and Kim, J. Aerosol Sci. 37, 1532 (2006)

Rietveld et al., Macromol. Mater. Eng. 293, 387 (2008)

Aal et al., Nanoscale. Res. Lett. 4, 627 (2009)

Wruk et al., J. Electrochm. Soc, 140, 1097 (1993)

Zhou et al., Mater. Chem. Phys. 98, 267 (2006)

Shu et al., J. Alloy. Compd. 496, 633 (2010)

Das et al., Physica E. 42, 1377 (2010)

Awais et al., Surf. Coat. Technol. 204, 2729 (2010)

Park et al., Sol. Energ. Mat. Sol. C 94, 2332 (2010)

Guo et al., Appl. Phys. Lett. 99, 083111 (2011)

Veerapandian et al., Carbon. 50, 4228 (2012)

Timpanaro et al., Chem. Phys. Lett. 394, 339 (2004)

Friend et al., Nature. 397, 121(1999)

Sariciftci et al., 258, 1474 (1992)

Hüttner et al., Appl. Phys. Lett. 92, 093302 (2008)

Groenendaal et al., Adv. Mater. 12, 481 (2000)

Ahlswede et al.,Appl. Phys. Lett. 92, 143307 (2008)

Hong et al., Org. Electron. 9, 864 (2008)

Yun et al.,ACS Appl. Mater. Interfaces, 3(1), 43 (2011)

Gaynor et al., Adv. Mater. 23, 2905 (2011)

Hu et al., ACS. Nano. 4, 2955 (2010)

Sun et al., Adv. Mater. 14, 833 (2002)

Kim et al., Chem. Eng. J. 167, 308 (2011)

Molina et al., Chem. Eng. J. 203, 212 (2012)

Ramadoss et al., Appl. Phys. Exp. 5, 085803 (2012)

Sriwong et al., Chem. Eng. J. 191, 210 (2012)

He et al., Chem. Eng. J.168, 931 (2011)

Duraisamy et al., Mater. Lett. 92, 227 (2012)

Korte et al., J. Mater. Chem. 18, 437 (2008)

Ramasamy et al., J. Mater. Chem. 22,11651 (2012)

Krishnamoorthy et al., Ultrason. Sonochem. 20, 644 (2013)

Memarzadeh et al., IMCS2012. 1105 (2012)

Lin et al., Sensor. Actuat. B. Chem. 140, 402 (2009)

Venugopal et al., Chem. Phys132, 29 (2012)

Muhammad et al., Thin Solid Films. 520, 6398 (2012)

Krishnamoorthy et al., Carbon. 53, 38 (2013)

Wang et al., Nanoscale. Res. Lett. 4(7), 613 (2009)

Farah et al., J. Appl. Phys. 112, 113709 (2012)

Yun et al., Adv. Mater. 24, 1321 (2012)

Chen et al., Org. Electron. 13, 1881 (2012)

Haacke et al., J. Appl. Phys. 86, 6451 (1999)

APPENDIX

List of Publications in International Journals

1. Nauman Malik Muhammad, Awais Muhammad Naeem, **Navaneethan Duraisamy**, Dong-Soo Kim, Kyung-Hyun Choi, Fabrication of high quality zinc-oxide layers through electrohydrodynamic atomization, Thin Solid Films 520 (2012) 1751–1756.
2. Kyung-Hyun Choi, **Navaneethan Duraisamy**, Nauman Malik Muhammad,Inyoung Kim, Hyunseok Choi, Jeongdai Jo. Structural and optical properties of electrohydrodynamically atomized TiO_2 nanostructured thin films.Appl Phys A 107 (2012) 715–722.
3. **Navaneethan Duraisamy**, Nauman Malik Muhammad, Hyung-Chan Kim, Jeong-Dai Jo, Kyung Hyun Choi. Fabrication of TiO_2 thin film memristor device using electrohydrodynamic inkjet printing. Thin Solid Films 520 (2012) 5070–5074.
4. **Navaneethan Duraisamy**, Nauman Malik Muhammad, Adnan Ali, Jeongdai Jo, Kyung Hyun Choi. Characterization of poly(3,4-ethylenedioxythiophene):poly(styrenesulfonate) thin film deposited through electrohydrodynamic atomization technique. Materials Letters 83 (2012) 80–83.
5. Nauman Malik Muhammad, **Navaneethan Duraisamy**, Hyun-Woo Dang, Jeongdai Jo, Kyung Hyun Choi. Solution processed Al doped ZnO film fabrication through electrohydrodynamic atomization. Thin Solid Films 520 (2012) 6398–6403

6. Nauman Malik Muhammad, **Navaneethan Duraisamy**, Khalid Rahman, Hyun Woo Dang,Jeongdae Jo, Kyung Hyun Choi. Fabrication of printed memory device having zinc-oxide activenano-layer and investigation of resistive switching. Current Applied Physics 13 (2013) 90−96.
7. Kyung-Hyun Choi, Ganeshthangaraj Ponniah, **Navaneethan Duraisamy**, Yang-Hoi Doh. Web tension optimization of slot die coated PEDOT: PSS based on resistance characteristics. International Journal of Engineering Research and Applications (IJERA) 2 (2012) 1497–1502.
8. Muhammad Naeem Awais, Nauman Malik Muhammad, **Duraisamy Navaneethan**, Hyung Chan Kim,Jeongdai Jo, Kyung Hyun Choi. Fabrication of ZrO2 layer through electrohydrodynamic atomization for the printed resistive switch (memristor). Microelectronic Engineering 103 (2013) 167–172.
9. Mustafa Maria, **Duraisamy Navaneethan**, Kim Hyung Chan, Hyeoun Myung Taek, Choi Kyung Hyun. Solution processed fabrication of single wall carbon nanotubes thin film by electrohydrodynamic atomization deposition technique and its characterization. Appl Phys A 109 (2012) 515–522.
10. **Navaneethan Duraisamy**, NaumanMalikMuhammad, Myung-TaekHyun, Kyung-HyunChoi. Structural and electrical properties of P3HT:PCBM/PEDOT:PSS thin films deposited through electrohydrodynamic atomization technique. Materials Letters 92 (2013) 227–230.
11. Kyung-Hyun Choi, **NavaneethanDuraisamy**, MuhammadNaeemAwais, Nauman MalikMuhammad, Hyung-ChanKim, Jeongdai Jo. Investigation

onswitchingbehaviorofZrO_2 thin filmformemory device applications. Materials Science in Semiconductor Processing, Article in press.

12. **Navaneethan Duraisamy**, Sung-Jei Hong, Kyung-Hyun Choi. Deposition and characterization of silver nanowires embedded PEDOT:PSS thinfilms via Electrohydrodynamic atomization. Chemical Engineering Journal, Article in press.
13. **Navaneethan Duraisamy**, Ganeshthangaraj Ponniah, Jeongdai Jo, and Kyung-Hyun Choi. Structural and Electrical Properties of AgGrid/Poly(3,4-ethylene dioxythiophene):Poly(styrenesulfonate) Coatings for Diode Application ThroughAdvanced Printing Technology. Journal of Nanoscience and Nanotechnology, Article in press.
14. **Navaneethan Duraisamy**, Nauman Malik Muhammad, Jeongdai Jo, and Kyung-Hyun Choi. Fabrication of Nanostructured Copper Indium diSelenide (CIS) Thin Films by Electrohydrodynamic Atomization Technique. Journal of Nanoscience and Nanotechnology, Article in press.

List of Conferences

1. Muhammad Naeem Awais, Nauman Malik Muhammad, **Duraisamy Navaneethan**, Dong-Soo Kim, Hyung Chan Kim, and Kyung Hyun Choi. Deposition of Non-stoichiometric ZrO_2 Thin Film through Electrohydrodynamic Atomization. NANO KOREA 2011 Symposium, Republic of Korea.
2. Mustafa Maria, Dang Hyun Woo, Park Jae Hee, **Navaneethan Duraisamy**, Doh Yang Hoi, Choi Kyung Hyun. Thin Film Fabrication of Single Wall Carbon Nanotubes by Electrospray deposition technique towards Supercapacitor, Republic of Korea.